NASA/CR—1999-209162

NSTAR Ion Thrusters and Power Processors

T.A. Bond and J.A. Christensen
Hughes Electron Dynamics, Torrance, California

November 1999

The NASA STI Program Office . . . in Profile

Since its founding, NASA has been dedicated to the advancement of aeronautics and space science. The NASA Scientific and Technical Information (STI) Program Office plays a key part in helping NASA maintain this important role.

The NASA STI Program Office is operated by Langley Research Center, the Lead Center for NASA's scientific and technical information. The NASA STI Program Office provides access to the NASA STI Database, the largest collection of aeronautical and space science STI in the world. The Program Office is also NASA's institutional mechanism for disseminating the results of its research and development activities. These results are published by NASA in the NASA STI Report Series, which includes the following report types:

- TECHNICAL PUBLICATION. Reports of completed research or a major significant phase of research that present the results of NASA programs and include extensive data or theoretical analysis. Includes compilations of significant scientific and technical data and information deemed to be of continuing reference value. NASA's counterpart of peer-reviewed formal professional papers but has less stringent limitations on manuscript length and extent of graphic presentations.

- TECHNICAL MEMORANDUM. Scientific and technical findings that are preliminary or of specialized interest, e.g., quick release reports, working papers, and bibliographies that contain minimal annotation. Does not contain extensive analysis.

- CONTRACTOR REPORT. Scientific and technical findings by NASA-sponsored contractors and grantees.

- CONFERENCE PUBLICATION. Collected papers from scientific and technical conferences, symposia, seminars, or other meetings sponsored or cosponsored by NASA.

- SPECIAL PUBLICATION. Scientific, technical, or historical information from NASA programs, projects, and missions, often concerned with subjects having substantial public interest.

- TECHNICAL TRANSLATION. English-language translations of foreign scientific and technical material pertinent to NASA's mission.

Specialized services that complement the STI Program Office's diverse offerings include creating custom thesauri, building customized data bases, organizing and publishing research results . . . even providing videos.

For more information about the NASA STI Program Office, see the following:

- Access the NASA STI Program Home Page at ***http://www.sti.nasa.gov***

- E-mail your question via the Internet to help@sti.nasa.gov

- Fax your question to the NASA Access Help Desk at (301) 621-0134

- Telephone the NASA Access Help Desk at (301) 621-0390

- Write to:
  NASA Access Help Desk
  NASA Center for AeroSpace Information
  7121 Standard Drive
  Hanover, MD 21076

NASA/CR—1999-209162

NSTAR Ion Thrusters and Power Processors

T.A. Bond and J.A. Christensen
Hughes Electron Dynamics, Torrance, California

Prepared under Contract NAS3–27560

National Aeronautics and
Space Administration

Glenn Research Center

November 1999

Available from

NASA Center for Aerospace Information
7121 Standard Drive
Hanover, MD 21076
Price Code: A08

National Technical Information Service
5285 Port Royal Road
Springfield, VA 22100
Price Code: A08

TABLE OF CONTENTS

TABLE OF CONTENTS

SECTION **PAGE**

TABLE OF CONTENTS

SECTION **PAGE**

TABLE OF CONTENTS

SECTION PAGE

TABLE OF CONTENTS

SECTION PAGE

1.0 BACKGROUND

The NASA Solar Electric Propulsion Technology Application Readiness (NSTAR) project is a program to validate ion propulsion technology for use on future NASA deep space missions. The first NSTAR flight Xenon Ion Thruster, Power Processor Unit (PPU) and Digital Control and Interface Unit (DCIU) were used as the primary propulsion on the Deep Space 1 mission that was launched in October 24, 1998.

The NSTAR program encompassed four major elements: (1) the development of Engineering Models including 30 cm ion thrusters and breadboard PPUs by NASA GRC, and development of a xenon propellant system by JPL; (2) ground testing of Engineering Model ion thrusters to validate performance and lifetime; (3) the design, development, production and qualification of Flight Model ion thrusters and PPUs by Hughes, Electron Dynamics (HED) and DCIUs by Spectrum Astro; and (4) in-space diagnostic measurements of the NSTAR Flight Model ion propulsion system on the DS1spacecraft.

The Engineering Model ion thrusters and breadboard PPUs were developed by NASA GRC. Several Engineering Model (EM) ion thrusters were built and tested demonstrating the required performance characteristics. This work is reported in several papers shown in the list of selected references at the end of this report. Wear testing was also performed for durations of 2000, 1000 and 8193 hours, which resulted in some design changes to the baseline design for the flight thrusters. No environmental testing was performed on the EM thrusters prior to the start of the NSTAR Flight hardware program at HED.
The HED NSTAR contract was initiated in September 1995. The primary objectives of the program were to develop, qualify and produce two sets of flight quality ion thrusters, PPUs and DCIUs that provided the same performance and life as the NASA EM thrusters and also met the dynamic and thermal environmental requirements of the Deep Space 1 (DS1) spacecraft. Thruster design changes to meet the flight environmental requirements (vibration, shock, and thermal) were carefully selected as to not invalidate the NASA EM thruster 8000 hour wear test that was conducted concurrently. In addition, the design of the DS1 spacecraft was not started until several months after the HED program, so the complete set of environmental requirements were not defined.

2.0 FLIGHT SYSTEM PROGRAM REQUIREMENTS

2.1 SOW Description

2.1.1 Paraphrased Version of the Statement of Work Tasks

Task 1. NSTAR Ground Tests

HED supported the NSTAR thruster ground tests at GRC and JPL to evaluate the results of the EM thruster wear tests and to integrate the HED Breadboard PPU with the NASA EM thruster.

HED participated in the integration of the Flight hardware with the DS1 spacecraft and the environmental testing. HED also supported analyses of the in-space operation and performance of the DS1 ion propulsion system.

Task 2. Design of the Flight Thruster

HED performed the initial design of the flight thruster, based closely on the NASA EM thruster designs and drawings provided. Conceptual and developmental subassembly and assembly drawings were generated. A preliminary structural dynamics model was developed. Test and product assurance plans were drafted. These results were presented at an informal PDR at Hughes with NASA, JPL and Spectrum Astro personnel in attendance.
HED generated the detailed thruster design, including parts and assembly drawings, parts lists, operations sheets (detailed assembly and process instructions) and installation control drawings. Thruster thermal analyses were performed by JPL. Structural dynamics and stress analyses were done by HED as well as a vibration test program using modified versions of the EM1 thruster. Manufacturing and test plans were prepared. The results of these efforts were presented in the CDR that was held at HED. The thruster flight design was approved for fabrication.

Task 3. Fabrication of Flight Thrusters

HED fabricated one Pathfinder and one Flight thruster using the approved design and assembly processes (OS). The Pathfinder thruster was used to prove out the parts designs and assembly processes. The Pathfinder thruster was later retrofitted to serve as a flight spare (FT2). Both thrusters were built using flight parts. Equipment logs with signed-off assembly procedures were provided.
The thrusters were shipped in containers provided by NASA for acceptance and qualification testing at NASA GRC.

Task 4. Vacuum Performance Test of the Pathfinder Thruster.

All the vacuum performance testing of the Pathfinder and Flight Model (FM) Thrusters was conducted by NASA at the NASA GRC or JPL test facility. These tests were performed in accordance with a test procedure and processes developed by NASA and HED.

Task 5. Design of the Flight Power Processor Units and Digital Interface and Control Units

HED designed the flight PPU to meet the NSTAR Thruster Element (TE) performance requirements and provide the electrical inputs required to operate the Thruster, DCIU and propellant feed system. The design process included the design, fabrication and test of a Breadboard PPU with a NASA EM thruster. The Breadboard PPU that was delivered to NASA used commercial parts and did not incorporate flight-type packaging. Two Flight Model PPUs were built, tested and delivered to NASA for integration and acceptance testing.
The design of the Digital Control and Interface Unit (DCIU) was subcontracted to Spectrum Astro. Spectrum Astro designed, built and tested one Engineering Model DCIU and two Flight

Model DCIUs. The DCIU provides the command and telemetry interface between the PPU, the xenon feed system (XFS) and the spacecraft computer. It also provided the control and telemetry for the propellant feed system sensors and solenoid valves. Spectrum Astro also designed and built the PPU slice subassembly that is the digital interface with the DCIU. The EM DCIU used commercial parts and was integrated and tested with the Breadboard PPU at HED and with an EM thruster at GRC. Two Flight Model DCIUs were built, integrated with the FM PPUs and delivered to NASA. HED also developed a power cable, which extended from the PPU to a DS1 field joint and then to the thruster.

The design of the Breadboard PPU and EM DCIU were presented at an informal PDR at HED. Schematics of the PPU circuits were analyzed and documented and preliminary Breadboard PPU test results were provided. Thermal and structural package design concepts were presented. Similar design information was presented for the DCIU. The PPU and DCIU designs were approved for detailed design of the Flight Models.

HED performed the detailed Flight Model PPU designs, including drawings, parts lists, assembly procedures and design analyses. The mechanical/package design was completed, and thermal and radiation analyses were performed. Operational sequences and fault logic were defined. Acceptance and Qualification Test Plans were documented. This data was presented in a Critical Design Review at HED.

The detailed Flight Model design of the DCIU was done by Spectrum Astro. Drawings, parts lists, package designs and design analyses were generated. Operational sequences, fault logic and telemetry circuits were defined. Test plans were documented. This data was presented at the Critical Design Review at HED.

The Flight Model PPU and DCIU designs were approved for fabrication at the conclusion of the CDR.

Task 6. Fabrication of Flight Model PPUs and DCIUs.

HED fabricated two Flight Model PPUs in accordance to the approved designs. Spectrum Astro fabricated two Flight Model DCIUs and two Flight Model PPU slices. Two DCIU to PPU wire harnesses were built and three sets of PPU to thruster power cables were assembled and delivered. Equipment logs were provided with each PPU and DCIU.

Task 7. Functional/Performance Tests of the PPUs and DCIUs Using a Load Bank.

Functional/performance tests were performed at HED on the Flight Model PPUs and DCIUs using resistive load banks to simulate the thruster electrical characteristics.

Following the successful completion of these tests, the Flight PPUs and DCIUs were delivered to NASA for integration with the thrusters and for performance and environmental testing.

Task 8. Integration and Functional Performance Tests of Ion Thrusters and PPUs.

The integration and functional performance tests of the Pathfinder and FM Thrusters with PPUs were performed by HED and NASA at the GRC test facility. These tests validated the performance, control, stability, and data system of the thruster/PPU subsystem.

Task 9 and 10 Environmental Acceptance **and Qualification Testing of Ion Thrusters, and PPUs.**

The thermal vacuum and final functional performance testing of the Pathfinder and FM Thrusters and PPUs was performed by NASA, with HED support, at the NASA GRC facility. These tests were performed using a manual propellant feed system and handling procedures documented in the NASA IPDs.

The vibration testing of the Pathfinder and FM Thrusters was performed by JPL with HED and GRC support. The thrusters were mounted to the Engineering Model DS1 gimbal assembly in order to simulate the spacecraft dynamic inputs to the thrusters during launch. These were non-operating vibration tests.

The vibration tests of the two FM PPUs and two FM DCIUs were performed at NASA GRC.

Task 11 Engineering Support

HED provided engineering support for spacecraft interface design coordination and design reviews. This effort also included the generation of Interface Control Documents for the NSTAR Thruster Element. HED prepared ICD drawings for the Thruster, PPU and DCIU.

Task 12 Reports of Work

HED prepared Reports of Work in accordance with the requirements of the contract.

Task 13 Product Assurance

HED documented and implemented a Product Effectiveness Program Plan that was approved by NASA.

Task 14 Thruster Spare Parts

HED provided spare parts and assemblies as requested by NASA.

Task 16 Integration of Thruster and Power Processor on the Spacecraft

HED assisted in the integration of the thruster and PPU with the DS1 spacecraft.

Task 21 Vibration Tests of EM Thrusters

HED performed vibration testing on EM thrusters in order to validate the computer structural models used for the FM thruster design and to verify that the final FM design could survive the Qualification vibration levels required for the DS1 Spacecraft. Low level resonance vibration tests were performed on the EMT1B thruster, which had two gimbal mounting pads. The EMT1 thruster was then modified to the C configuration, which incorporated nearly all the FM thruster design features, including three high strength gimbal mounting pads. Low level resonance vibration tests were performed, followed by step stress testing up to Protoflight Qualification random vibration levels. The EMT1C thruster was also vibration tested in the Engineering Model DS1 gimbal assembly at JPL.

2.2 Program Schedule

The NSTAR program at HED began on September 20, 1995. The following items were designed, built, and delivered:

Pathfinder Thruster (later reworked to be a flight spare FT2)
Flight Thruster (FT1)
2 Flight power processor units
2 Flight digital control units
3 Flight PPU/Thruster power cables
2 PPU Test Consoles (SPOTHs)
2 DCIU Simulators (PCs with DCIU-like software)*
2 DS1 Spacecraft Computer Simulators (PCs to control DCIU)*
2 XFS Simulator*
1 PPU Simulator
2 Sets of Spare Thruster Optics Parts
2 Sets of Spare Thruster Cathodes
1 Breadboard PPU
2 Engineering PPU Slice Boards
PPU Drawing Package
Thruster Drawing Package
PPU Test Data
DCIU Test Data
Miscellaneous Test Cables and Connectors
1 Heat Exchange Plate for PPU/DCIU Testing
1 Final Report

* Includes one supplied directly to JPL by Spectrum Astro, Inc.

Key dates are given in the following section.

The work on this contract culminated on Friday, April 30, 1999 with the submittal of this, The Final Report.

Figure 1. DS1 Spacecraft Showing NSTAR IPS Ion-Thruster

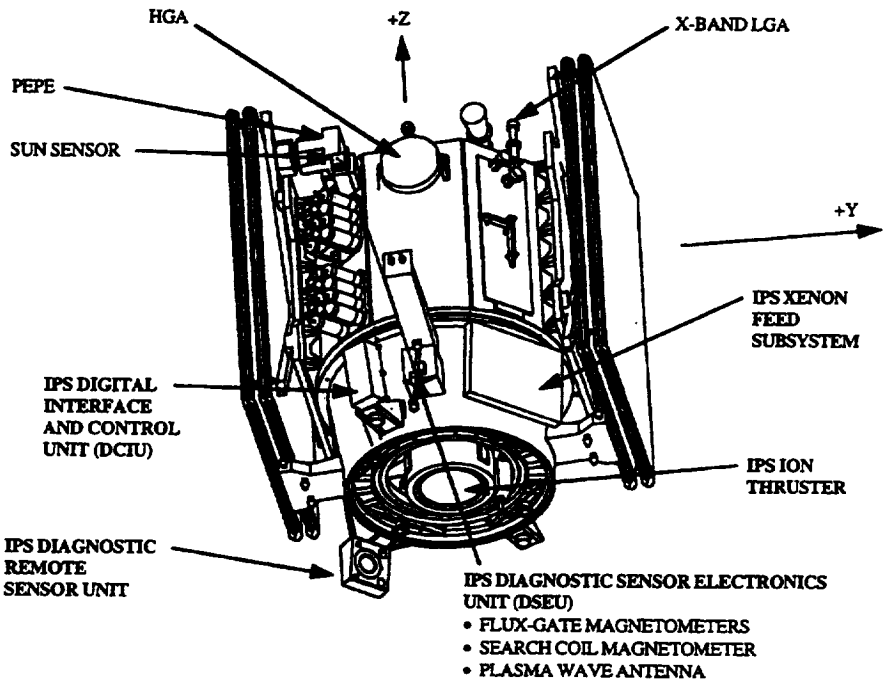

Figure 2. PHOTO OF THRUSTER - Side View

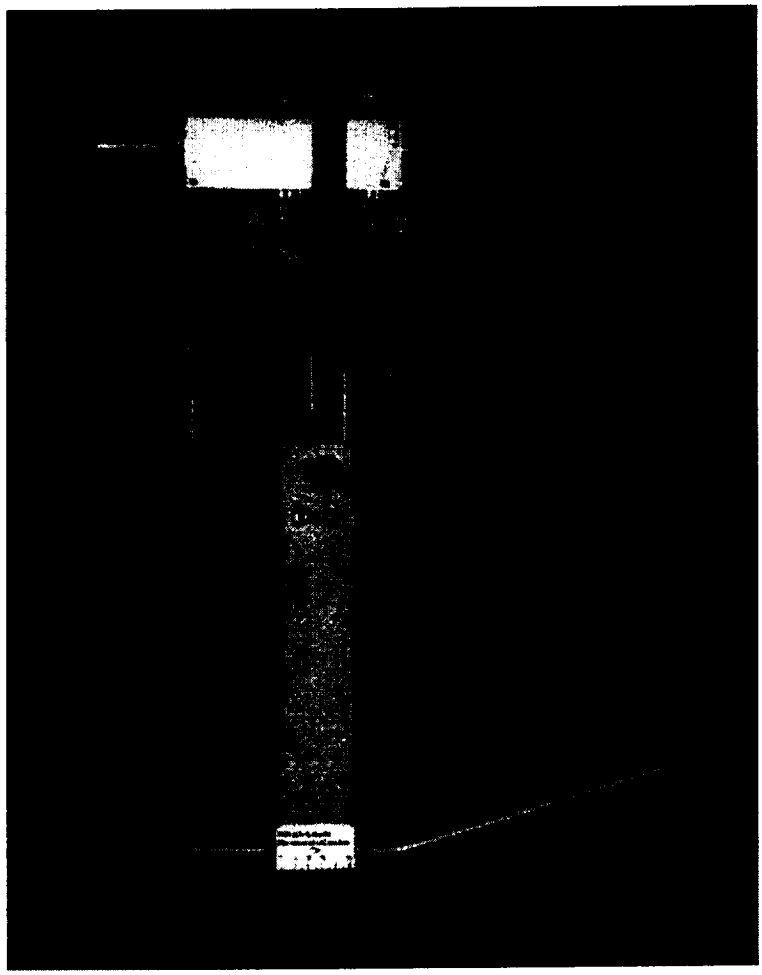

Figure 3. PHOTO OF THRUSTER –Downstream End

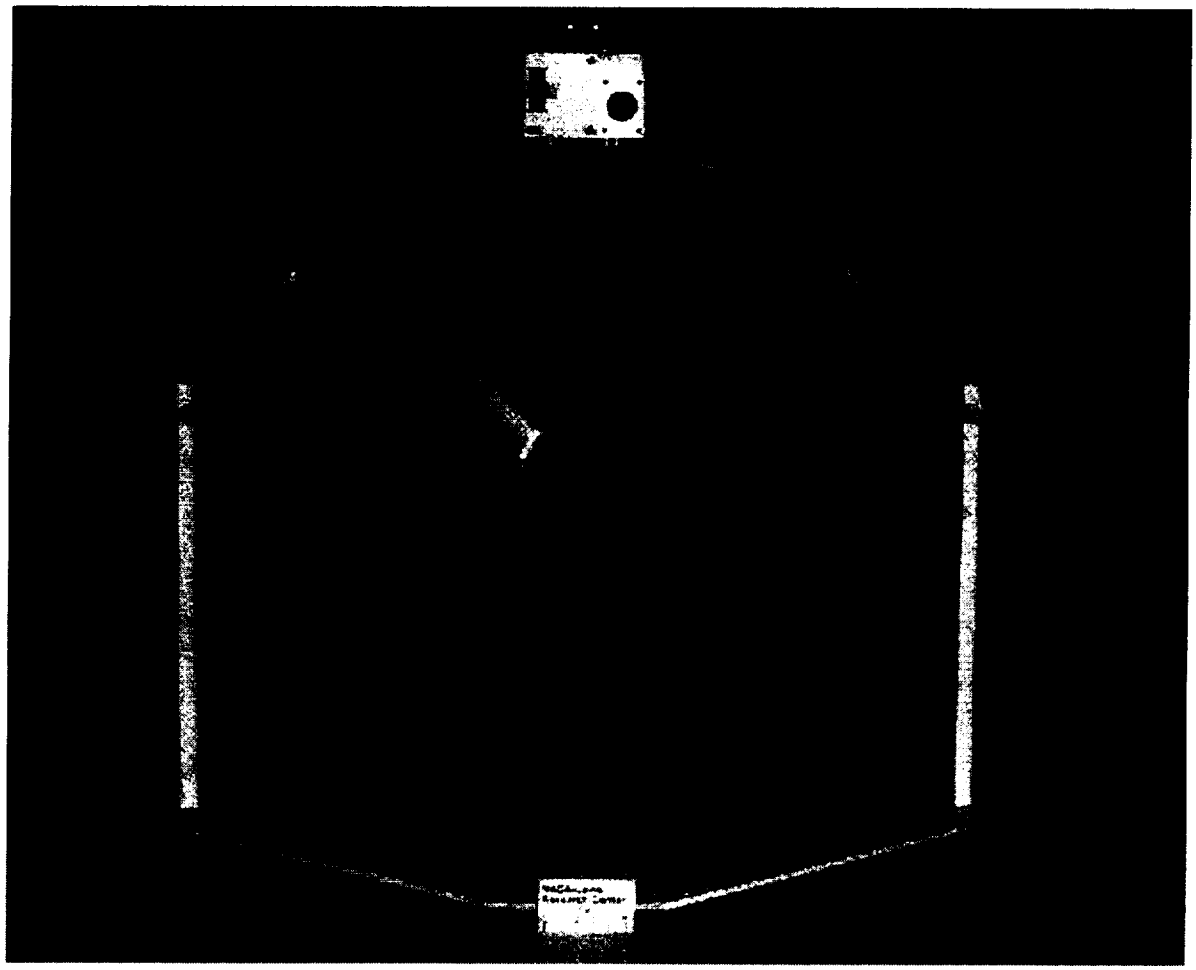

Figure 4. PHOTO OF THRUSTER

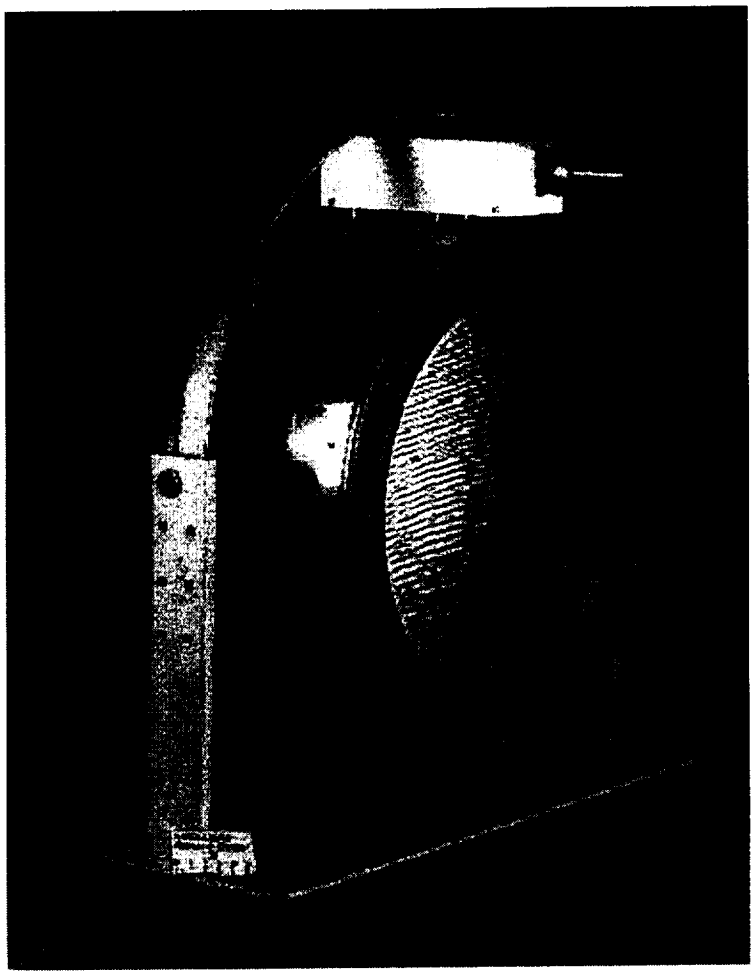

2.3 Key Delivery Dates

Event	Date
Contract Start	Sept 20, 1995
PDR	Jan 17-18, 1996
CDR	Oct 1-3, 1996
Deliver Pathfinder (PFT)	Sept 10, 1997
Deliver Flight Thruster (FT1)	Oct 28, 1997
Deliver PPU1	Oct 26, 1997
Deliver PPU2	Dec 19, 1997
Deliver DCIU1	Oct 26, 1997
Deliver DCIU2	Dec 19, 1997
Acceptance Testing of FT1 At NASA GRC	Nov '97 – Jun '98
PFT Reworked to become FT2	April '98
PPUs Thermal Upgrade	May – Jun '98
DS1 Launch	Oct 24, 1998

3.0 FLIGHT SYSTEM REQUIREMENTS

This section presents the thruster performance requirements as specified in the governing contract and the NSTAR Element Technical Requirements Document (ND-310, JPLD-13638)

3.1. The Thruster

3.1.1. Performance

The 30 cm NSTAR ion thruster is designed to operate over a large range of thrust levels as required for the intended deep space mission applications. The primary throttling performance requirements are shown in Table 1.

The typical Operating Parameter Set Points for these thrust levels are shown in Table 2. These set points were based on the NASA EMT performance data. The operating parameters for different thrust levels were selected in order to minimize the complexities of the PPU and DCIU. At each of the thrust levels, the xenon flows to the discharge cathode and neutralizer cathode were kept about the same to simplify the propellant feed system design. This resulted in only a small reduction in thruster efficiency.

The thruster is capable of operating through the entire range of thrust levels. The operating condition at each thrust level is controlled by the DCIU, which contains a 16 set-point parameter look up table. This table can be reprogrammed from Earth to accommodate changes in the mission profile.

The 30 cm thruster provides a total impulse of more than 2.7×10^6 Ns for input power level between 0.5 and 2.3 kW. The total xenon propellant throughput capability is greater than 83 kg at any combination of thrust levels. This is equivalent to continuous operation at an input power of 2.3 kW for more than 8000 hours.

The thruster is capable of completing more than 200 operating cycles.

Table 1. Thruster Throttling Performance Requirements

Power to thruster, kW	2.31	2.06	1.48	1.00	0.49
Maximum xenon mass flow, mg/s	2.86	2.65	1.86	1.51	1.02
Thrust, mN	92.0	83.0	58.0	40.0	19.5
Specific impulse, s	3280	3190	3180	2700	1950
Efficiency	0.64	0.63	0.61	0.53	0.38

Table 2. Thruster Parameter Set Points for Throttling

Power to thruster, kW	2.31	2.06	1.48	1.00	0.49
Beam power supply voltage, V	1110	1100	1100	1100	650
Accel voltage, V	180	180	180	150	150
Nominal beam current, A	1.76	1.58	1.09	0.72	0.50
Main plenum flow, sccm	23.5	21.3	14.3	9.0	6.0
Cathode flow, sccm	3.00	2.48	2.10	2.10	2.10
Neutralizer flow, sccm	3.00	2.48	2.10	2.10	2.10
Neutralizer keeper current, A	1.50	1.50	1.50	2.0	2.0
Maximum discharge voltage, V	28.0	28.0	28.0	29.0	30.0

Note: Cathode and Neutralizer flow rates were later modified to conform to the conditions of the 8000 hour life demonstration test at JPL. See section 8.

3.1.2. Mechanical

Thruster Mechanical Design Requirements

The discharge and neutralizer cathode assemblies, including the cathode insert and heater were to be identical to the NASA EMT designs. Except for minor changes, the ion optics assembly was to be identical to the NASA EMT. Additional requirements for the flight thruster design were the inclusion of cathode keeper electrodes in both the discharge and neutralizer cathode assemblies, wire mesh liner throughout the discharge chamber for spalled flake control, and low pressure propellant high voltage electrical isolators.

The flight thruster outline and mounting configuration, as shown in Fig 5. The main body of the thruster is approximately 41 cm. in diameter and 33 cm. long excluding the neutralizer assembly. The thruster is attached to the spacecraft gimbal assembly using three equally spaced mounting pads located at the outer diameter of the plasma shield. The mass of the ion thruster is 8.2 kg., excluding the electrical cable to the PPU.

Figure 5. NSTAR Thruster Outline and Mounting

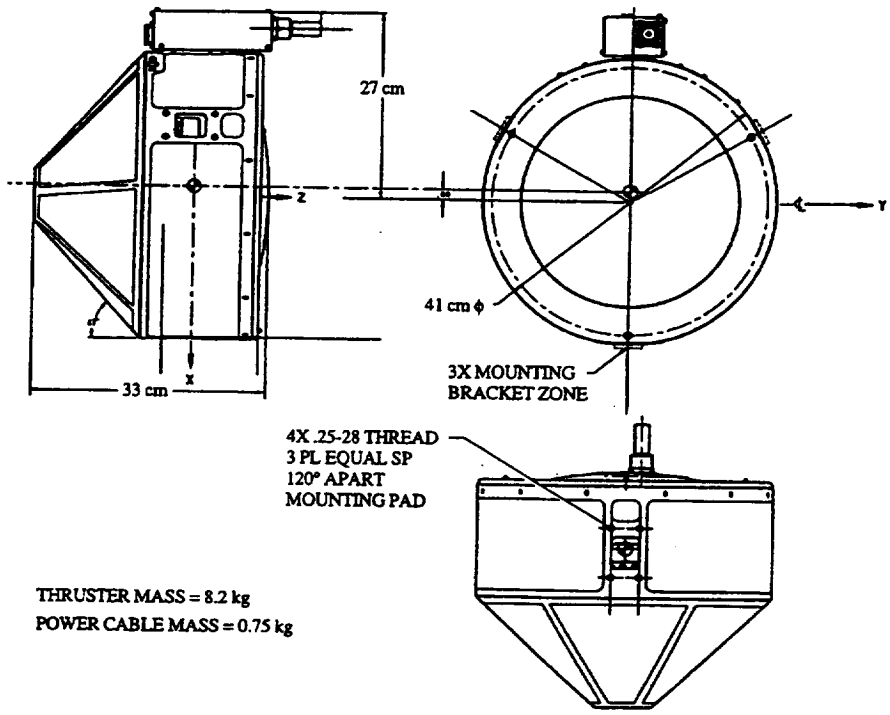

3.1.3. Environmental

The dynamic environmental requirements established for the NSTAR ion thruster were intended to envelope the characteristics of several launch vehicles including the Delta 7920. At the time of the initial design of the flight thruster, the structural characteristics of the DSI spacecraft and the gimbal assembly, which attaches the thruster to the spacecraft, were undefined. Specifications for the thruster random vibration and shock levels were selected based on typical component requirements for similar spacecraft. These are shown in Table 3. The design safety margins for the mechanical stresses within the thruster were also specified. This necessitated the development of a detailed computer structural model of the thruster using a Pro/MECHNICA finite element code to predict the resonance modes and stresses. Meeting the stress safety margins presented a significant challenge in the structural design of the thruster given the high levels of vibration and the low thruster mass requirements. Extensive vibration testing of a NASA EMT was also performed to validate the thruster structural model results.

The thruster is self cooled during operation. Due to the construction of thruster and the gimbal assembly, there is very little heat conduction in or out of the thruster. Radiation is the dominant cooling mechanism to minimize heat input to the DS1 spacecraft. To minimize heat input to the DS1 spacecraft, a heat shield covers much of the body of the thruster. As a result, internal thruster temperatures reach high levels during operation. When the thruster is off, radiation to deep space causes the temperatures to drop below -100 C. The mounting configuration of the NSTAR thruster in DS1 is shown in Figure 6.

At the start of the program, little was known of the internal operating temperatures of the thruster components under the various modes of operation. In order to evaluate the thermal design of the thruster and the effects of the DS1 spacecraft, NASA and JPL developed a detail thermal model of the thruster. The DS1 thermal interfaces were added as they were defined. This model was validated by means of several thermal vacuum tests at NASA using EMT and flight model thrusters.

Based on the results of the thermal modeling and test efforts, the thermal vacuum test requirements for the thruster were defined as shown in Figure 7. The specified temperatures are measured at the down-stream face of the thruster front mask, which covers the outer flange portion of the accelerator (negative) grid.

Table 3 - NSTAR Thruster Dynamic Structural Requirements

- Stress safety margins over yield ≥1.25
- Random vibration (with force limiting)

Conditions for All Axes	Frequency (Hz)	PSD Level (g^2/Hz)	Slope (dB/Oct)	Overall (g_{rms})	Duration (sec/axis)
Protoflight	20-50 50-500 500-2000	— 0.2 —	+6 — -6	13.0	60
Acceptance	20-50 50-500 500-2000	— 0.1 —	+6 — -6	9.2	60

- Shock analysis or test
- Shock response levele (Q = 10)

Frequency (Hz)	Acceptance (G PK)	Protoflight (G PK)
100 100-1500 1000	40 9.2 dB per Octave 2500	60 9.2 dB per Octave 3750

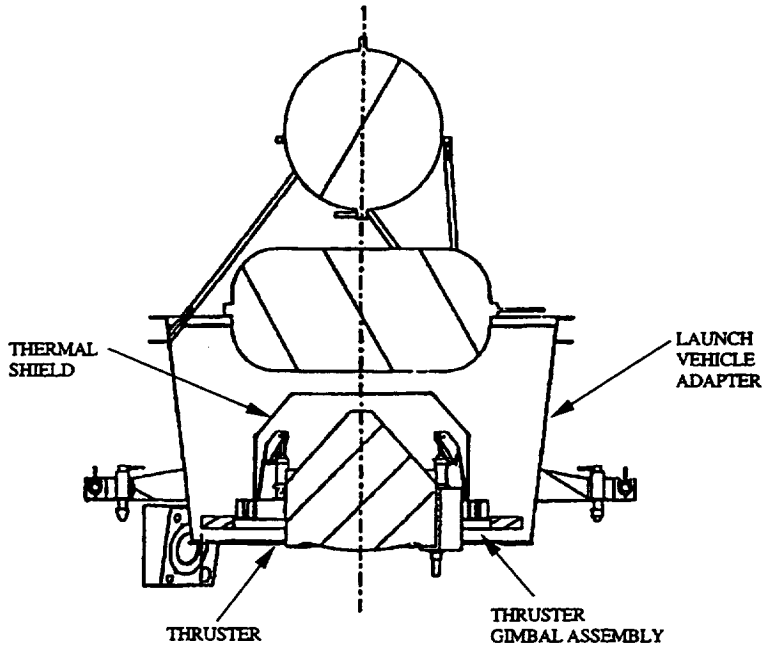

Figure 6. NSTAR Thruster DS1 Thermal Environment

Note: This is a functional layout of subassemblies and is not necessarily geometrically correct.

Component		Cold (°C)	Hot (°C)	Notes
Flight allowable	Operating	–93	+138	Temperatures at thruster mask. Thruster max temperatures are based on self heating of operating thrusters. Non-operating maximum temperatures will be less.
Flight allowable	Non-operating	–93	<+138	
Acceptance	Operating	–98	+143	
Acceptance	Non-operating/survival	–98	<+143	
Qualification	Operating	–109	+153	
Qualification	Non-operating/survival	–109	<+153	

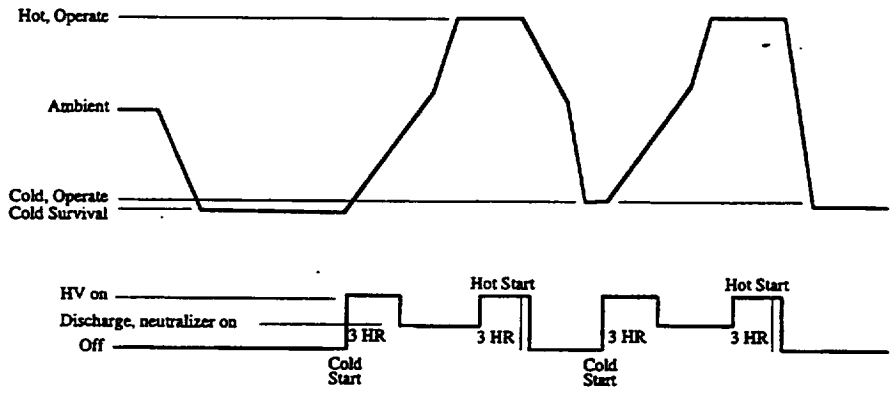

Figure 7. NSTAR Thruster Thermal Vacuum Test Requirements for DS1

3.2. The PPU

3.2.1. General Requirements, PPU

3.2.1.1. Component Description

The PPU is a separate box mounted to the spacecraft structure and is connected electrically by harnesses to the following (refer to block diagram):

1. Spacecraft +28 Vdc unregulated power from the Power Distribution Unit (PDU) in the spacecraft PPS for the PPU housekeeping power supply.
2. Spacecraft unregulated high-power (+80 to +160 Vdc) from solar arrays via the PDU to PPU converters for FT power.
3. DCIU and PPU microcontrollers MIL-STD-1553 interface for command and telemetry input/output.
4. PPU output power for the FT.

3.2.1.2. Recycle Logic

The PPU shall contain logic that detects and recovers from thruster short circuits and other anomalous events. The events, which shall cause a recycle and the recovery processes, are listed in a later section

3.2.1.3. Electromagnetic Interference (EMI) filters

EMI filters shall be installed on the input power busses to the PPU, which ensure compliance with MIL-STD-461C.

3.2.1.4. Power Converters

Power converters shall be included which convert spacecraft +80 to +160 Vdc bus power-to-power for the following.

1. Neutralizer cathode heater
2. Main cathode heater
3. Neutralizer
4. Discharge
5. Beam
6. Accelerator grid

HouseKeeping Power shall be derived from the spacecraft +28 ±6 Vdc bus.

3.2.1.5. Grid Clearing Circuit

The PPU shall contain switches that facilitate application of the discharge power supply to the ion optics to clear short circuits caused by flakes of sputtered material. (See Appendix 1.)

3.2.1.6. Thruster Selection Switches

Switches shall be provided which allow connection of two thrusters to the PPU. Power shall be supplied to the selected thruster via DCIU command.

3.2.1.7. Sensor and Telemetry Circuits

Power supply current and voltage sensors shall be included to measure the outputs of each of the above listed power converters in addition to the 80 - 160 V bus voltage and current. The outputs of these sensors shall be digitized within the PPU and passed to the DCIU in digital format.

3.2.2. Performance

3.2.2.1. Efficiency

The PPU minimum efficiency shall be as follows.

Table 4. PPU EFFICIENCY REQUIREMENTS

3.3.Output Power Level	3.4.Efficiency
2.3 kW	.90
0.5 kW	.84

3.2.2.2 Power Supplies

Power supply performance shall be as listed in section 5.5.6 for all thruster power converters. The housekeeping power supplies shall be designed as required to operate the PPU internally. Their individual requirements shall be determined by the contractor.

3.2.3 Design Resource Allocations

3.2.3.1 Mass

The PPU mass shall not exceed 12 kg including all mass contingencies. Micrometeorite shielding may require an additional 1.7 kg.

3.2.3.2 Envelope

The external dimensions of the PPU shall be as outlined in HED document B768329-500, Installation Control Drawing, Power Processing Unit (PPU). For additional details, refer to ND-312.

3.2.3.3 Power

Total PPU power consumption in the thruster power converters, excluding the housekeeping power supply, should not exceed 250 W at maximum 2.35 kW power output to the thruster.

3.2.4 Mechanical Design Requirements

3.2.4.2 Structural Design

The structural design of the PPU shall be consistent with requirements listed in the design resources section and shall ensure compliance with the New Millennium CVS (unless otherwise specifically stated elsewhere in this document).

3.2.4.3 Mechanical Interfaces

The PPU shall be mounted to the spacecraft via the baseplate. Bolt hole patterns and mounting torques shall be as listed in drawing B768329-500.

3.2.5 Electrical Design Requirements

3.2.5.1 DC Power

The PPU shall accept unfiltered power from two separate busses, an 80-160 Vdc unregulated high-power bus (for thruster power), and a 28 $\pm$ 6 Vdc unregulated low-voltage bus for control and housekeeping power. The maximum power input to the PPU shall not exceed 2.55 kW.

3.2.5.2 Undervoltage and Overvoltage Protection

The PPU shall not operate if the high-power bus input voltage falls below 75 VDC or exceeds 165 VDC. The PPU shall not operate with low-voltage bus input voltages below 23.5 V. The PPU shall not provide any power to the thruster if the low-voltage source is lost.

3.2.5.3 Power Interlock

28 V power shall not be applied to the PPU unless power has been applied to the DCIU. In the event of DCIU power loss, the 28 V power shall be removed from the PPU immediately.

3.2.5.4. Fusing

The PPU shall have no internal fuses on its input power buses.

3.2.5.5. Grounding and Isolation

3.2.5.5.1 Power Busses

The 28 V and 80 - 160 VDC power inputs shall be compatible with negative ground or floating power busses. For floating power busses, the potential between power bus returns and the spacecraft structural ground shall not exceed 5 VDC.

3.2.5.5.2 Internal Power Converters

All PPU power converter outputs to the thruster shall have line/load isolation. Transformer isolation capability shall exceed 2 kVdc.

3.2.5.6. Thruster Power Converters

The PPU shall convert spacecraft high-power bus input into independently controllable regulated dc power outputs for the ion thruster as follows:

Beam Power Supply

Output Voltage:	650 - 1100 VDC
Output Current:	0.5 - 1.8 ADC
Regulation Mode:	Constant Voltage
Ripple:	< 5 % of Setpoint, Regulated Parameter

Accelerator Power Supply

Output Voltage:	-150 to -180 VDC
Output Current:	0 - 0.02 ADC, 0.2 A surge for 100 ms
Regulation Mode:	Constant Voltage
Ripple:	< 5 % of Setpoint, Regulated Parameter

Discharge Power Supply

Output Voltage:	15 - 35 VDC
Output Current:	4 - 14 ADC
Regulation Mode:	Constant Current
Ripple:	< 5 % of Setpoint, Regulated Parameter

Discharge Pulse Igniter

Pulse Amplitude:	650 V peak
Pulse Duration:	10 μs
Rate of Rise:	150 V/μs
Repetition Rate:	10 Hz minimum

Neutralizer Power Supply

Output Voltage:	8 - 32 VDC
Output Current:	1 - 2 ADC
Regulation Mode:	Constant Current
Ripple:	< 5 % of Setpoint, Regulated Parameter

Neutralizer Pulse Igniter

Pulse Amplitude:	650 V peak
Pulse Duration:	10 μs
Rate of Rise:	150 V/μs
Repetition Rate:	10 Hz minimum

Discharge Cathode Heater Power Supply

Output Voltage:	3 - 12 VDC
Output Current:	3.5 - 8.5 ADC
Regulation Mode:	Constant Current
Ripple:	< 5 % of Setpoint, Regulated Parameter

Neutralizer Cathode Heater Power Supply

Output Voltage:	3 - 12 VDC
Output Current:	3.5 - 8.5 ADC
Regulation Mode:	Constant Current
Ripple:	< 5 % of Setpoint, Regulated Parameter

3.2.5.7 Line and Load Regulation

The output line/load regulation for the neutralizer and discharge power supplies shall be better than 5%.

3.2.5.8 Engineering Telemetry

PPU telemetry shall be as listed in the Command and Telemetry section (Section 7).

3.2.5.9 Electromagnetic Compatibility (EMC)

The PPU shall be designed using MIL-STD-461C for conducted and radiated EMI as a baseline. The PPU shall not generate electromagnetic interference that would adversely affect the spacecraft; it's own functioning, other components, or the safety and operation of the launch vehicle and the launch site. Components shall not be susceptible to emissions that could adversely affect safety and performance. This applies whether emissions are self generated or emanate from other sources, whether intentional or unintentional. Applicable military standards for test and compliance are MIL-STD-461C, 462, 461C Part 3 class A2a.

3.2.5.10 Connectors, Receptacles, and Cabling

The PPU shall provide four connectors or terminal blocks, one for input power, two for output power (one for each thruster), and one for the RS-422 DCIU data interface. Connector types and pin-outs are listed in ND-312, Thruster Element ICD.

3.2.6 Thermal Design Requirements

3.2.6.1 General

The PPU supplier shall ensure that flight hardware meets spacecraft requirements for thermal isolation and waste heat rejection. The thermal interface design shall be determined jointly between the spacecraft and PPU contractors. Except for its baseplate, the PPU shall be thermally isolated from surrounding spacecraft elements.

3.2.6.2 Heat Rejection

The PPU shall reject all internally generated waste heat through the baseplate and/or top cover. The heat split shall be modifiable by design and shall be configurable as listed in the following table:

Table 5. Thermal Design Requirements/Heat Rejection.

Baseplate Rejection	Cover Rejection
100 %	0 %
50 %	50 %
0 %	100 %

The baseplate shall allow attachment to a waste heat dissipation element provided by the host spacecraft and designed to control the baseplate temperature within the following flight allowable ranges:

1. PPU Operating: -5° C to +50° C.
2. PPU Non-operating: –25° C to +55° C.

If necessary, the spacecraft shall maintain the PPU baseplate non-operating temperature range by supplying power to survival heaters. The temperature range shall be regulated by sensor signals to thermal control circuits furnished by the spacecraft. The spacecraft shall ensure that the baseplate is within the operating range prior to applying power to the PPU.

3.2.6.3 Junction Temperature

The Junction Temperature rise in any PPU electronics component junction shall not exceed 75°C above the PPU baseplate operating temperature range.

3.2.7 Environmental Design Requirements

3.2.7.1 Launch Environment Requirements

Launch environment design requirements shall be as listed in the New Millennium DS1 Component Verification Specification (unless otherwise stated in this document).

3.2.7.2 Radiation Environment

3.2.7.2.1 Total Ionizing Dose (TID)

All PPU flight parts shall operate within specifications following exposure to a 100 kRad (Si) Total Ionizing Dose (TID) at box surface. The assumed TID environment shall include all space radiation components. The total shielded dose limits shall apply to the radiation design margins specified below.

3.2.7.2.2 Radiation Design Margin (RDM)

The Radiation Design Margin (RDM) shall be at least two (2) for the TID received at the end of the mission. If spot shielding is used, the RDM shall be three (3). The RDM is defined as the ratio of the part dose capability to the localized radiation environment for the part.

3.2.7.2.3 Single-Event Effects (SEE)

A Single-Event Upset (SEU) shall not cause the PPU to be stressed or permanently damaged. Devices in the PPU susceptible to Single-Event Latchup (SEL) shall recover without damage at worst-case rated voltages and maximum rated temperatures. Devices with power FETs operated in the off mode shall

not be susceptible to permanent failure from particle-induced Single-Event Burnout (SEB) and Single-Event Gate Rupture (SEGR).

3.2.7.2.4 Electrostatic Discharge (ESD)

The flight PPU shall operate as specified in the Earth orbital environment without electrostatic discharge (ESD). Surface and internal ESD events shall not degrade PPU performance and reliability.

3.2.7.3 Altitude

The PPU shall operate at sea level or at an altitude in excess of 100 km. No requirement to operate at intermediate altitudes or pressures exists.

3.2.8 Life and Reliability

3.2.8.1 Post-launch Operational Lifetime

The PPU shall meet performance requirements for a period of not less than two (2) years of continuous full power post-launch operation, after being subjected to pre-launch operation and ground storage. As a goal, the PPU design shall not preclude three (3) years of continuous post-launch operation.

3.2.8.2 Pre-launch Operation

All flight PPU electronic assemblies shall undergo burn-in for a minimum of 168 hours at the unit level. The PPU design shall also allow the NSTAR project and the spacecraft contractor to perform electronics testing on the PPU up to a combined total of 2,000 hours before launch.

3.2.8.3 Electronics On/Off and Thermal Cycle Fatigue

PPU electronics on/off and solder joint thermal cycling capability shall be greater than or equal to twice the combined cycles expected during pre-launch and post-launch operations. The number of expected cycles is 200.

3.2.8.4 Ground Storage Life

The PPU flight hardware shall be capable of up to five (5) years of ground storage.

3.2.8.5 Reliability Design

The baseline PPU design shall be single string. Single-Point Failures (SPFs) are permitted, except for personnel and launch vehicle safety items. PPU parts and functions whose failure may result in loss of control or commandability of the spacecraft shall include mitigating reliability design features.

3.2.8.6 Redundancy

Redundant elements and components shall be used only if significantly improved reliability is required and their use is cost effective.

3.2.8.7 PPU Operational Reliability

PPU reliability shall conform to the reliability requirements as listed in ND-12, Project Policies and Constraints.

3.2.9 Fault Protection

3.2.9.1 Input Bus Failures

The PPU shall survive and recover to a known and verifiable state (by telemetry) from input power bus short circuits or other faults, which result in bus voltage failure and their removal.

3.2.9.2 Output Short Circuits

All power converters shall survive and recover from output short circuit faults and survive arbitrary short circuits that connect any two PPU outputs. Pin-to-pin or pin to structure short circuits in direct access connectors shall not damage the PPU, other NSTAR assemblies or the spacecraft.

3.2.9.3 Recycle Conditions

The following conditions shall cause a recycle. The recycle procedure is outlined in a later section.

3.2.9.3.1 High Beam Current

If the beam current exceeds 3.0 A, a recycle shall be initiated. High beam current results from any of the following conditions. These faults shall not cause damage to the PPU.

1. Screen Grid to Accelerator Grid Short
2. Screen Grid to Ground (Structure) Short
3. Accelerator Grid to Structure Short

3.2.9.3.2 Discharge Extinction

If the discharge current falls below 1.5 A, a recycle shall be initiated.

3.2.9.3.3 Neutralizer Extinction

If the neutralizer keeper current falls below 0.5 A, a recycle shall be initiated.

3.2.9.4 Recycle Procedure

The recycle procedure shall be executed as follows. The total time for recycle recovery shall be minimized to the greatest extent possible. It is anticipated that PPU/Thruster integration testing will be required to define the timing of the recycle sequence.

1. **High Voltage Off**
   The beam and accelerator power supplies shall be immediately turned off upon the detection of a fault. The energy in the output filters of the power supplies shall be allowed to discharge through the fault. A "crowbar" circuit is not required. Removal of the high voltage shall disable the throttling algorithm as listed in the Throttling section.
2. **Discharge Cutback**
   The discharge current shall be cut back to 4.0 A upon the detection of the fault. The ramp down rate shall be such that no undershoot of the discharge power supply occurs, and shall be completed within one second.
3. **High Voltage On**
   If and only if the fault which has caused the recycle clears, and the discharge current is at the cutback value, the high voltage shall be reapplied. The beam and accelerator power supplies shall be turned on simultaneously, with timing as listed in the Thruster Ignition section. In the cases of neutralizer or discharge extinction, the PPU controller shall take the necessary corrective actions as listed in the Fault Recovery section prior to the application of the high voltage.

4. **Discharge Current Ramp Up**
   Following the application of the high voltage to the thruster, the discharge current shall be returned its nominal level prior to the recycle. The ramp up time shall be such that the increase in discharge current will not precipitate another recycle.

3.2.10 Ground Support Equipment (GSE)

The following GSE are required for stand-alone PPU operation.

3.2.10.1 Housekeeping Power Supply

A laboratory grade 28 V ±6 V, 1 A DC power supply shall be required to provide housekeeping power to the PPU during ground operations. Housekeeping power shall be applied prior to the application of the main power supply.

3.2.10.2 Main Power Supply

A laboratory grade 80 - 160 V, 35 A DC power supply shall be required to provide power for the thruster main power converters.

3.2.10.3 DCIU Simulator

An IBM compatible PC with an RS-422 interface board, running the control program entitled "PPU Test" is required to provide a command and telemetry interface with the PPU.

3.2.10.4 Thruster Simulator

A resistive load shall be used to simulate the thruster. The resistive load shall provide the following loads to the thruster. Variable Resistors shall be capable of operating at a minimum of five points within the specified range. Continuous variability is not required.

1. Neutralizer Heater

Resistor Type:	Variable
Resistance Range:	0.3-3.2 ohms
Power:	75 W
Resistance Control:	Manual

2. Discharge Heater

Resistor Type:	Variable
Resistance Range:	0.3-3.2 ohms
Power:	75 W
Resistance Control:	Manual

3. Neutralizer

Resistor Type:	Variable
Resistance Range:	4-32 ohms
Power:	64 W
Resistance Control:	Manual

4. Discharge

Resistor Type:	Variable
Resistance Range:	1-8.8 ohms
Power:	500 W
Resistance Control:	Manual

5. Accelerator

Resistor Type:	Variable
Resistance Range:	7.5-200 kohms
Power:	5 W
Resistance Control:	Manual

6. Beam

Resistor Type:	Active Load
Resistance Range:	350-2200 ohms
Power:	2 kW
Resistance Control:	Closed Loop Proportional

3.2.10.5 Beam Load Closed Loop

The resistance of the beam load shall be controlled proportionally by the discharge current. A discharge current of 4.0 A shall result in a beam current of 0.5 A. A discharge current of 14 A or higher shall result in a beam current of 1.75 A. The control law is thus:

$$Ibeam = Idischarge/8.0$$

The 3dB bandwidth of the control loop shall be at least 500 Hz. In the event of zero discharge current, the beam load shall be 2200 ohms.

3.2.10.6 Recycle Simulation

The thruster simulator shall simulate the following short circuits in response to front panel push-button commands.

1. Accelerator Grid to Screen Grid Short
2. Accelerator Grid to Ground Short
3. Anode to Ground Short

The thruster simulator shall also allow for the "hot" interruption of current in the discharge and neutralizer loads in response to front panel commands.

3.2.10.7 Cooling

All PPU GSE shall be forced air cooled if cooling is required.

3.2.10.8 Cabling

The following cables are required for PPU GSE. AC power cables are omitted from these descriptions. AC power cables shall conform to all standards in the National Electric Code and applicable range safety documents.

1. PPU to thruster simulator
2. DCIU simulator to PPU data cable
3. PPU input power cable

3.2.10.9. Calibration

PPU telemetry sensors shall be calibrated to ensure that the accuracy of the telemetered data is within the specifications listed in the command and telemetry list in Section 7, Software Requirements.

3.2.10.10. Telemetry Sensors

Calibration curves shall be generated by the PPU manufacturer, which relate the digital telemetry output of the microcontroller with the engineering unit values of the telemetry parameters. These calibration curves shall have an accuracy of better than ± 2% of the measured value.

3.3 The DCIU

3.3.1 General Requirements, DCIU

3.3.1.1 Subsystem Description

The DCIU is a separate box mounted to the host spacecraft structure and is connected electrically by separate harnesses to the following (Figures 21 and 22):

1. Spacecraft +28 Vdc power from the PDU in the spacecraft Power/Pyrotechnic Subsystem (PPS).
2. Spacecraft Command and Data Subsystem (CDS).
3. NSTAR PPU microcontroller (MIL-STD-1533B interface).
4. XFS valve drives.
5. XFS engineering data sensors.

3.3.1.2 EMI Filter

The EMI filter shall ensure compatibility with MIL-STD-461C on the +28 Vdc power bus with regard to conducted and radiated EMI.

3.3.1.3 Command & Telemetry Interface

The DCIU shall receive commands from and transmit telemetry to the spacecraft via a MIL-STD-1553B interface.

3.3.1.4 Housekeeping Power Supply

The housekeeping power supply shall draw power from the 28 VDC bus to power the internal DCIU circuitry.

3.3.1.5 Microcontroller

The DCIU microcontroller shall verify, decode and process commands from and transmit telemetry data to the Command & Telemetry Interface, execute stored

operating sequences in response to ground commands, control PPU and XFS transition to the commanded operating mode and state, control XFS solenoid and latch valve drivers, regulate pressures in the Xenon Plenum Tanks to one of sixteen (16) stored set points, receive, store and process PPU telemetry data, receive, store and process XFS telemetry from sensor and Telemetry Signal Conditioning Circuits, and execute safing commands in response to autonomous fault protection or ground commands.

3.3.1.6 Sensor and Telemetry Signal Conditioning Circuits

Pressure and temperature engineering sensors in the XFS will provide analog input to the DCIU. The DCIU will process and digitize this analog output data and relay it to the spacecraft.

3.3.1.7 XFS Valve Drivers

The DCIU will open/close two (2) dual solenoid valves sequentially and five (5) latch valves in response to commands from the DCIU microcontroller or the spacecraft. Valve actuation shall be electrically isolated from the DCIU valve control circuits.

3.3.2 Performance

3.3.2.1 Processor Utilization

The DCIU shall perform all control functions as listed in the software requirements. A processor time margin of 25 % shall exist in the delivered unit. Processor time margin is defined as time when the processor is idling or not executing critical control software, i.e., waiting for a new command.

3.3.2.2 Memory Utilization

The final delivered flight software shall reside completely within 75 % of the total non-volatile memory integrated to the processor.

3.3.2.3 Digitization Accuracy

Digitization accuracy shall be ± 2 LSB, or better.

3.3.3 Design Resource Allocations

3.3.3.1 Mass

The DCIU mass shall not exceed 2 kg.

3.3.3.2 Envelope

The external dimensions of the DCIU box should be less than 30 cm x 15 cm x 10 cm, including electrical connectors but excluding thermal insulation and mounting brackets.

3.3.3.3 Power

The DCIU shall consume less than 30 W internally.

3.3.4 Mechanical Design Requirements

3.3.4.1 Structural Design

The structural design of the DCIU shall ensure compliance with all applicable requirements in the New Millennium CVS (unless otherwise specifically stated elsewhere in this document).

3.3.4.2 Mechanical Interfaces

The DCIU shall be mounted to the spacecraft via its baseplate. The mounting hole pattern and other details can be found in ND-312.

3.3.5 Electrical Design Requirements

3.3.5.1 DC Power

The DCIU shall draw all power from the 28 V bus. The DCIU shall have no fusing on the spacecraft +28 Vdc input power bus circuit. The spacecraft will provide fuses.

3.3.5.2 Grounding and Isolation

The DCIU electrical design shall meet host spacecraft grounding, isolation and electromagnetic compatibility design and testing requirements (to be specified in ICD ND-510).

3.3.5.3 MIL-STD-1553 Interface

The DCIU shall provide a MIL-STD 1553B compatible data interface with the host spacecraft. Detailed interface requirements can be found in ND-312, Thruster/PPU Interface Control Document, ND-510, NSTAR Thruster Element Interface Control Document, and in the Software Requirements Section herein.

3.3.5.4 EMC and EMI

The DCIU shall be compatible with MIL-STD-461C.

3.3.5.5 Connectors, Receptacles, and Cabling

All DCIU connectors shall be located on one face of the DCIU enclosure. Connectors shall be clearly labeled. Connector types, exact location, and pin-out can be found in ND-312.

3.3.6 Thermal Design Requirements

3.3.6.1 General

The spacecraft shall provide thermal control elements for maintaining specified DCIU operating and non-operating temperature ranges at the DCIU mounts, if necessary by supplying power to survival heaters. Heater power shall be regulated by temperature sensor signals to thermal control circuits furnished by the spacecraft.

3.3.6.2 Temperature Limits

The DCIU operating and non-operating flight allowable temperature ranges at the mounts to the spacecraft shall be:

DCIU operating	-15°C to +50°C
DCIU non-operating	-25°C to +55°C

3.3.6.3 Junction Temperatures

The temperature rise in any DCIU electronics component junction shall not exceed 75°C above the operating temperature range of the DCIU mounts.

3.3.7 Environmental Design Requirements

3.3.7.1 Launch Environment Requirements

The DCIU shall be designed to ensure compliance with the Launch Environment Requirements in the New Millennium Component and Spacecraft Verification Specifications, 1069-EW-Q00108, Rev B, April 1997.

3.3.7.2. Radiation Environment Requirements

3.2.7.2.1 Total Ionizing Dose (TID)

All PPU flight parts shall operate within specifications following exposure to a 100 kRad (Si) Total Ionizing Dose (TID) at box surface. The assumed TID environment shall include all space radiation components. The total shielded dose limits shall apply to the radiation design margins specified below.

3.2.7.2.2 Radiation Design Margin (RDM)

The Radiation Design Margin (RDM) shall be at least two (2) for the TID received at the end of the mission. If spot shielding is used, the RDM shall be three (3). The RDM is defined as the ratio of the part dose capability to the localized radiation environment for the part.

3.2.7.2.3 Single-Event Effects (SEE)

A Single-Event Upset (SEU) shall not cause the DCIU to be stressed or permanently damaged. Devices in the DCIU susceptible to Single-Event Latchup (SEL) shall recover without damage at worst-case rated voltages and maximum rated temperatures. Devices with power FETs operated in the off mode shall not be susceptible to permanent failure from particle-induced Single-Event Burnout (SEB) and Single-Event Gate Rupture (SEGR).

3.2.7.2.4 Electrostatic Discharge (ESD)

The flight DCIU shall operate as specified in the Earth orbital environment without electrostatic discharge (ESD). Surface and internal ESD events shall not degrade DCIU performance and reliability.

3.3.8. Life and Reliability

The lifetime and reliability requirements for the DCIU are the same as for the NSTAR PPU, except the DCIU design lifetime shall not be less than three (3) years of continuous post launch operation, after being subjected to 2000 hours of pre-launch operation and up to 5 years of ground storage.

3.3.9 Fault Protection

3.3.9.1 General

The DCIU shall process telemetry from the detection of faults, and command the safing of the ion propulsion subsystem in response to anomalous conditions, such as software errors, EMI interference, single event effects, loss of command and telemetry, anomalous hardware conditions, or electrical performance deficiencies in the PPU. The objective shall be to supplement fault protection functions performed by the spacecraft. Thruster fault detection and recovery shall be as listed in the software requirements.

3.3.9.2 Ground Test

To the extent practical, the fault protection design shall allow for testing on the ground without potential for damage to the NSTAR flight system.

3.3.9.3 Input Bus Failure

The DCIU shall survive and recover to a known and verifiable state from spacecraft +28 Vdc input power bus short circuits and their removal.

3.3.9.4 Output Short Circuit

DCIU housekeeping power supplies shall survive and recover from output short circuit faults and survive arbitrary short circuits, which connect any two outputs.

3.3.10 GSE Required

The following GSE are required for stand-alone DCIU operation.

3.3.10.1. Spacecraft Computer Simulator

An IBM compatible PC with a 1553B interface board, running the control program entitled "DCIU Test" is required to provide a command and telemetry interface with the DCIU.

3.3.10.2. XFS Simulator

A load box to simulate the XFS is required.

3.3.10.3. PPU Simulator

A load box to simulate the PPU is required.

3.3.10.4. Housekeeping Power Supply

A laboratory grade 28 V ±6 V, 1 A DC power supply shall be required to provide housekeeping power to the PPU during ground operations. Housekeeping power shall be applied prior to the application of the main power supply.

3.4. System Interfaces

The-NSTAR TE mechanical configurations and system interfaces are defined in HED Drawings CDB768329 (4 sheets). The Thruster has three Xenon propellant input lines for the discharge cathode, discharge chamber plenum and neutralizer. Each of the propellant lines is a stainless steel tube with a resistoflex male connector. The propellant lines are located near the neutralizer with the connectors hard mounted to the thruster.

The thruster is capable of being mounted on a spacecraft gimbal assembly so that the actual thrust vector is aligned within an 18 mrad tolerance (shims may be used at the gimbal interface).

The electrical inputs to the thruster are all provided through an integral cable harness with two high voltage connectors.

The actual masses of the thruster, PPU, DCIU and cable harness are shown in Table 6.

Table 6. Masses of NSTAR Thruster Element DS1 Flight Components

Component	Mass (kg)
DS1 Flight Thruster (FT1)	8.21
Flight Cable, Power, PPU/Thruster	1.72**
DS1 Flight PPU (PPU #1)	14.50*
DS1 Flight DCIU (DCIU #2)	2.51

* Includes 1.7 kg for micrometeoroid shielding.

** PPU portion of cable weighs 0.95 kg; Thruster portion weighs 0.77 kg.

4.0 FLIGHT SYSTEM DESCRIPTION

4.1 The Thruster

Flight Thruster Design Description

The baseline electrical design for the NSTAR flight ion thruster was the NASA Engineering Model 1b (EMT1b) thruster design that resulted from initial performance and wear test program. The development of the EM thruster is described in previous papers.

The EMTs were developed to implement the conical discharge chamber and box-beam construction concepts (seen in Figure 9), and to optimize thruster performance and demonstrate life. Flight thermal and structural requirements were not addressed.

The NSTAR 30 cm thruster is comprised of four major subassemblies: the discharge chamber assembly, the discharge hollow cathode-keeper assembly, the neutralizer hollow cathode-keeper assembly, and the ion optics assembly. The schematic for the flight thruster is shown in Figure 8. The ion optics assembly is comprised of a screen grid operating at the discharge cathode potential and an accelerator grid at -180 V for full power operation. The discharge chamber operates at voltages up to 1100 V. The thruster body, except for the ion optics assembly, is enclosed in the plasma screen, which is at spacecraft ground.

The discharge chamber assembly is the main structural element of the NSTAR thruster. All of the other thruster components are mounted to the chamber. The up-stream end is a conical configuration to reduce overall thruster mass. A detailed cross section of the flight thruster is shown in Figure 9.

The discharge chamber of the early NASA EMTs was fabricated of 0.79 millimeters thick spin-formed aluminum except for the down-stream cylindrical section that supports the ion optics assembly, which was made of titanium. The EMT4 had an anode structure primarily fabricated of titanium. See IEPC Paper 97-051, August 1997 for a general description of the EMT designs.

The discharge chamber of the flight model thruster is fabricated entirely of titanium. This design change reduced the stress levels due to flight vibration and shock in the regions where the discharge

cathode and the cathode magnet assemblies are mounted onto the cone end of the chamber. The all titanium discharge chamber also eliminated thermal distortion that was observed on the EMTs at the interface where the aluminum and titanium chamber parts are riveted together. The higher strength of titanium allowed the thickness of the chamber to be reduced to 0.51 mm., so that there was no increase in the chamber mass. After spinning and stress relieving, the discharge chamber parts were finished machined to achieve precise interface alignment and ease of assembly. The parts were cleaned and grit blasted to enhance thermal emmissivity. The flight thruster discharge chamber is assembled using rivets, similar to the NASA EMTs.

The entire inside surface of the flight thruster discharge chamber is covered with a stainless steel fine mesh screen material to capture and prevent spalling of ion sputtered grid material. The liner was comprised of wire mesh diffusion bonded to 0.09 mm stainless steel sheet. This liner was fabricated using flat pattern cutouts of the fine mesh which were riveted and resistance spot welded to the inner chamber surfaces. Pull tests were conducted on sample assemblies to develop and qualify the spot weld process. The fine mesh liner is also used to fasten the propellant feed line plenum into the down-stream end of the discharge chamber. Lining the entire inside surface of the chamber with fine mesh provides the maximum containment of sputtered material throughout the operating life of the thruster.

The magnetic circuit for the NSTAR thruster is a ring-cusp design, which does not utilize a soft iron flux return path. It is essentially identical to the EMT design. Three samarium-cobalt magnet rings are used which have alternating polarities, one in the region of the discharge cathode, one at the discharge chamber conic-cylinder intersection, and one at the ion optics end. The magnets are of samarium cobalt that is temperature stabilized to 350 degrees C. Thermal tests at GRC on these magnets indicated less than a 12% irreversible drop in magnetic field when exposed to 350°C for 2200 hours. The magnet temperatures are estimated to be less than 310°C in the worst case thermal environment of the DS1 mission. The magnet retainers for the flight thruster, which are an integral part of the discharge chamber assembly are also made of titanium. Lightening holes were incorporated in the retainer designs, which also improved the radiation cooling of the magnets.

The EM thruster is supported by means of two aluminum gimbal mounting pads, 180 degrees apart that are fastened to the outer diameter of the discharge chamber. Alumina and Vespel insulators are used between the mounting pads and the chamber to provide the voltage standoff.

The flight thruster design uses three gimbal mounting pads, 120 degrees apart, to support the thruster. The use of three mounting pads significantly increases the thruster stiffness and reduces the vibration stresses during spacecraft launch.

The gimbal mounting pads for the flight thruster are made of a high strength titanium alloy (6A1-4V) in order to minimize mass and meet the stress safety margin requirements at the 210 degrees C mounting pad operating temperatures predicted. These high temperatures at the mounting pads are the result of the heat shield that encloses the thruster body in the DS1 spacecraft and the low heat conduction through the gimbal assembly.

The mounting pad insulators for the flight thruster are made of alumina ceramic and Vespel rather than the all-Vespel insulators that were used on the EMTs. The alumina insulators are held in compression to withstand the launch vibration stresses and the large operating temperature cycles

without cracking or creeping. The gimbal pad insulators are enclosed by overlapping sputter shields to prevent electrical leakage during prolonged thruster operation. The neutralizer assembly is attached to the discharge chamber using a similar mounting pad and insulator design.

The ion optics assembly for the NSTAR flight thruster is identical to the NASA EMT2 that was used for the 8000 hour wear test. A photograph of the flight thruster ion optics assembly is shown in Figure 10.

This ion optics assembly uses a domed two-grid design. The screen grid is 0.38 mm thick molybdenum with 1.91 mm diameter apertures and is electrically connected to the discharge cathode. The accelerator grid is 0.51 mm thick molybdenum with 1.14 mm diameter apertures. The grids are fabricated by hydroforming flat sheets, which have been coated with the appropriate photoresist pattern followed by photoetching. Selective grit blasting of the optics assembly components is performed to improve the adherence of sputtered grid material. The outer flanges of the finished grids are attached to molybdenum stiffener rings using specially modified rivets. These processes are very robust and produced grids of excellent quality. The resulting optics assemblies achieved the required alignment without difficulty. The ion extraction performance of the flight thruster optics assemblies also closely matched the NASA EMT performance.

The flight thruster grids are supported by a precision-machined titanium alloy ring. Alumina insulators with overlapping sputter shields are used to mount the grids and the ring to the discharge chamber.

The hollow cathode and heater designs and assembly processes for the flight thruster discharge cathode and neutralizer assemblies were derived from the Plasma Contactor Development Program for the International Space Station. The electrical design, heater and cathode insert designs were retained from the NASA EMTs so as to preserved the validity of the EMT2 wear tests and the extensive testing performed on the Plasma Contactor. The discharge and neutralizer cathode designs are nearly identical, except for differences in the cathode and keeper orifice configurations. However, changes were made to improve the structural design and assembly processes. This represents a significant change from EMT design where the discharge cathode keeper was a separate assembly supported by the discharge chamber. Figure 11 shows a cross-section of the hollow cathode and keeper assembly for the neutralizer.

The cathode assembly is comprised of a cathode support tube brazed to an insulator. The cathode orifice plate is welded to the end of the support tube. The cathode electron emitter (insert) is contained within the support tube. The coaxial swaged heater is positioned directly over the cathode insert on the support tube outer diameter and brazed to the insulator. The cathode keeper assembly is then welded to a flanged brazed to the outer diameter of the insulator. Assembly tooling is used to achieve the required spacing and concentricity. The low voltage propellant insulator is welded to the end of the support tube to complete the assembly.

An exploded view of the final assembly of the NSTAR flight thruster is shown in Figure 12.

The discharge cathode assembly is mounted at the conical end of the discharge chamber. The design allows accurate positioning of the cathode orifice within the magnetic field. It also permits

replacement of the discharge cathode assembly. The electrical and propellant line connections to the discharge cathode are contained within a lightweight cylindrical terminal housing.

The neutralizer cathode assembly is mounted in a rectangular housing which also serves as a junction box for the thruster electrical connections. The electrical power cable and neutralizer propellant feed line also attach to this housing.

The high voltage propellant isolators for the discharge cathode and chamber plenum are mounted to the neutralizer mounting pad inside the plasma screen.

Resistoflex gas fittings are used for the connections to spacecraft propellant lines.

The body of the thruster is enclosed in the plasma shield. This is a lightweight cover fabricated of photoetched stainless steel that is 0.25 mm thick. The plasma screen design prevents electrons from entering the thruster and allows radiation heat transfer out of the thruster. At the ion optics end of the thruster, the front mask is used to provide the spacecraft ground surface. A thermal sensor is mounted directly on the face of the front mask to monitor thruster temperatures during flight acceptance testing and the DS1 mission.

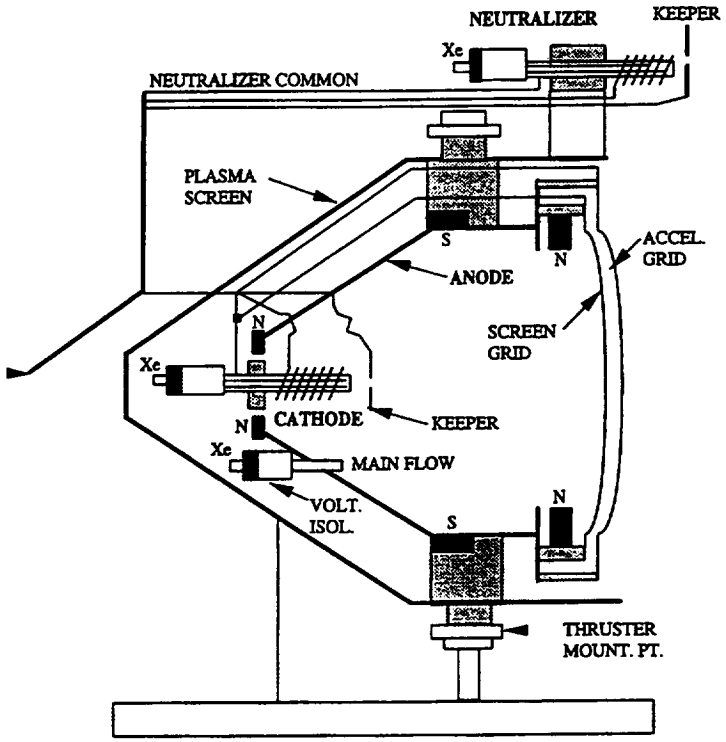

Figure 8. Schematic of the NSTAR Ion Thruster

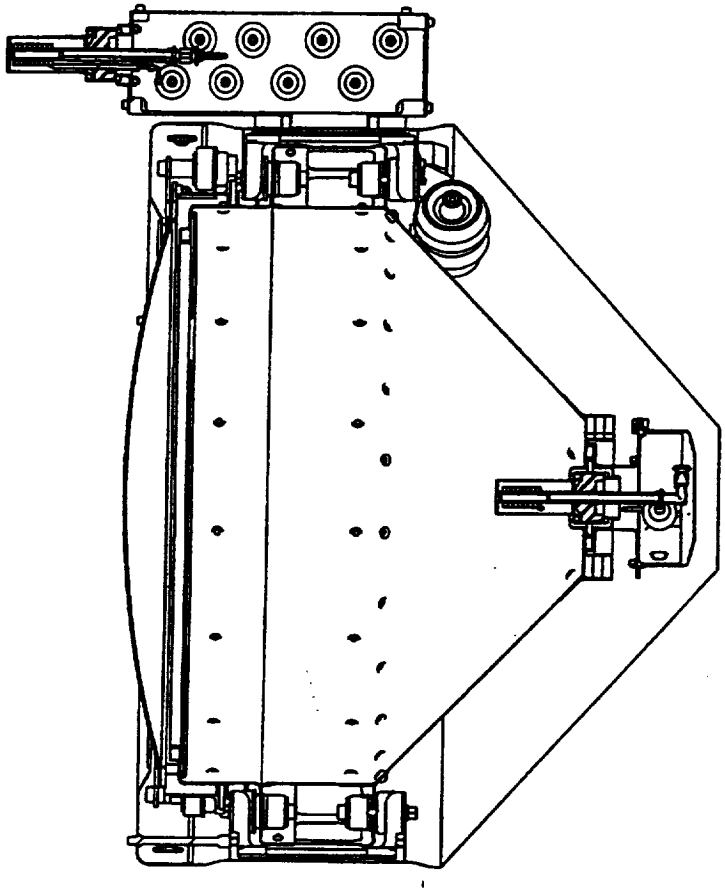

Figure 9. Cross Section of the NSTAR Flight Thruster

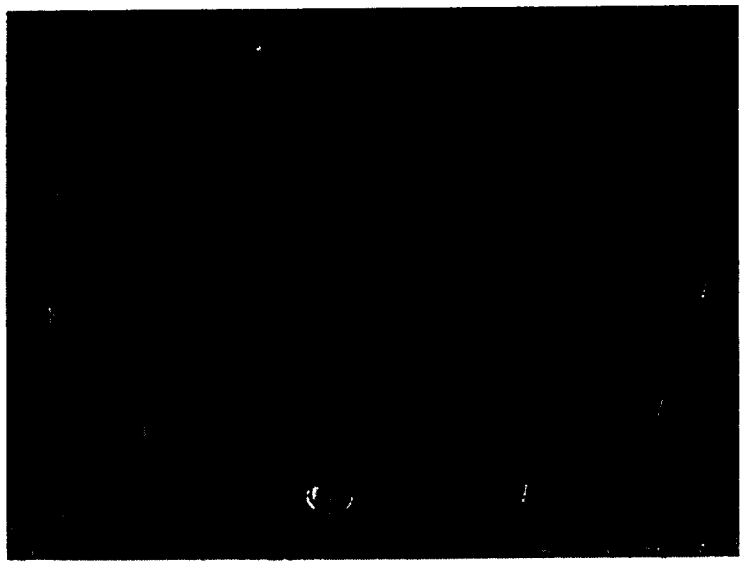

Figure 10. Flight Thruster Ion Optics Assembly

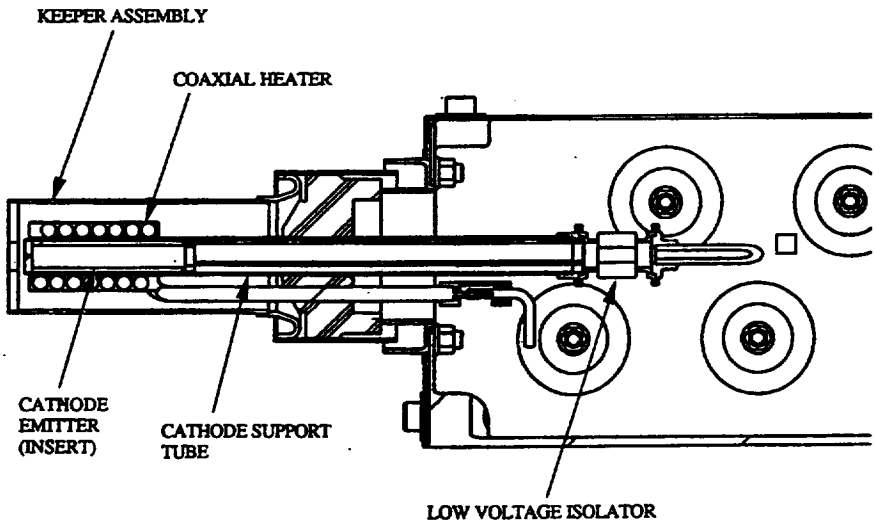

Figure 11. Flight Thruster Neutralizer Hollow Cathode Keeper Assembly

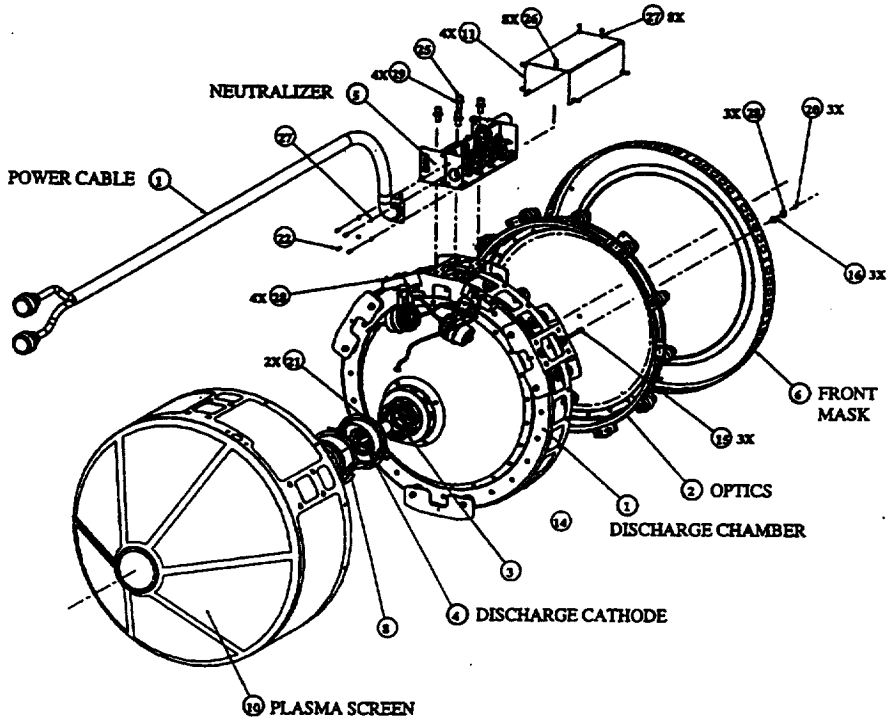

Figure 12. NSTAR Flight Thruster Final Assembly

4.2 The PPU

4.2.1 Overall Architecture – Block Diagram

BASIC POWER PROCESSOR DESIGN - The PPU contains the six (6) power supplies required to operate the thruster (refer to block diagram – Figure 20). In addition, the PPU contains a "slice" board that performs all required digital-to-analog (A/D) and analog-to-digital (D/A) conversions as well as an RS-422 command/telemetry interface. A set of high voltage vacuum relays to allow power switching between two thrusters is also contained in the PPU box. Two power inputs are required from the spacecraft. Primary power is supplied from the spacecraft power bus (80 to 160 V), while housekeeping power is supplied from a separate 28 V spacecraft bus. A description of the grid clear function is given in the appendix to this report.

4.2.2 Description of Individual Power Supplies

	NEUTRALIZER	DISCHARGE	CATHODE HEATER	BEAM	ACCEL	
Input Voltage	80 to 160 Volt high power bus and 22 to 34 Volt low power bus					
Output Voltage	8.0 32.0	15.0 35.0	3.0 12.0	650 1100	-180 -150	VDC
Output Current	1.0 2.0	4.0 14.0	3.5 8.5	0.5 1.80	0.00 0.02	ADC
Regulation Mode	CC	CC	CC	CV	CV	
Reg w Line/Load	5%	5%	5%	5%	5%	
Ripple	5%	5%	5%	5%	5%	Pk to Pk
Max Power Out	64	490	75	1980	3.6	Watts

Maximum Total Output Power	2538	Watts
Max Input Power @90% Eff	2820	Watts

Slice power ignored in table

Parameter	Nominal Value	Command Range	Slice to PPU Voltage	Resolution (12 bit)	Accuracy (± %FS)
Beam Voltage	650 -1100 VDC	0 - 1200 VDC	0 - 10 V	0.3 V	2
Accelerator Voltage	150 - 180 VDC	0 - 250 VDC	0 - 10 V	0.05 V	2
Discharge Current	4 - 14 ADC	0 - 15 ADC	0 - 10 V	4 mA	2
Neutralizer Keeper Current	1.5, 2.0 ADC	0 - 2 ADC	0 - 10 V	0.5 mA	2
Neutralizer Heater Current	3.5 - 8.5 ADC	0 - 10 ADC	0 - 10 V	2.5 mA	2
Discharge Heater Current	3.5 - 8.5 ADC	0 - 10 ADC	0 - 10 V	2.5 mA	2

PPU Design

The PPU contains the slice board, which interfaces the PPU to the DCIU and the six power supplies, which operate the thruster, as shown in Figures 20 and 21. Power for housekeeping is drawn from a 28, –4, +6 V bus. The high power input for the six converters used to operate the thruster is rated for 80 -160 VDC operation. Low voltage cutoffs are in place at 24 and 75 V for the housekeeping and high power busses, respectively, and an overvoltage trip is set at 165 V for the high power bus. The housekeeping power supply is capable of operation without damage at input voltages as high as 60 V.

All PPU power supplies operate at a switching frequency of 20 kHz, and no resonant switching is used. Ferrite cores are used for all power transformers and the beam supply output inductor. The remaining DC inductors are made from a metal tape core construction.

Thermal management is accomplished by conducting heat from the power components to the baseplate and PPU cover. The DS1 spacecraft mounts the PPU externally, on the ram face. The PPU is covered with metallized tape, which converts the enclosure to a radiator.

Baseplate cooling is also utilized to keep the PPU temperatures within limits.

In the event of a high voltage fault on the thruster, the PPU must set a fault flag and automatically shut down the beam and accelerator power supplies and operate the thruster discharge at a cutback level to reduce ion production. The DCIU then assesses the status of the system, resets the fault flag, and increments the recycle counter. Normal thruster operation is resumed. In the event of a discharge extinction, the DCIU automatically restarts the thruster.

Slice

The slice board contains an RS-422 interface for digital communications with the DCIU. Six digital to analog converters provide setpoint reference signals for the PPU power supplies. Fifteen analog inputs are available for PPU telemetry. Four temperature sensors are interfaced to the slice, which measure internal PPU temperatures. All of these components are controlled by a central FPGA.

Beam Power Supply

The beam power supply, sometimes referred to as the screen power supply, processes up to 80% of the total power in the NSTAR system. The wide dynamic range in the specifications and operating space (500 - 1200 VDC output, 80 - 160 VDC input) complicates the design, making single stage design solutions nearly impossible to execute and remain within the efficiency and weight constraints. For example, to achieve the performance required by the specification, the beam power supply must demonstrate an efficiency in excess of 0.93 while keeping the specific mass of the power converter near 1-1.5 kg/kW.

To deal with this wide dynamic range and high efficiency requirement, a four-stage non-resonant bridge topology was selected. The beam power supply consists of four individual power modules, each capable of 300 VDC output with an 80 VDC input. The outputs of each power module are connected in series, as shown in Figure 13. Each of the power converters is pulse-width modulated in a novel, sequential fashion. Depending on input and output conditions, the operation of the power supply is as follows; module #1 increases pulse width until a duty cycle of 100% is achieved. Module #2 then begins to phase up to 100%, and so on.

For an 1100 V output at 80 V input, for example, modules #1, 2, and 3 operate at 100% duty cycle and #4 will operate at approximately 66%. This allows 3 of the four modules to operate at maximum efficiency while the fourth is modulated. Further, the voltage ripple at the output of the rectifier sections of the power supply is greatly reduced, which allows a reduction in size of the output smoothing inductor when compared to a standard single stage converter. The mass savings also translate to the input filter, as the input current ripple is also reduced by this topology.

Discharge Power Supply

The discharge power supply is second to the beam power supply with respect to the level of power processed. For the NSTAR PPU, a standard, single stage, non-resonant bridge topology was selected, as shown in Figure 14. A single current smoothing inductor is used as the output filter.

A novel approach to the ignition circuit was applied here. Previous designs used a second winding on the output inductor for pulse generation. This winding was generally excited directly from the main power bus, which had the disadvantage of introducing large current transients when the winding was excited. The NSTAR PPU uses a tapped output inductor, as shown in Figure 15, to generate the high voltage ignition pulse.

The power supply is energized, and generates full output voltage into the unit discharged. A transistor connected between the inductor tap and the power supply return is turned on, which places the tapped winding directly across the output of the discharge power supply, energizing the pulse winding. The transistor is turned off, and the tapped winding generates a flyback pulse, which is amplified by autotransformer action in the pulse inductor.

Neutralizer, Accelerator, and Cathode Heater Power Supplies

The remaining four power supplies required to operate the thruster have output power levels below 70 W in normal operating conditions (Neutralizer and Accelerator) or are mainly used only to start the thruster (Cathode Heaters). This characteristic led to the topology shown in Figure 16. The four power supplies are based on a bridge topology, except that the upper two transistors of the bridge are shared by all four power stages. The four transformers are connected to these transistors through isolating diodes, and transistors are operated at a constant 50% duty cycle. A pair of lower bridge transistors is provided for each of the transformer primaries, and this pair is operated in the pulse-width-modulated mode. This configuration eliminates three sets of upper bridge transistors, and their associated gate drive circuits.

All of these components are integrated into a single enclosure.

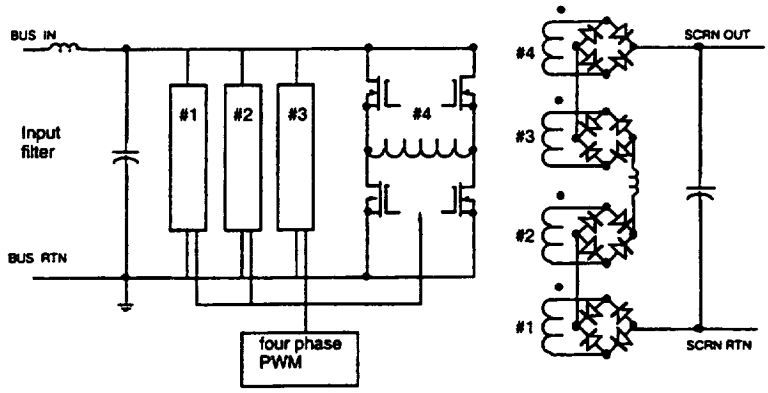

Figure 13. Beam Power Supply Topology

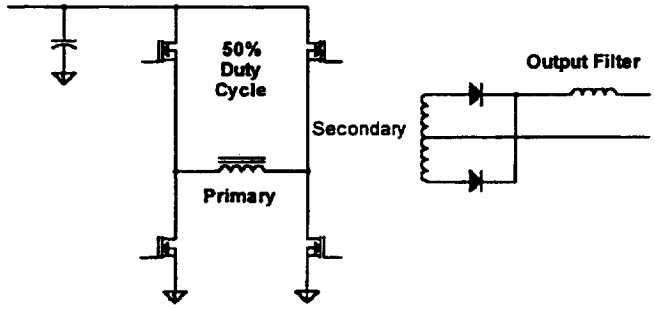

Figure 14. Discharge Power Supply Topology

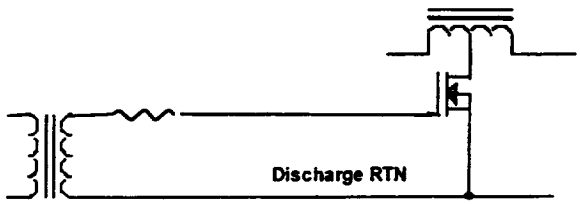

Figure 15. NSTAR Arc starter schematic

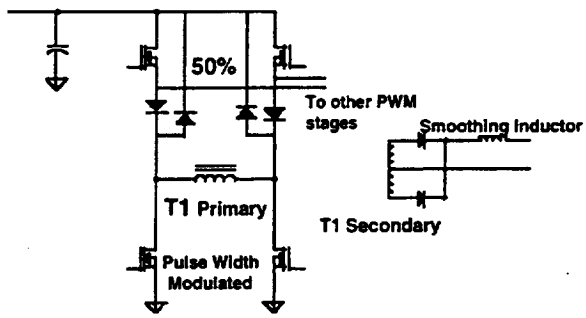

Figure 16. Neutralizer/Accelerator/Cathode Heaters Power Supplies Topology

Figure 17. Photo of PPU – Interior (Top View)

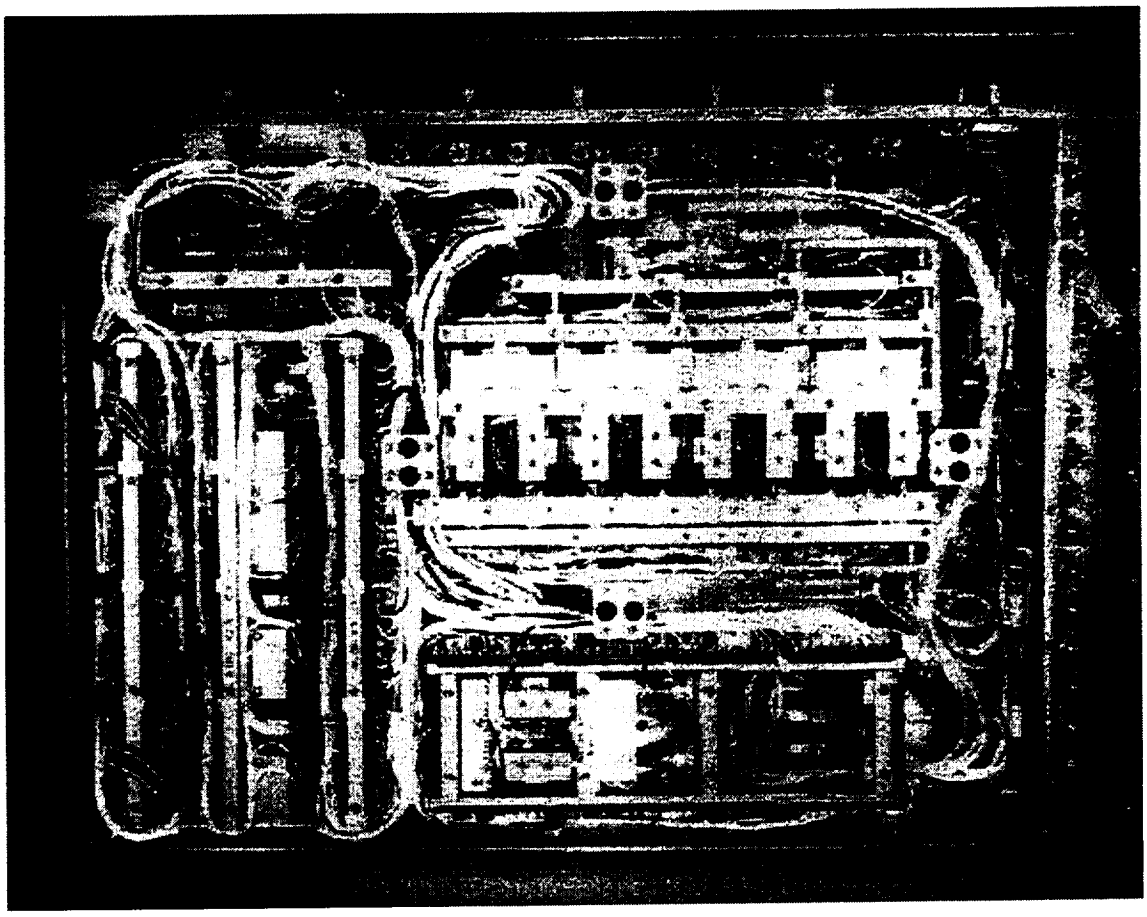

Figure 18. Photo of PPU - Interior

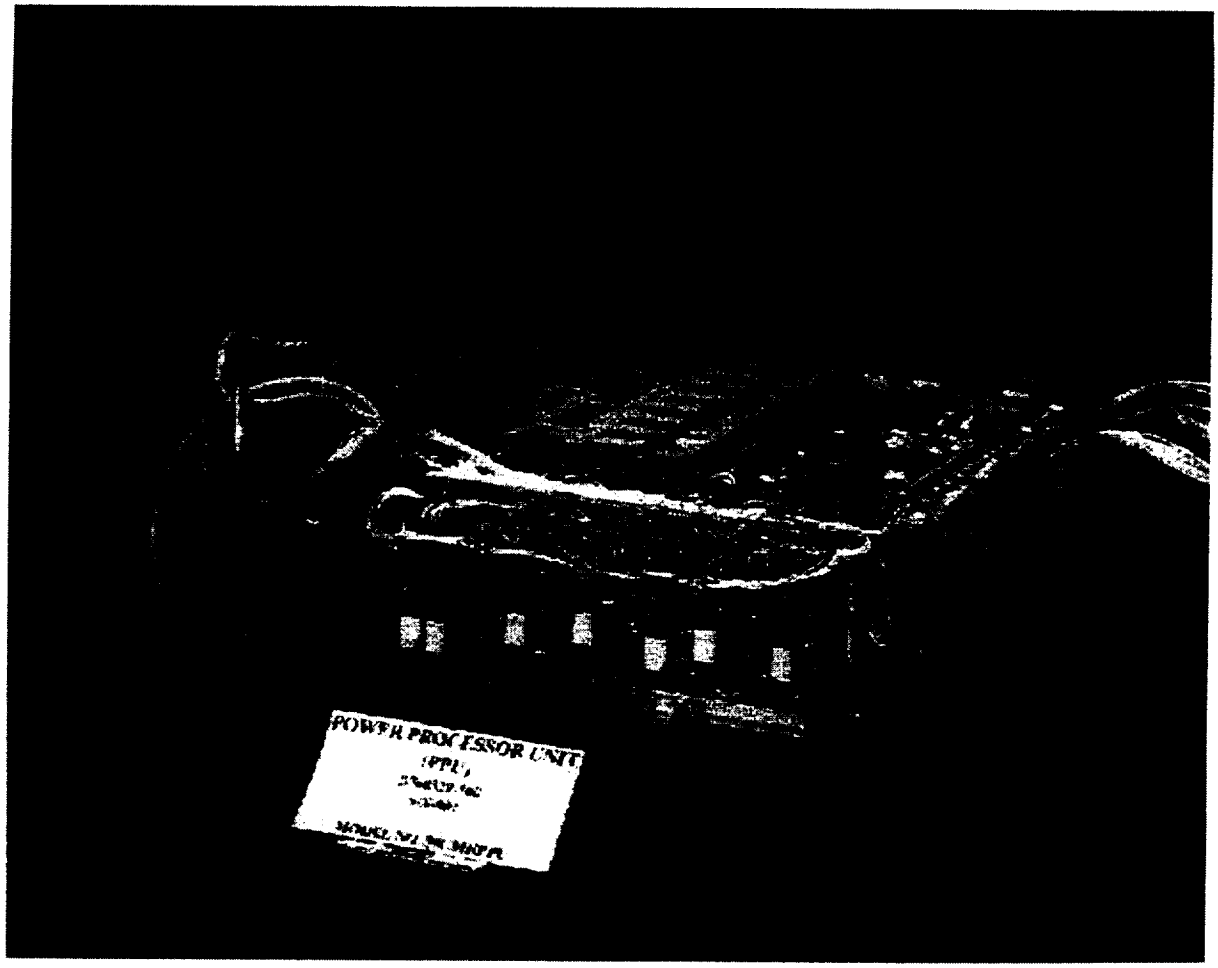

Figure 19. Photo of PPU – Outside View

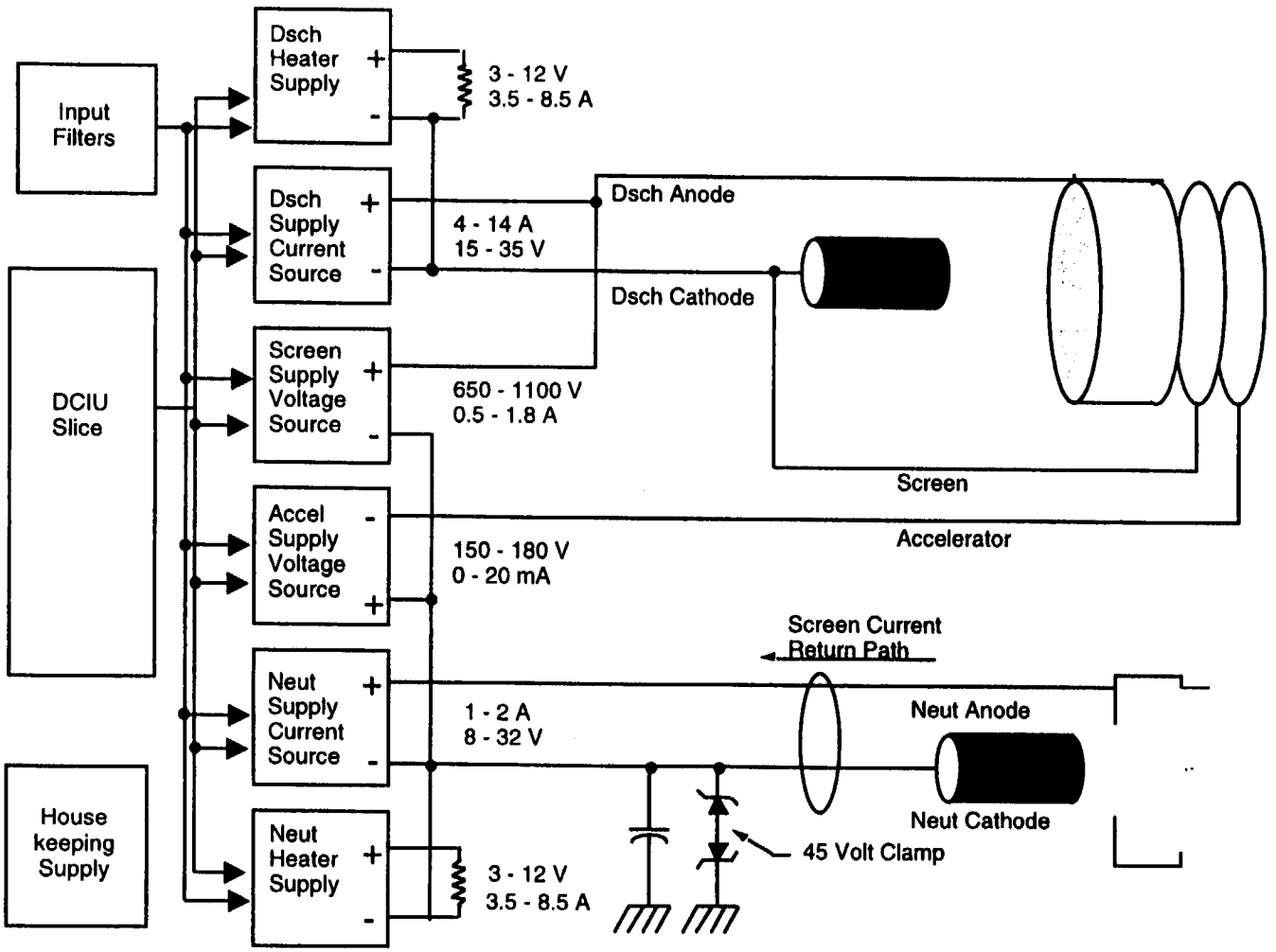

Figure 20. Block Diagram of NSTAR PPU with Thruster

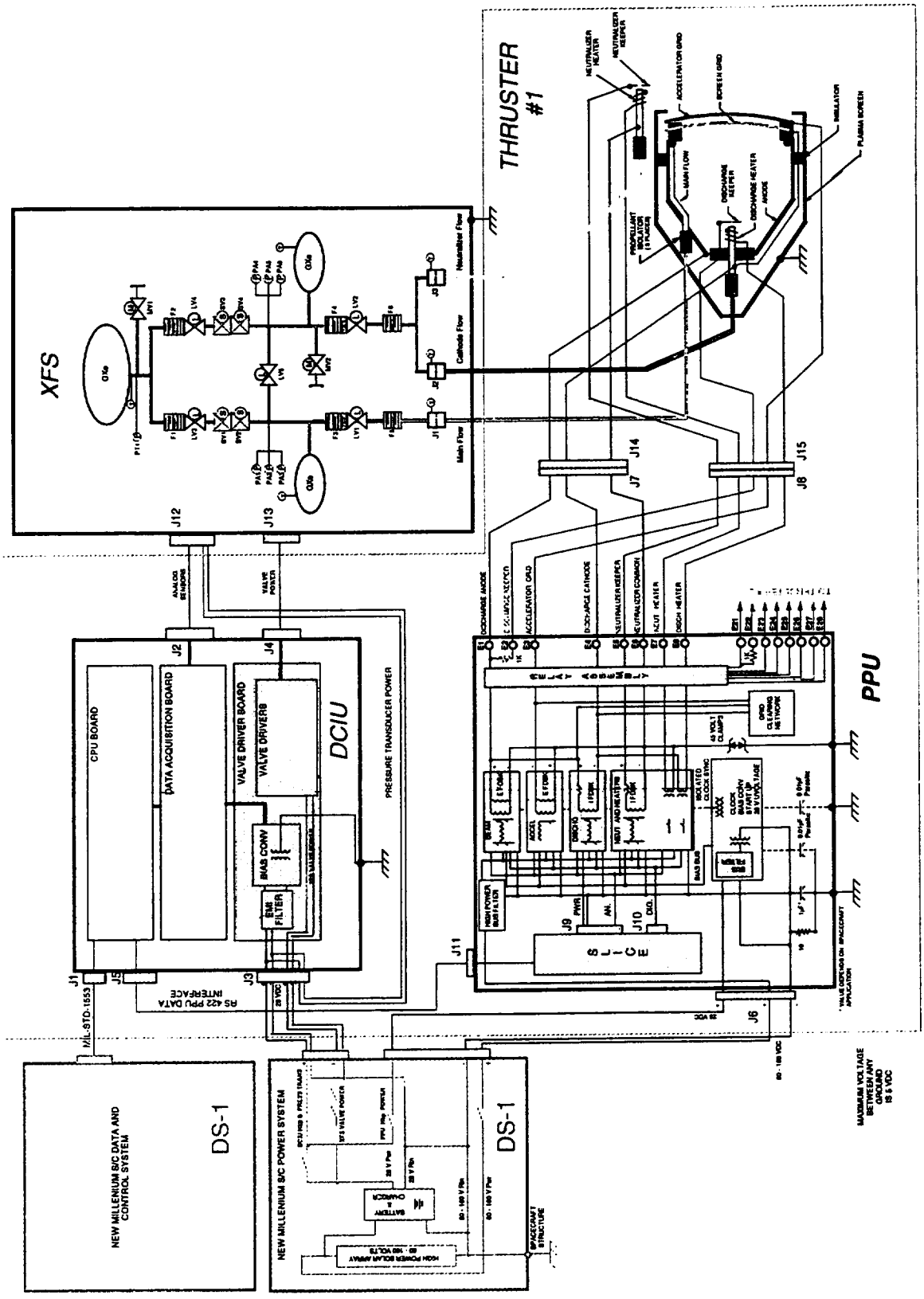

Figure 21. Block Diagram of the NSTAR Subsystem

4.3 The DCIU

4.3.1 Overall Architecture – Block Diagram

DCIU Design

The DCIU consists of three circuit boards, each conforming to the 1/2 width VME bus standard. The CPU, Valve Driver, and Data Acquisition boards will be discussed in following sections. These boards are installed into a five-slot backplane. Two slots are open for expansion for future applications. These slots are flown empty on the DS1 spacecraft. A block diagram of the DCIU appears in Figure 22.

The DCIU interfaces to the spacecraft via connectors on one face of the DCIU enclosure, as shown in Figure 23. The data interfaces with the spacecraft and PPU reside on the CPU board. The Data Acquisition Board is the analog data interface with the XFS. Power is brought into the DCIU on the valve driver board, which also interfaces with the solenoid and latch valves on the XFS. Radiation hardened components are used throughout to ensure a total dose capability of 100 kRad.

CPU Card

The CPU card is designed around an 80C86 microprocessor operating at 4 MHz. The flight software is loaded into a 64 k EEPROM, and 64 k of RAM is available on board. A MIL-STD-1553B chipset provides the command and telemetry interface for communication with the PPU. A Field Programmable Gate Array (FPGA) is used to interface these devices with the microprocessor. The flight software operates on a one second timed loop, which reads a full telemetry scan, polls for system errors and executes any steady state concerns.

Valve Driver Card

The valve driver board contains the DC/DC converter used to provide ± 15 V and 5 VDC power to the DCIU form a nominal 28 V bus. 28 V power is also routed to the pressure transducers in the XFS through the power connector on the valve driver card. 4 solenoid and 5 latch valve drivers are provided to operate the propellant valves in the XFS. All of the valve drivers are optically coupled for electrical isolation, and contain flyback diodes to suppress the switching transients on the valve coils. The solenoid drivers can source up to 420 mA, and the latch drivers can source up to 550 mA. The pulse lengths for each valve type are variable via spacecraft command.

Data Acquisition Card

The Data Acquisition Card provides high accuracy, 12 bit analog to digital conversion for 8 Platinum Resistance Thermometers (PRTs) and 7 pressure transducers in the XFS. The PRTs are excited by a precision 1 mA current source. On-board, precision, temperature compensated resistors are used for self calibration of the A/D converter.

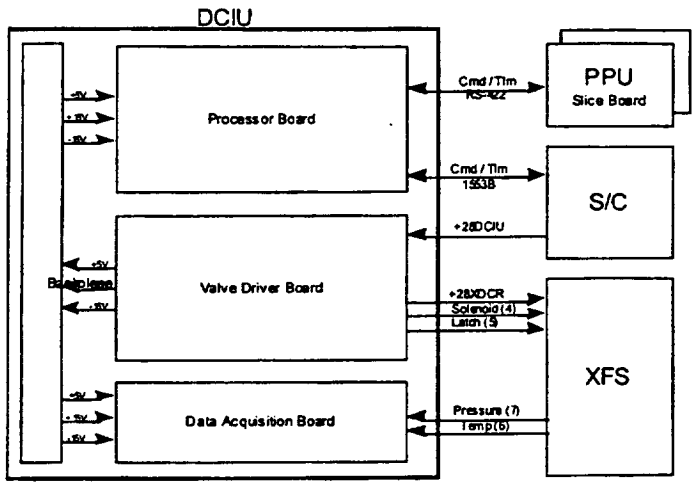

Figure 22. DCIU Block Diagram

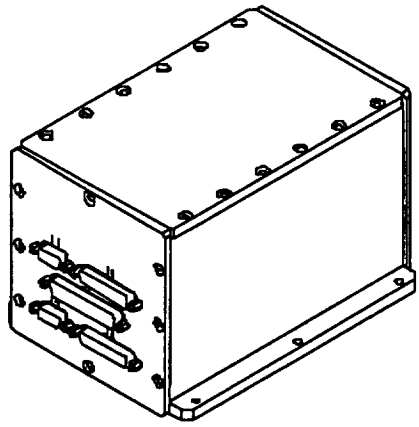

Figure 23. Isometric View of the DCIU

5.0 FLIGHT SYSTEM STRUCTURAL DESIGN AND ANALYSIS

5.1. Flight Thruster Structural Design and Analysis

One of the major challenges and risk areas of the NSTAR flight thruster program was the redesign of the NASA thruster to meet the DS1 vibration and shock tests and to satisfy the component stress safety margin requirements without significantly increasing the thruster mass. This effort was further complicated by the fact that the DS1 spacecraft, the thruster gimbal design and dynamics characteristics were not defined until late in the flight thruster development program. As a result, most of the thruster structural design was performed using an assumed gimbal strut configuration.

The Hughes EDD approach was a combination of structural modeling and analysis coupled with a vibration test program using modified versions of the NASA EMT thruster. The steps that were followed in developing the flight thruster structural design were as follows:

1. Development of a detailed computer structural model of the EMT1b with two mounting pads.
2. Vibration testing (sine resonance searches) on EMT1b to refine and validate the structural model in January 1996.
3. Modification of the computer model for the proposed flight thruster design with three mounting pads.
4. Modification of the EMT to near flight thruster configuration (EMT1c).
5. Vibration testing (resonance searches) on EMT1c to validate the model.
6. Vibration of EMT1c to protoflight random vibration levels to demonstrate that the flight design meets the requirements in August 1996.
7. Use the measured resonance data from EMT1c to complete the stress analyses, modify the design, as required, and demonstrate that it has the required safety margins.

The thruster was modeled using the MECHNICA structural analysis computer code. The final model of the 30 cm flight thruster is shown in Figure 24.

Excellent correlation between the structural models of the EMT1b and 1c configurations and the vibration test data was achieved. A comparison of the modal analyses of EMT1c and the flight thruster with the vibration test data on EMT1c is shown in Table 7.

The lowest thruster resonance is at 77 Hz, well above any predicted spacecraft resonances.

The EMT1c configuration, which is close to the flight thruster structural design, was successfully step-stress tested to protoflight levels of random vibration with no changes in resonant frequencies or measured dimensions.

The stress analysis of the flight thruster was performed using effective static loads based on peak levels measured during the EMT1c random vibration tests. These loads were estimated conservatively to be 75 g in the lateral axes and 120 g along the thruster axis. The results of the analysis showed a safety factor on yield of 1.25 everywhere except in some small zones of the discharge chamber box beam near the gimbal mounting pad bolt locations. These were judged to be low risk stressed.

DS1 component level pyroshock tests were not performed on the thruster as the levels were expected to be less than the peak random vibration responses. The Pathfinder thruster was successfully shock tested during the DS1 spacecraft integration tests in November 1997.

The DS1 flight gimbal design was completed after the thruster design was frozen and parts were procured. To assure that the gimbal dynamic characteristics did not result in excessive forces on the thruster, the EMT1c thruster was installed in the flight prototype gimbal assembly and vibration tested to spacecraft protoflight levels in October 1997. The vibration levels measured at the thruster mounting points were less than the specified thruster component vibration test levels. The EMT1d thruster successfully completed these tests.

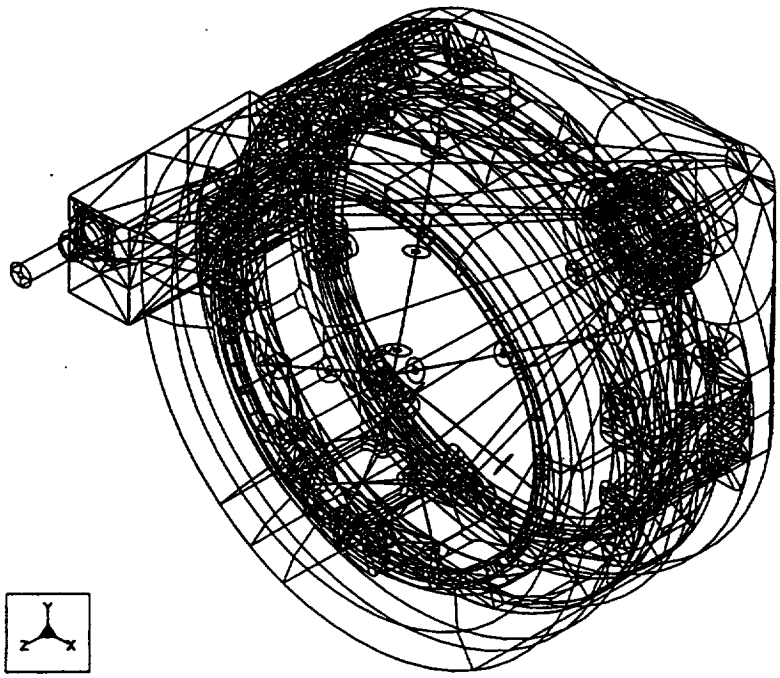

Figure 24. Mechanica Structural Model of the NSTAR Flight Thruster

Table 7. - Comparison of Modal Analysis Results of Flight with EMT-1C Analyses and Test

Mode Shape	Analysis – Flight Total Mass = 18.31 lb Frequency (Hz)	Analysis – EMT-1C Total Mass = 17.85 lb Frequency (Hz)	Test – EMT-1C Total Mass = 16.77 lb Frequency (Hz)
Assembly TR along X	76	77	76-77
Assembly TR along Y	77	78	79
Assembly TR along Z	101	107	109
Neutralizer Bending	144	120	120
Assembly ROT about Y	147	158	170-171
Assembly ROT about X	148	159	175
Assembly ROT about Z	159	162	—
Optics TR along Z	—	507	470

The flight Thruster (FT1) successfully completed non-operating random vibration tests to acceptance levels (see Table 3). These tests were performed at JPL using the Engineering Model DS1 gimbal assembly in March 1998. Force limiting was used during these tests.

The spare Flight Thruster (FT2) also successfully completed random vibration testing to flight acceptance levels in May 1998.

5.2. The PPU

5.2.1 Mechanical Design

Refer to the Installation Control Drawing (CDB768329) in Appendix A of this report for external dimensions, predicted mass, installation notes ...etc. Figure 25 is a sketch of the internal PPU layout.

By requirement, the PPU has a short/broad aspect ratio which resulted a box design with:

Top and Bottom surfaces of machined aluminum

Sheet metal covers on the side surfaces

All major internal assemblies bridge the top and bottom surfaces - this enhances thermal characteristics and adds structural rigidity.

The bottom surface or baseplate has peripheral feet as well as four through-holes in a box pattern, for PPU attachment to the spacecraft surface. All mounting holes are designed for #8 hardware. The PPU box is not hermetic and is vented through fine mesh screens in the metal side covers.

Figure 25. Interior PPU Layout

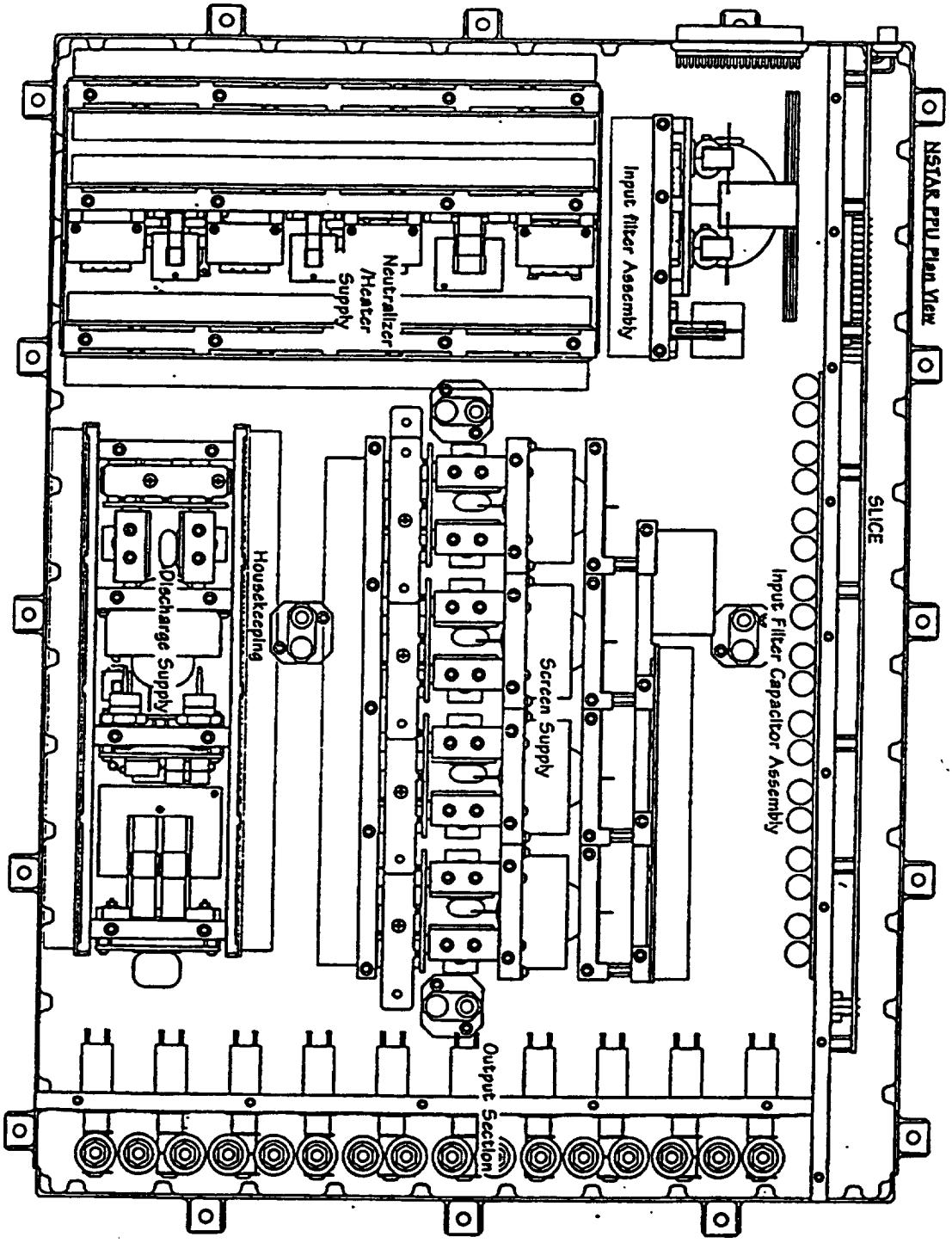

5.2.2 Structural Analysis

A structural analysis was carried out on the PPU. The model and results were submitted in a report to NASA GRC dated 27 January 1997. The abstract is reprinted here.

Abstract:

This report contains the fastener analysis of the NSTAR Power Processing Unit (PPU) for NASA. It is intended to verify the structural integrity of the fasteners attaching the highest loaded components in the assembly. The analysis does not cover the details or other subassembly components such as printed boards or electrical components. This report is a verification of the structural integrity of the PPU when subjected to the protoflight qualification levels of the random vibration and shock environments as defined in the DS1 Specification identified in Paragraph 3.3.7.1.

Part of the analysis involved determining the shock response curve to test the unit with, since the original curve would have dictated a redesign of many of the subassemblies. A curve was chosen which would minimize the impact of any redesign. The curve described in Table 2.3 of the CVS requires changing eight of the most critical fasteners to high strength fasteners. The proposed curve is described in Section 2.0 of this report and all fastener calculations are according to the "Protoflight – Revised" environment levels required by the CVS. The results of this analysis show that the preloads on all of the major structural fasteners in the PPU are not compromised by the protoflight qualification random vibration or the proposed protoflight qualification shock test.

The unit was analyzed by creating a finite element model (FEM) of the entire assembly and predicting the overall natural frequency of the unit. Only the major structural components were included in the model. The fastener analysis itself was performed using a combination of finite element analysis results and hand calculations (see Section 3.0). Calculations were performed to determine the load of the main fasteners for all of the major subassemblies and chassis details. During protoflight qualification testing, the worst caseloads will occur during the shock tests. If the preload on the bolts is exceeded during shock, the epoxy staking of the screw head would serve to maintain preload in the joint, as long as the elastic limit (yield strength) was not exceeded. During shock, the minimum Margin of Safety of the fasteners was determined to be 0.011 against the preload for the worst case bolt. However, when considering the yield strength of the same bolt, the Margin of Safety is 1.2.

The PPU is constructed using a bolted-panel assembly method. It consists of six distinct subassemblies, which are grouped in terms of electronic functionality. Each of the subassemblies is constructed using at least one metal support panel, which is bolted at the top and bottom to the cover and baseplate. Some of the subassembly panels are also bolted into the sidewalls. These panels comprise the major mechanical support for the PWBs, magnetics and other discrete electronic components required for each subassembly. The support panels also function to remove heat generated from the electronics. The unit is completed by bolting four sidewalls to flanges on the cover and baseplate (and to two of the subassemblies). All of the panels are machined from 6061-T6 Aluminum, while the sidewalls are formed from 6061-T4 Aluminum sheet. The unit is shown in Figures 26 and 27, which provide an overview of the construction and assembly breakdown.

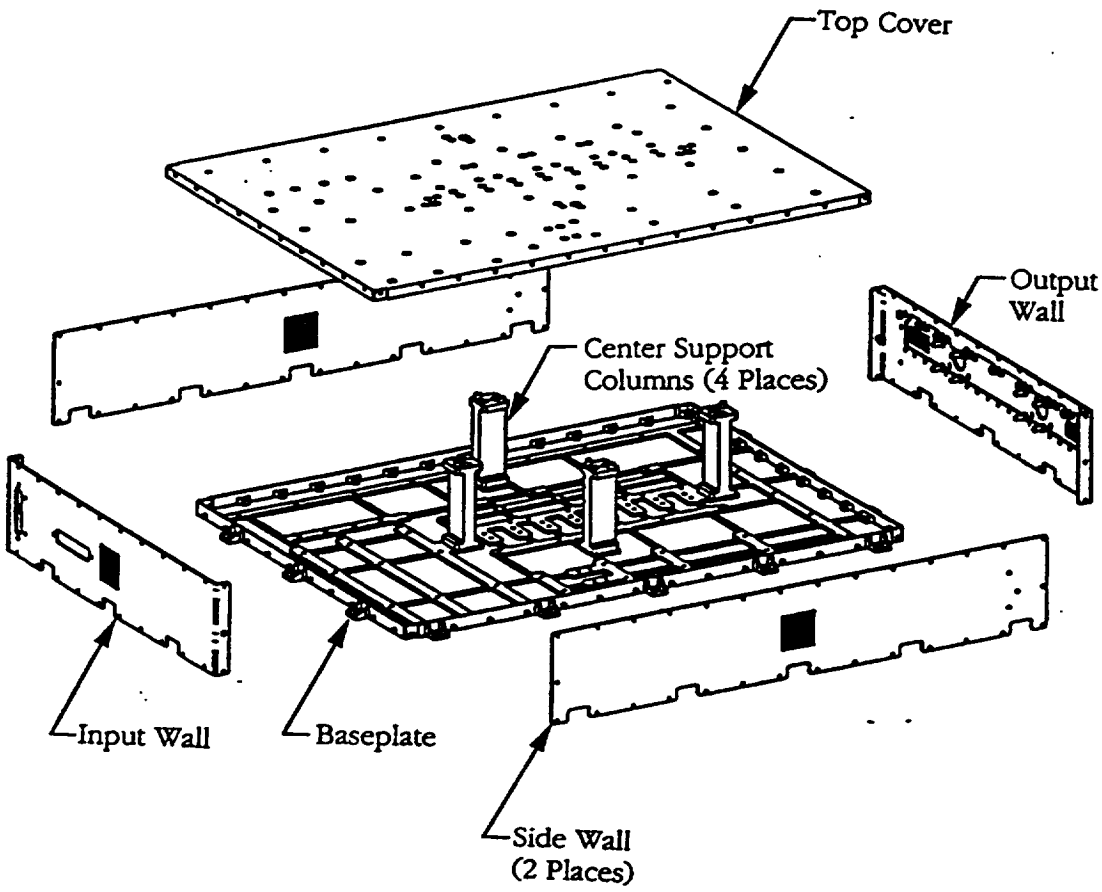

Figure 26. NSTAR PPU Structural Details - Exploded View (All Electronic Subassemblies Removed for Clarity)

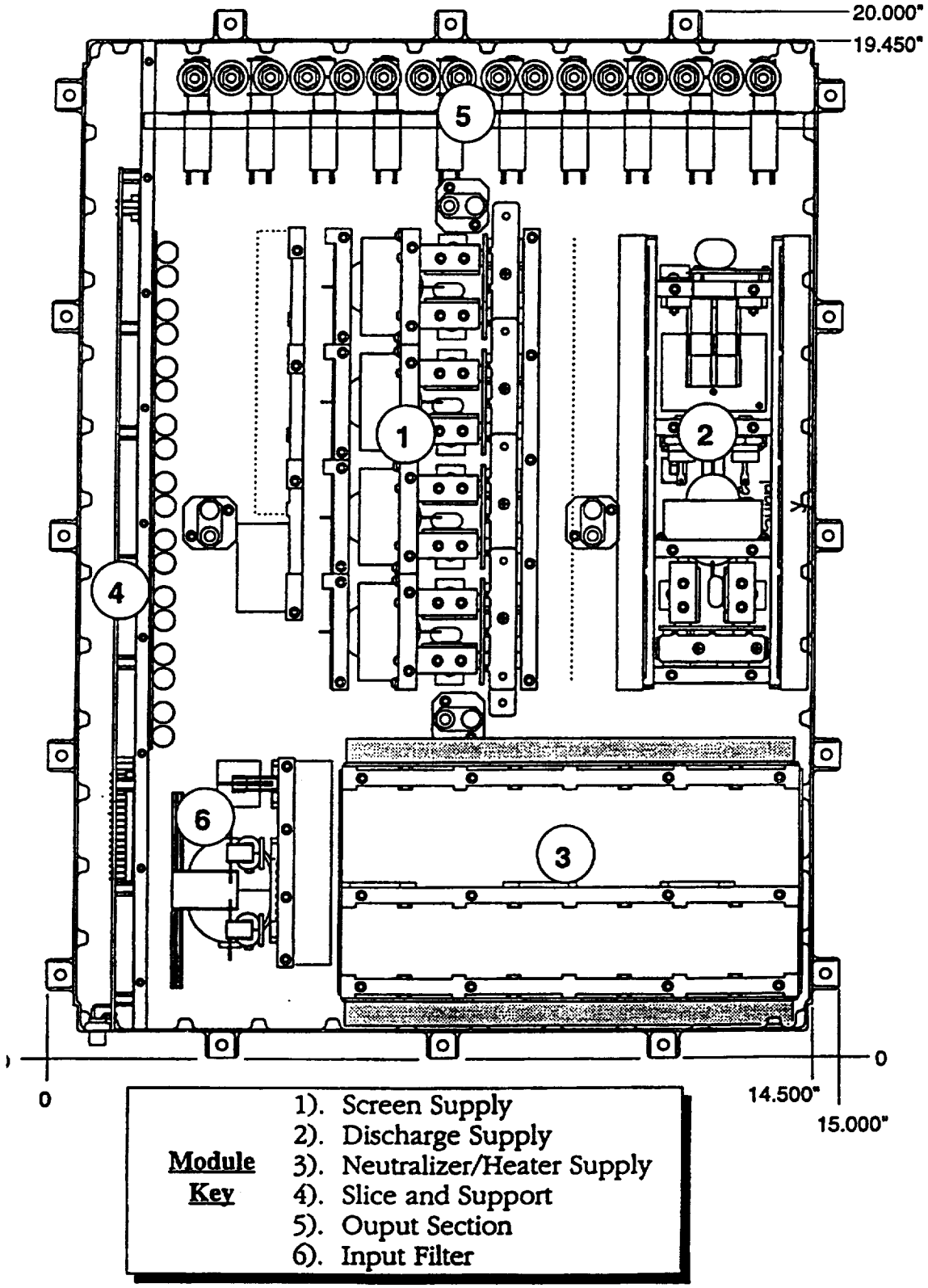

Figure 27. NSTAR PPU Electronic Subassemblies - Top View (Cover Removed)

As a result of this analysis the following waiver was generated by HED and sent to NASA GRC for resolution.

> **W003**: The CSVS pyroshock requirement (which was generated after the PPU mechanical design was complete) for protoflight (also qualification) is too severe for the 57 screws securing the baseplate and cover. Estimated margins of safety (worst case) range from 0.0 to –0.6. Resolution: DS1 spacecraft requirements were revised making this waiver unnecessary.

5.3 The DCIU

5.3.1 Mechanical Design

Refer to the Installation Control Drawing (CDB768329) in Appendix A of this report.

6 FLIGHT SYSTEM THERMAL AND ELECTRICAL DESIGN AND ANALYSIS

6.1 The Thruster

6.1.1 Thermal Model and Analysis

The thermal design was another essential element in the development of the NSTAR flight thruster. Thermal modeling was necessary to determine the internal temperatures of the thruster components in order to complete the materials selection and stress analyses and to assure that the discharge chamber magnetic field would not degrade due to overheating of the permanent magnets. A thermal model was also needed to determine the thermal interface with the DS1 spacecraft and to define the appropriate thermal vacuum test levels for the thruster.

The NSTAR thruster thermal model was developed by Ray Becker of JPL. This model incorporates the component designs of the flight thruster and the thermal interfaces of DS1. The results of the thermal model are shown in figures 28 through 32 for various operating conditions.

The thruster internal heat dissipation distribution is shown in figure 28 for two input power levels – TH15 (2.3 kW) and TH-10 (1.7 kW).

Figures 29 and 30 show the predicted thruster temperatures for TH10 with no solar input and with 1 sun at 30 degrees off-axis, respectively.

Figures 31 and 32 show the predicted temperatures for TH15 with no solar input and with 1 sun at 30 degrees off-axis, respectively.

For the worst case conditions, the discharge chamber operates at temperatures in the range of 239 to 306°C. The discharge cathode magnets reach 291°C. The plasma shield and gimbal mounting pads operate around 195°C. Extensive thermal vacuum

tests were performed at NASA GRC using EMT3 and EMT4 with a simulated DS1 thermal interface. These tests, performed in the March to October 1997 timeframe, were used to validate the thermal model and to determine minimum and maximum thruster internal temperatures and performance effects. The EMT3 was subjected to three cold starts at -117°C and steady state operation at +120°C, measured on the front mask. No start-up or performance problems were seen. The results of these tests were used to select the flight thruster thermal vacuum test limits. Excellent agreement was achieved between the measured thruster temperatures and those predicted by the thermal model.

Based on the thermal modeling and test results, the thruster flight acceptance thermal vacuum test levels were specified at -98°C minimum and +143°C maximum; measured at the face of the front mask. The flight thruster successfully passed these tests at NASA GRC as well as the solar thermal vacuum tests of the DS1 spacecraft at JPL in February 1998.

Figure 28.

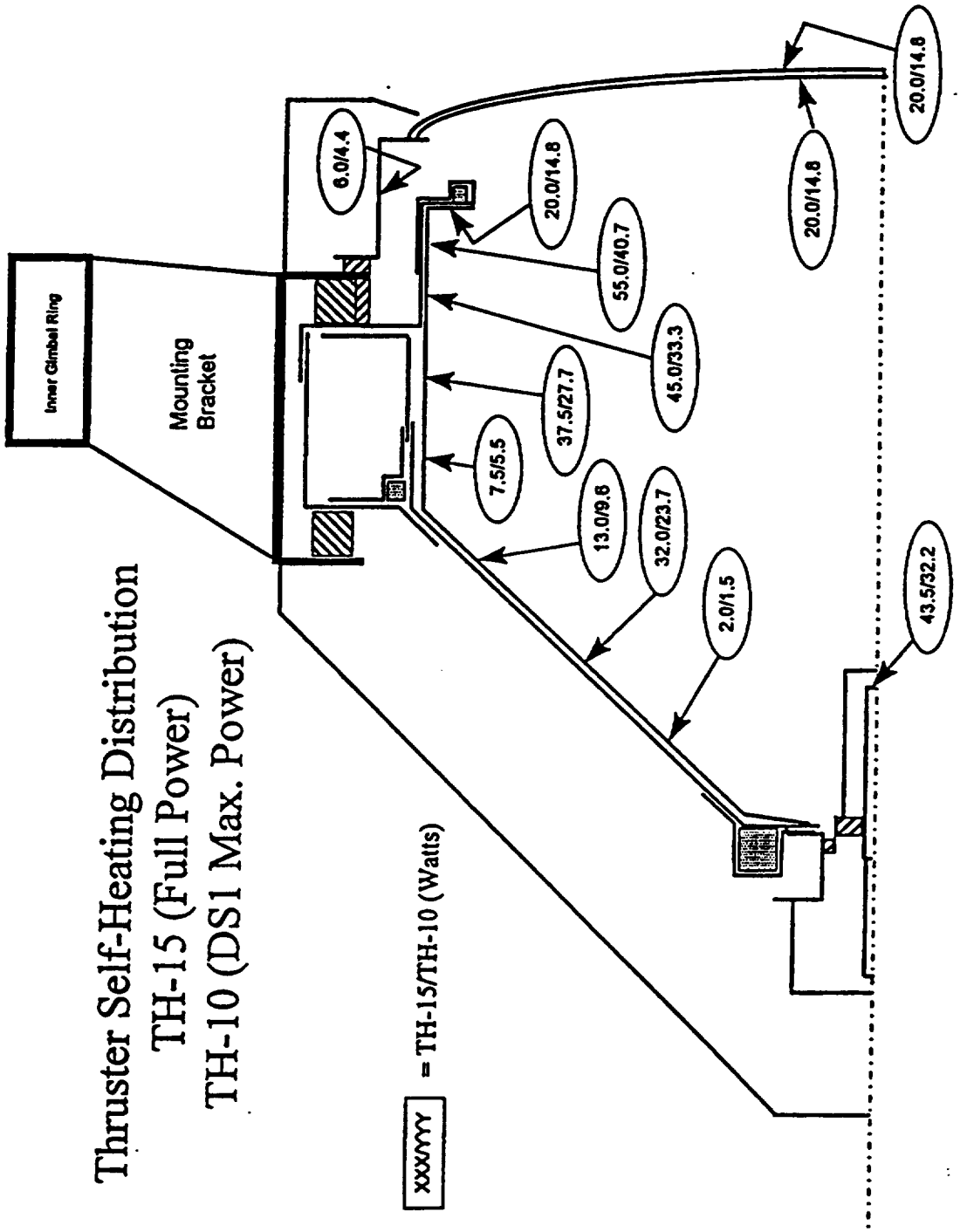
Thruster Self-Heating Distribution
TH-15 (Full Power)
TH-10 (DS1 Max. Power)
XXX/YY = TH-15/TH-10 (Watts)
Inner Gimbal Ring
Mounting Bracket
6.0/4.4
20.0/14.8
55.0/40.7
45.0/33.3
37.5/27.7
7.5/5.5
13.0/9.8
32.0/23.7
2.0/1.5
20.0/14.8
20.0/14.8
43.5/32.2

Figure 29.

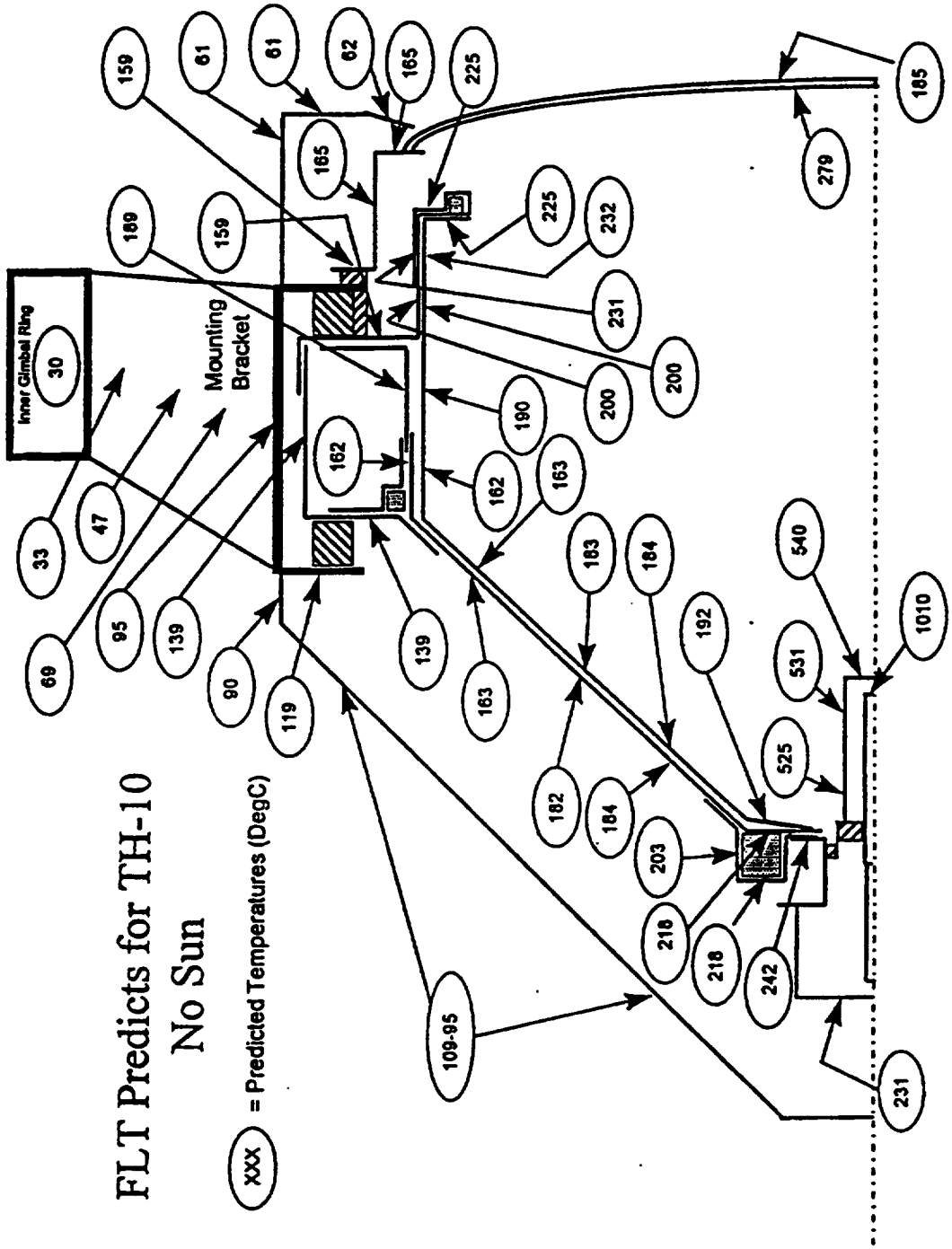
FLT Predicts for TH-10
No Sun
XXX = Predicted Temperatures (DegC)
Inner Gimbal Ring
30
Mounting Bracket
159
61
61
62
165
225
165
185
279
159
160
225
232
231
200
200
190
162
162
163
33
47
69
95
139
90
119
139
163
183
184
182
184
203
218
218
192
540
1010
531
525
242
109-95
231

Figure 30.

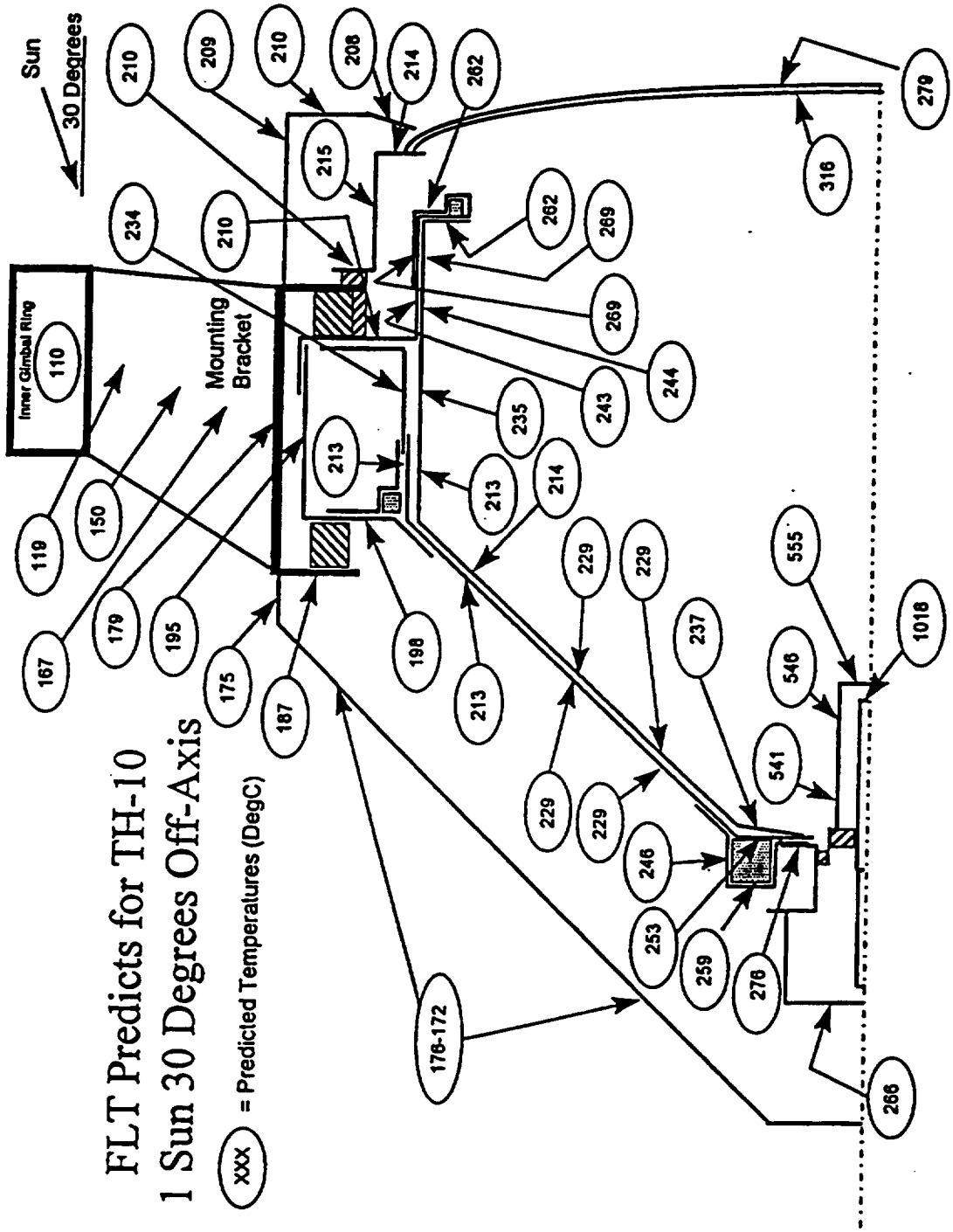
FLT Predicts for TH-10
1 Sun 30 Degrees Off-Axis
XXX = Predicted Temperatures (DegC)
Sun
30 Degrees
Inner Gimbal Ring
110
Mounting Bracket
167
119
150
179
195
175
187
198
213
178-172
210
209
210
208
214
282
215
234
210
262
269
269
244
243
235
213
214
213
229
229
237
555
546
1018
541
229
229
246
253
259
276
316
279
266

Figure 31.

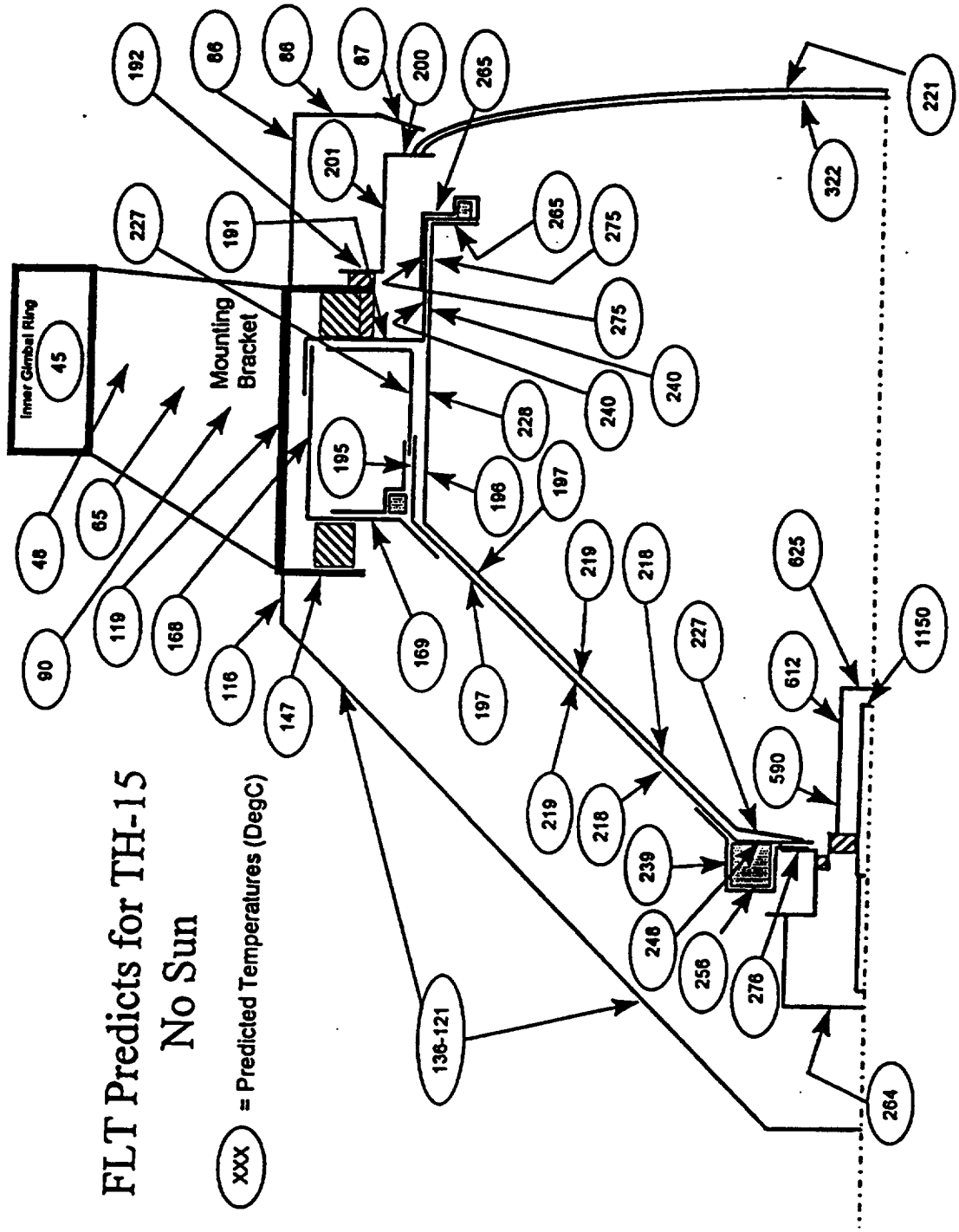
FLT Predicts for TH-15
No Sun
XXX = Predicted Temperatures (DegC)
Inner Gimbal Ring
45
Mounting Bracket
192
86
86
87
200
265
201
221
322
227
191
265
275
275
240
240
228
195
196
197
48
65
90
119
168
116
147
169
197
219
218
227
625
612
1150
590
219
218
239
248
256
278
136-121
264

Figure 32.

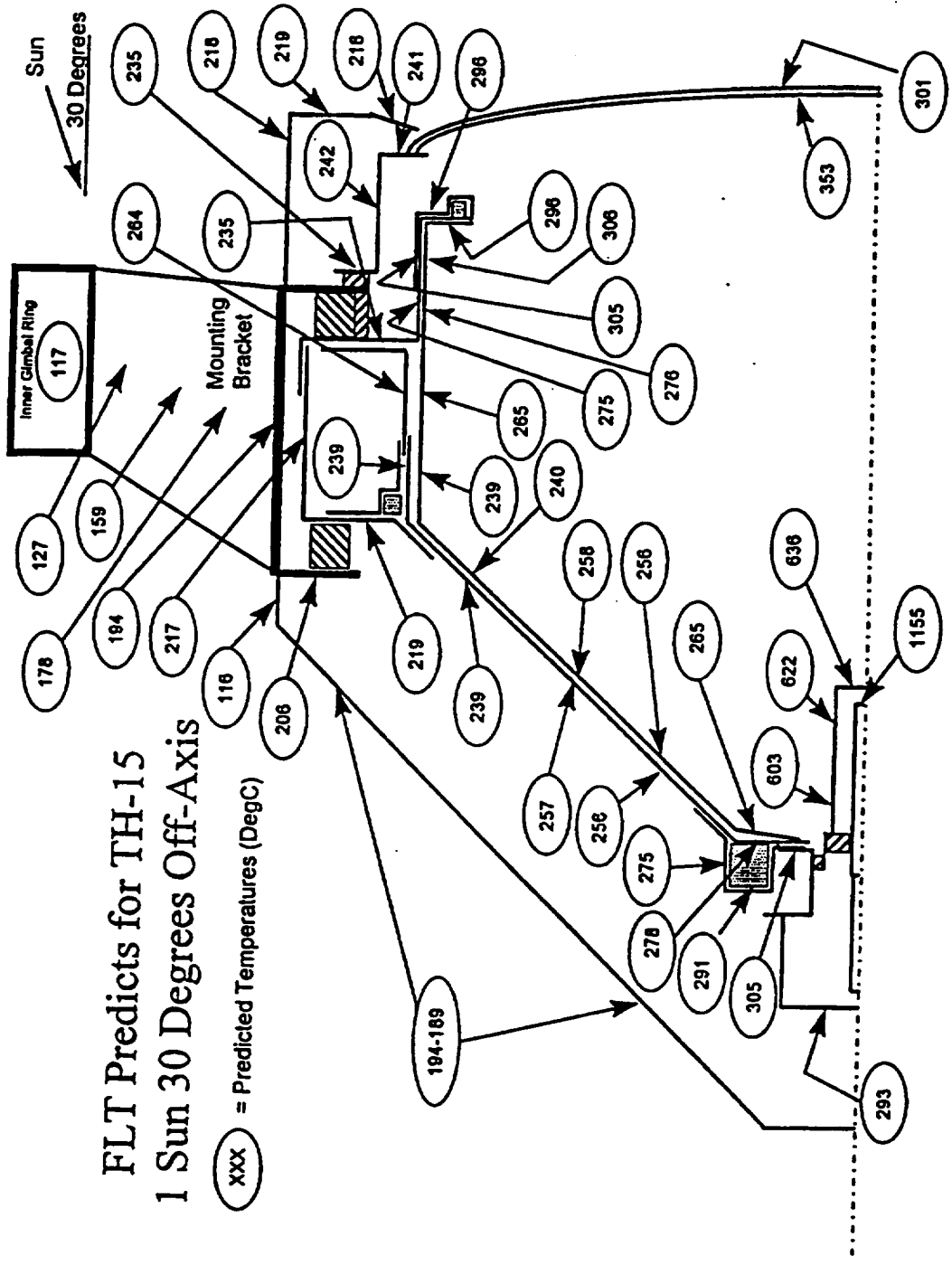
FLT Predicts for TH-15
1 Sun 30 Degrees Off-Axis
XXX = Predicted Temperatures (DegC)
Sun
30 Degrees
Inner Gimbal Ring
117
Mounting Bracket
127
159
178
184
217
116
206
219
239
240
265
275
276
284
235
218
219
216
241
242
296
306
305
301
353
258
256
265
622
636
1155
603
257
256
275
278
291
305
194-189
293

6.2 The PPU

6.2.1 Thermal Analysis

A thermal model of the PPU was generated by HED and a report of the results was submitted to NASA Lewis on 17 February 1997. The report abstract is repeated here.

ABSTRACT

This analysis is a verification of the thermal integrity of the NSTAR XPC30 PPU for the 30 cm Xenon Ion Thruster in relation to the requirements of Component Verification Specification New Millennium Deep Space Mission #1, Specification Number: 6446-361, revision A, signed September 9, 1996.

The analysis was performed using a version of SINDA 3G finite difference code that runs on a Macintosh personal computer. Both pre and post processing of the various elements of the data were performed on an MS-DOS PC using custom software. The component limitation requirements used in the analysis are specified by the applicable requirements of the specifications outlined in HED – Standard Parts Program Document, Document No. B850401, dated October 27, 1995. It should be noted that this document is primarily used for reliability predictions for life requirements of up to 22 years. This was chosen for the PPU's eventual use of station positioning and is considerably longer than the requirements of the NSTAR program. Maximum allowable temperatures not called out specifically in this document were provided by the appropriate material property limits suitably derated. The results show that a single electronic part operates beyond its maximum limits while the EPC package is mounted to an infinite heat sink maintained at the acceptance temperature of 50.0°C, as per analysis specification. That part is capacitor C12 of the Housekeeping PWB that operates at 87.1°C versus 85°C maximum.

The low line condition has been determined to be of primary importance (since the high line condition occurs when the spacecraft is much cooler) and is analyzed in the report. Of this case, three specific thermal cases have been performed to get the results presented in this report. The three conditions are called *full power*, *heaters on* and *neutralizer/accelerometer* on. The latter two conditions refer to power in the switching assembly of the neutralizer supply. The full power case combines the two secondary cases. Since the second and third conditions dissipate considerable power and they do not occur simultaneously, it would be prohibitive to design the PPU for both states to be operated at the same time. On pages 17 and 18 the operational temperature are reported for the switcher assembly for the two individual cases. The temperatures predicted for the rest of the PPU were determined at the full power condition.

Note that the analysis was done for a fixed baseplate temperature of 50°C; which was the original design requirement. Actual PPU tests established that increased heatsinking of the beam supply was required. Therefore, both flight and flight spare PPUs were upgraded with improved heatsinking (see the production section of this report). The following Waiver was generated by HED and approved by NASA GRC.

W001: Capacitor C12 (CSR13, 5.6μFd, 10%, 35V) on the Housekeeping PWB was predicted to have a worst case temperature of 87.1°C. The derating guideline is 85°C maximum. Resolution: Use as is. HED derating is more stringent than Military specification which allows 85°C operation. Specification operating temperature range is -55°C to +125°C.

6.2.2 Electrical Stress Analysis

6.2.2.1 Electronic Component Stress Analysis

An electrical stress analysis was performed and summarized in a report (dated 13 November 1996 with an addendum dated 4 February 1997) submitted to NASA Lewis. The abstract is repeated below.

STRESS ANALYSIS DESCRIPTION

This is the analysis of the component stress in the NSTAR Power Processor Unit (PPU) Model 30CMHPPU for NASA-Lewis Research Center. The power dissipation results are fed into a separate thermal analysis, which guarantees operation of devices within their specified temperature limits. The stress analysis is made under the following assumptions:

1. Nominal operating parameters and power dissipation for every electronic component in the design
2. Steady state input voltage – 80 Vdc minimum or 160 Vdc maximum
   (Minimum or maximum input voltage is used to provide the worst case condition)
3. Transient high input voltage – same as steady state input voltage
4. Maximum output dc voltages
5. Maximum output dc currents
6. Maximum Average or RMS voltage or current for all power supply internal circuitry
7. Maximum peak current for duty related circuits and turn on and off surge conditions

Parameters of interest may include current, voltage or power, depending on device type. Derating tables have been constructed for each component, with manufacturer's specified maximum values used as a baseline. These maximums are then derated by percentage in accordance with HED B850401, MIL-STD-975M and PPL21 derating criteria and are linked to the allowed entry in the stress analysis table. In some cases where derating criteria is not available from that document, the source of the derating is noted. The constants and variables table indicating the PPU operating voltages and currents are also linked to the actual calculated stress analysis table.

The stress analysis power dissipation subassembly subtotals are made under the assumption of normal operating conditions. Parts that are not on during normal operation are noted in the stress analysis comment column and are not included in the subassembly power dissipation subtotals. Power subtotals for all the components in the stress analysis are shown for major subassemblies.

Where the stress on a component is known to be higher at some special condition, that condition is individually identified or is listed in the comments column of the stress analysis. When a stress is only present for a short time, like when a command is energized, the voltage and/or current is presented for comparison to the surge or energy stress limit of the component.

The temperature is not relevant to the actual stress, but the derating allowed stress is often a function of temperature. The derating temperature formula for allowed voltage or power has been incorporated into the stress analysis for voltage on all capacitors (except ceramic) and for power on all IC's, resistors and transistors. The temperature in the stress tables are set at 85°C for all parts except those parts where the temperature has to be reduced (70°C minimum) or increased to meet the actual vs. allowed maximum power ratio of 1 and/or meet the actual component temperature based on the thermal analysis using a conduction cooling surface of 50°C. The actual temperature of most parts is 20 to 30°C below the 85°C assumed part temperature. As indicated by the thermal analysis, those parts above 85°C will be increased in the stress analysis and those parts reduced <85°C will be verified to assure proper parts derating. The temperature of IC's and transistors is based on case temperature, which has to be derived from the thermal analysis junction temperature by the formula $Tc = Tj - R\theta jc*Pwr$. The temperature of capacitors, diodes, resistors, and zener diodes are based on thermal analysis board temperature. Diode power derating is not required per PPL21 and MIL-STD-975M. The thermal analysis calculates the diode and zener junction temperature based on lead length and mounting method.

Every page of the analysis includes a logic statement that automatically prints an asterisk (*) in the Comments column if the actual vs. allowed ratio exceeds 1 for voltage, current and/or power. In the IC stress for –Vin, a negative ratio number is still interpreted as a number < 1 which is acceptable.

MAXIMUM STRESS CONCERNS

No parts in the NSTAR PPU design are operated in an overstressed condition, except those listed in the Out of Derating Summary.

OUT OF DERATING SUMMARY

Input Filter Assembly

Capacitor PWB

Input filter Capacitors: C1 through C8 and C14 through C23 56 uF, 125V, 10% CLR79 type

75V allowed at 70°C 80V actual per capacitor at Vin = 160V (2 capacitors in series)

Stress Ratio = 1.07

Comment: 125V is the highest voltage rating for CLR79 type capacitor

FET's operating with Vds at Vin = 160V

Comment: To meet efficiency of PPU, it was agreed between NASA and HED that the 200V FET's with a Rds(on) = 0.1 Ohms could be used in place of the 500V FET's with a Rds(on) = 0.45 Ohms

Discharge/Housekeeping Assembly

Converter Transistors: Q301 through Q304 IRHM7250

Vds(rating) = 200V Vds(allowed) = 150V Vds(actual) = 160V

Stress Ratio = 1.07

Comment: Used for lower Rds(on) = 0.1 Ohm

Neutralizer/Heater Assembly

Converter Top Transistors: Q1 and Q2 IRHM7250

Vds(rating) = 200V Vds(allowed) = 150V Vds(actual) = 160V

Stress Ratio = 1.07

Comment: Used for lower Rds(on) = 0.1 Ohm

Converter Bottom Transistors: Q3 through Q10 IRHF7230

Vds(rating) = 200V Vds(allowed) = 150V Vds(actual) = 160V

Stress Ratio = 1.07

Comment: Used for smaller size FET – TO205AF (IRHF7230) vs. TO254AA (IRHM7450)

Relay Module

Relay Switching Transistors: Q2, Q3 and Q5 IRHF7230

Vds(rating) = 200V Vds(allowed) = 150V Vds(actual) = 160V

Stress Ratio = 1.07

Comment: Used for smaller size FET – TO205AF (IRHF7230) vs. TO254AA (IRHM7450)

Screen Supply

Converter Transistors: Q301 through Q317 IRHM7250

Vds(rating) = 200V Vds(allowed) = 150V Vds(actual) = 160V

Stress Ratio = 1.07

Comment: Used for lower Rds(on) = 0.1 Ohm

CONCLUSION

All parts used in the NSTAR PPU design are operating well within their derating criteria based on HED B850401, MIL-STD-975M and PPL21, except for the capacitors and transistors listed in the

Out of Derating Summary. Based on the thermal analysis, the actual temperature of most parts is 20 to 30°C below the 85°C assumed part temperature and only a few parts had to be decreased below the 85°C to meet the derating criteria.

As a result of this analysis the following 2 Waivers were generated by HED and granted by NASA GRC.

W002: Stress model indicates Input Filter Assembly (B207201) capacitors C1 through C8 and C14 through C23 (CLR79, 5.6μFd, 10%, 125V) to have a worst case voltage stress of 80V. Derating guideline is 75V maximum. Stress ratio is 1.07. Resolution: Use as is. Worst case will only occur when input line voltage is above 150V, which cannot occur on the DS1 spacecraft.

W004: Input line voltage of 160Vdc causes some FETs to operate worst case above the derating guideline of 150Vdc maximum. The FETs affected are:

Discharge/Housekeeping	Q301-Q304	(IRHM 7250)
Neuralizer/Heaters	Q1, Q2	(IRHM 7250)
Neuralizer/Heaters	Q3-Q10	(IRHF 7230)
Relay Module	Q2, Q3, Q5	(IRHF 7230)
Screen Supply	Q301-Q317	(IRHM 7250)

Resolution: DS1 spacecraft input voltage will never exceed 150Vdc. Higher rated FETs would significantly impact PPU efficiency. Therefore, use as is.

6.2.2.2 Worst Case AC Circuit Analysis

A Worst Case AC Circuit Analysis was performed and summarized in a report (dated January 1997 with an addendum dated 21 February 1997) submitted to NASA Lewis. The abstract is repeated here.

NSTAR PPU AC WORST CASE ANALYSIS

The worst case analysis of the six AC control loops in the NSTAR PPU has been completed. The six regulators include the screen voltage regulator, the discharge current regulator, the neutralizer current regulator, the heater current regulators (two identical circuits), the accelerator voltage regulator and the internal auxiliary voltage regulator. AC computer models, which include the nominal DC bias conditions, were developed and tested for the nominal conditions for each of the regulators using PSPICE operating on a Power Macintosh 9500 platform. A sample of the schematic drawings of these models is included in this report and the computer net lists are available for inspection and review at Hughes EDD. In order to do the worst case analysis each component that influences the phase or gain of the control loop was identified. PSPICE was then used to determine the sensitivity to change of each of these components. A sample of this sensitivity analysis output and component shift printout is included for the discharge current regulator circuit. These sensitivity data can be used to determine if there is any particular component, which has an excessive effect upon the worst case performance of the circuit. After determining the sensitivity of each component, all of the components were changed the direction to generate the worst case for the parameter being studied i.e., bandwidth or phase margin. In order to determine the amount of degradation, Hughes has developed a degradation data base which, in one form or another, used on virtually all of space programs conducted at HED. There were numerous sources used in the development of the referenced data base. The first source used was the MIL-STD 1547. Where this standard was lacking other sources were used which include MIL-R 39005, MIL-R 39007, MIL-R 39008-C, MIL-R 55182F, MIL-C 39003, MIL-C 39006, MIL-C 123, MIL-STD 198E, and MIL-STD 19500. The HAC S&CG PUB. #609 was also used for some resistors capacitors and diodes. The MIL-STD 19500, HAC S&CG PUB. #609 and data from MATRA/MARCONI test report MRCS/NCEG/N 919 was used for some of the semiconductors. Each component type and the total ± degradation forced for each component type is shown in the tables on the following pages. It is very important to note that as the analysis was done there was no attempt to RSS the effects of the component changes. Further, no attempt was made to correlate direction of component shifts with reality. For example, if a worst case condition is developed by allowing the Beta of one transistor to increase while the Beta of a second transistor decreased this was allowed in the analysis. It is known that the Beta degradation of transistors is in the same direction with radiation or temperature and that one transistor cannot experience an increase in Beta while another transistor, in the same environment, has a decrease in Beta. The results of this analysis is in effect a "worst/worst" case. If any regulator had exhibited unacceptable performance when this worst/worst case condition was analyzed then intelligence would have been applied to direction of component shifts. In fact, all the regulators in the NSTAR PPU have acceptable A.C. performance predictions based upon the worst/worst case analysis. The results of this very conservative analysis indicate that all control loops will meet the requirements of Paragraph 8.5.4 of ND-310, which requires and minimum of 35° phase margin and 6 dB of gain margin. In addition, per a JPL CDR action item request, all of the control loops have demonstrated more than 40° of worst case phase margin. The individual Bode plots shown in this analysis predict performance in the nominal and worst case conditions. The data below summarized the results of the analysis. These results can be compared to the breadboard measured data and

from the comparison it is clear that the models accurately represent the circuits being analyzed.

The accelerator (accel) supply is a special case in that it operates in two distinctly different modes. As stated, the power supplied by this supply is nominally very low but in some conditions the load can be at least one order of magnitude above the nominal load. In order to optimize the size and weight of the supply, the engineering decision was made to allow the converter to operate in either the continuous current or the discontinuous mode. What is implied by the statements "continuous current" and "discontinuous current" is the state of the current in the output filter inductor. The basic topology of the converter is that of a "buck" converter. This topology is usually operated in the continuous current mode which causes the transfer function of the converter duty cycle to output voltage to be a second order system. The output voltage is determined by the time average of duty cycle and the input voltage and any transformer ratio if a transformer is used. Furthermore, the output voltage is ideally independent of the load current, provided that the current is above the value that causes the converter to operate in the continuous current mode. The implication in this statement is that there is always some low load current where upon the mode changes to the discontinuous current mode. This is in fact the truth and is the case with this particular design. When a buck converter is operated in the discontinuous current mode, its transfer function changes and becomes first order in nature. The output voltage is dependent upon the energy transferred in each cycle of operation, from the input into the output inductor. This means the output voltage is dependent upon the load current as well as the duty cycle and the input voltage. The computer model of the converter must consider the on time, off time and the discontinuous current time to determine the transfer function of the converter.

Quite often, these converters are modeled as discrete time models and the analysis is performed in the transient mode with the computer simulating the actual switching conditions of the converter. These models, which can be accurate are also very cumbersome. They require a great deal of computer power and computing time. To do a worst case analysis, where many components must be varied in order to determine component sensitivity, the transient switching model becomes almost impossible to apply. An average model, if appropriately designed and constructed, can be used to analyze a buck converter operating in the discontinuous mode. There have been a number of papers published which address average modeling of discontinuous current mode converters, including papers by R.D. Middelbrook, V. Vorperian and others. The model used to do the discontinuous current mode worst case analysis reported in this document was developed by Dr. Kiran Kantak of Hughes Electronics. The model has shown itself to be very accurate when compared to actual laboratory measurements. The continuous current model used in this analysis was developed by G. I. Cardwell and has also proven to be an appropriate continuous mode model.

6.3 The DCIU

6.3.1 Thermal Analysis

A SINDA3D model of the DCIU was generated and presented during the Critical Design Review held on October 1-3, 1996. The worst case temperatures for each of the three DCIU boards (and the PPU Slice) are presented here in graphic format.

Conclusion:
The thermal design of the DCIU provides sufficient conduction cooling and maintains all component junction temperatures at or below the maximum allowable temperature of 100°C.

Figure 33. Photo of DCIU

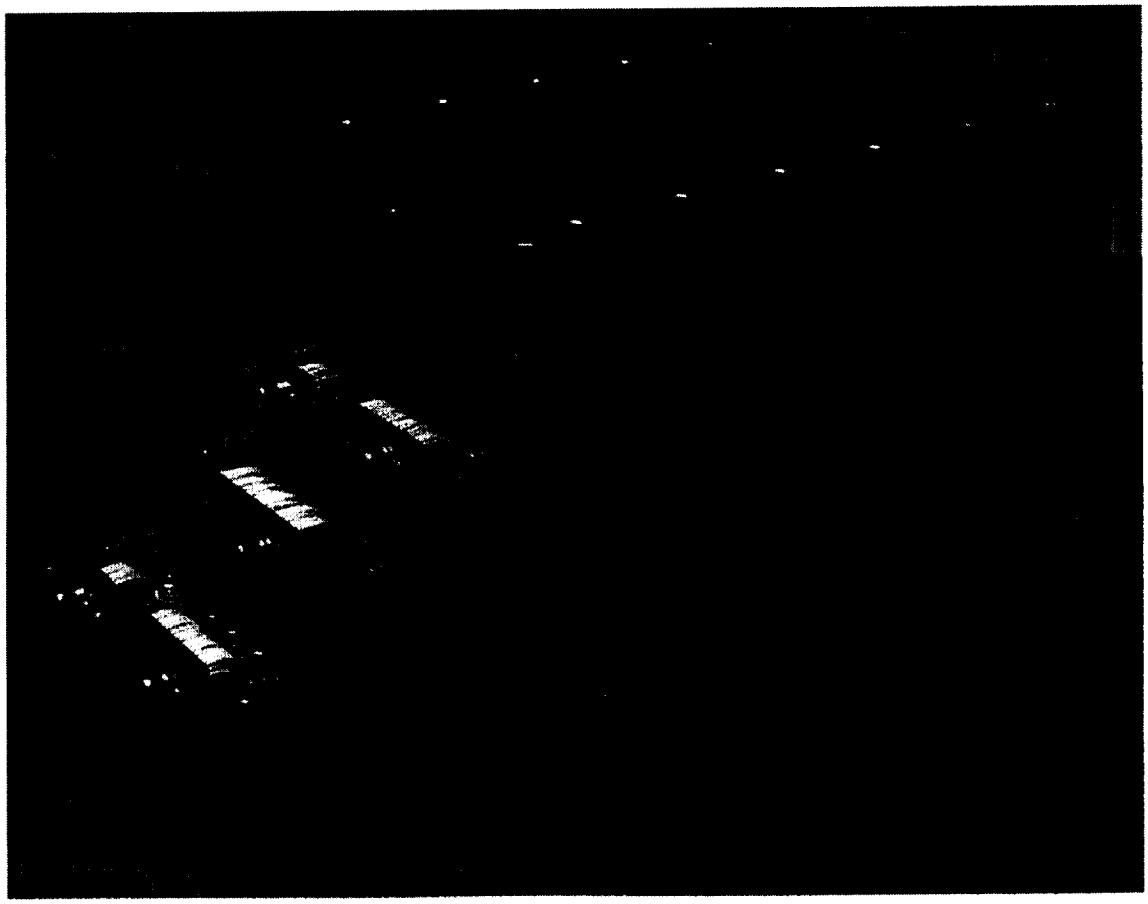

Figure 34. CPU, Data Acquisition, and Valve Driver Boards

Figure 35. PPU Slice

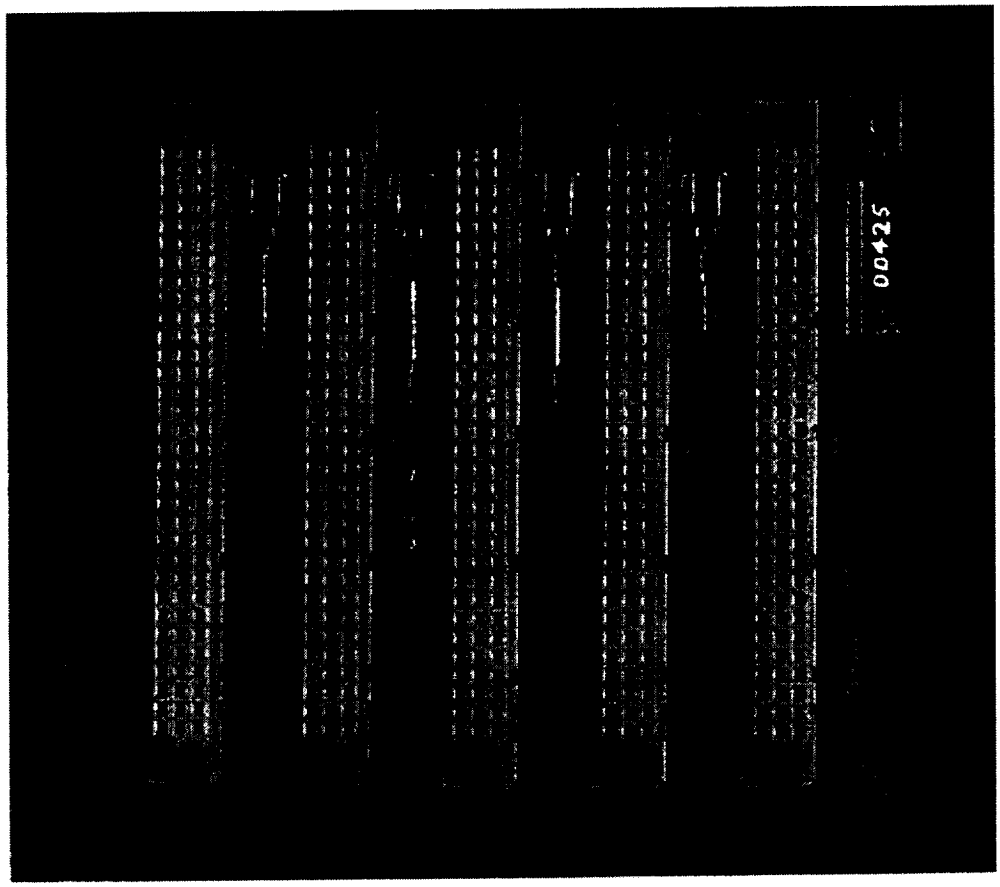

Figure 36. DCIU Backplane

- **Predicted Temperature Distribution for Data Aquisition PWB**

  - Fixed Chasis Temperature of 71 °C
  - Wedge Lock Thermal Resistance of 0.875 °C/W
  - Total Power Dissipated in Model 1.710 Watts

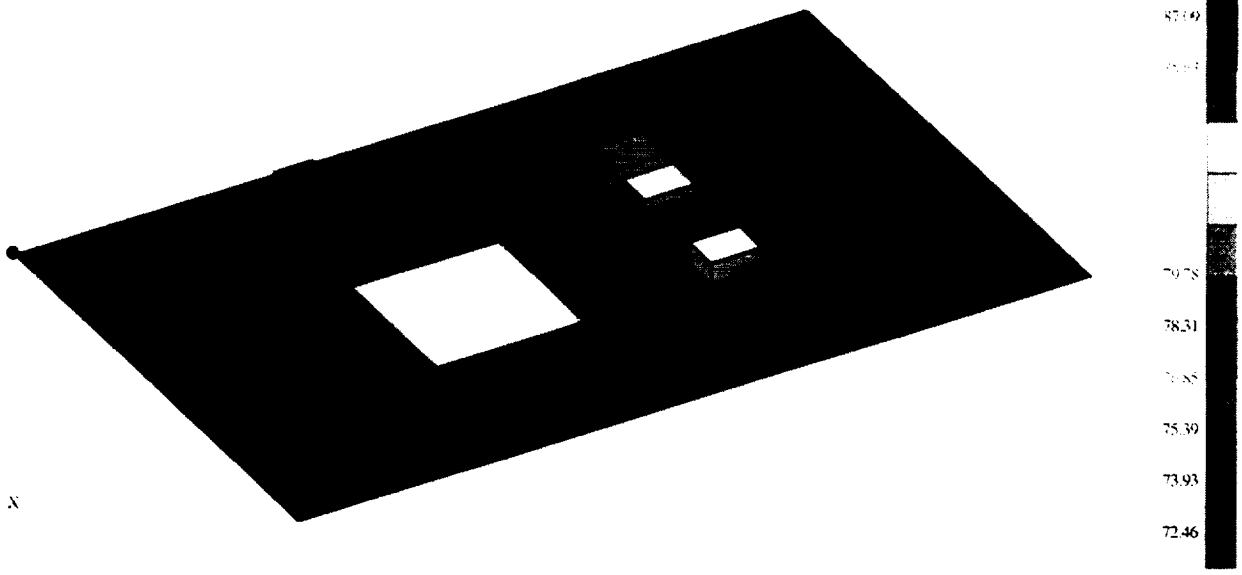

- **Predicted Temperature Distribution for Valve Driver PWB**

- Fixed Chasis Temperature of 71 °C
- Wedge Lock Thermal Resistance of 0.875 °C/W
- Total Power Dissipated in Model 3.700 Watts

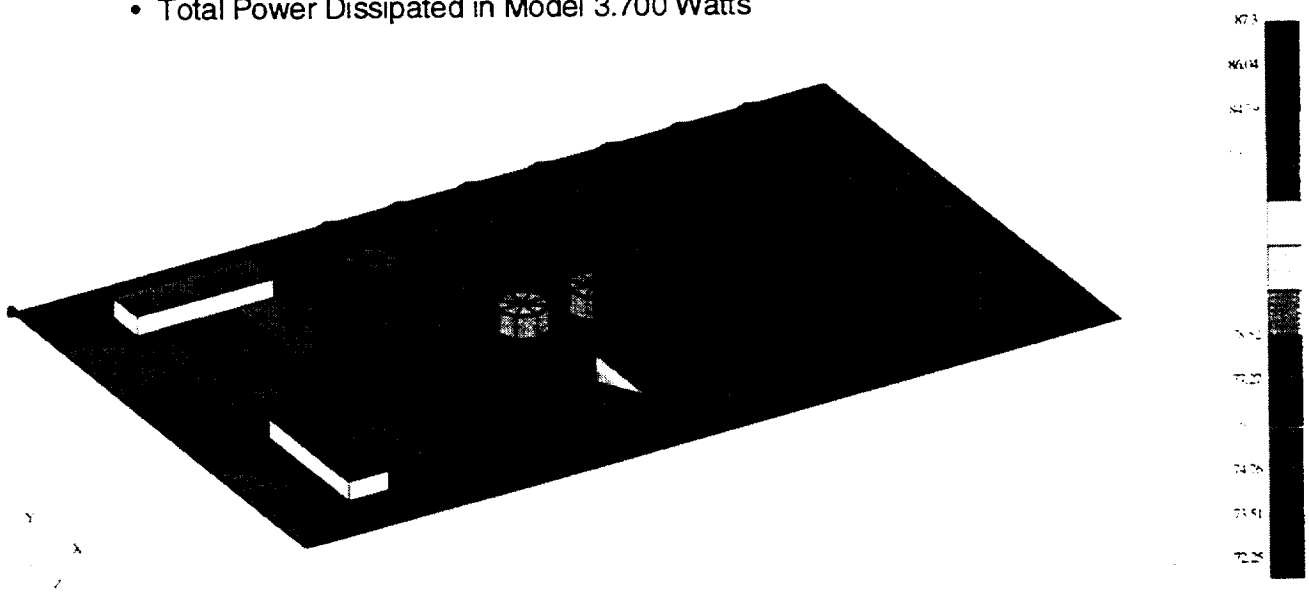

- **Predicted Temperature Distribution for Slice PWB**

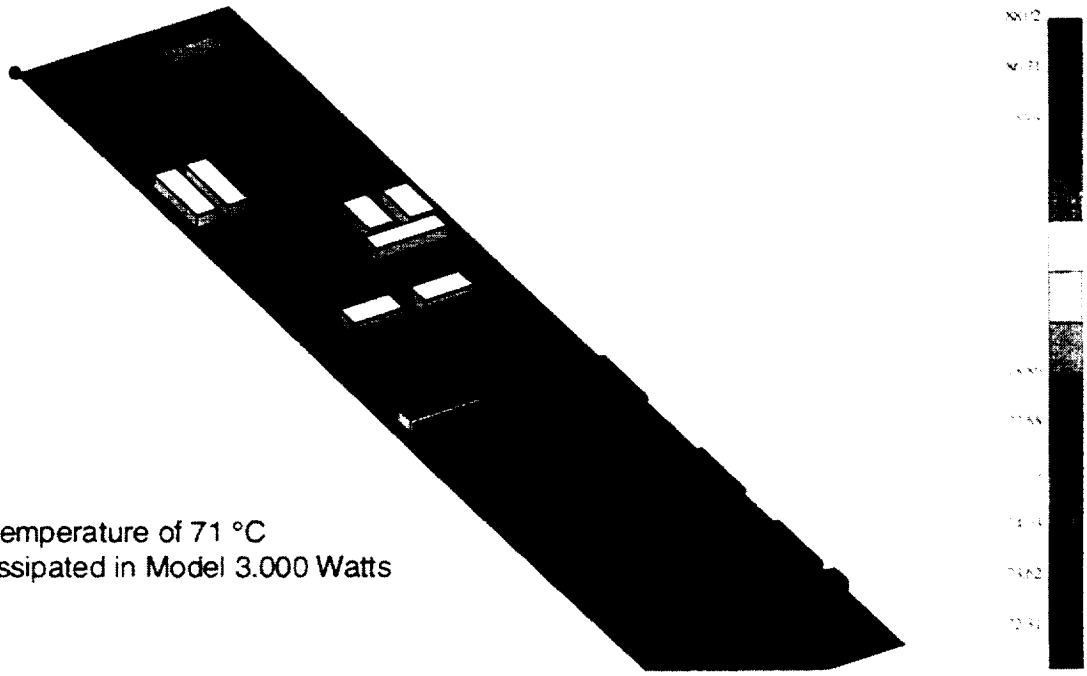

- Fixed Chasis Temperature of 71 °C
- Total Power Dissipated in Model 3.000 Watts

- **Predicted Temperature Distribution for Processor PWB**

- Fixed Chasis Temperature of 71 °C
- Wedge Lock Thermal Resistance of 0.875 °C/W
- Total Power Dissipated in Model 4.260 Watts

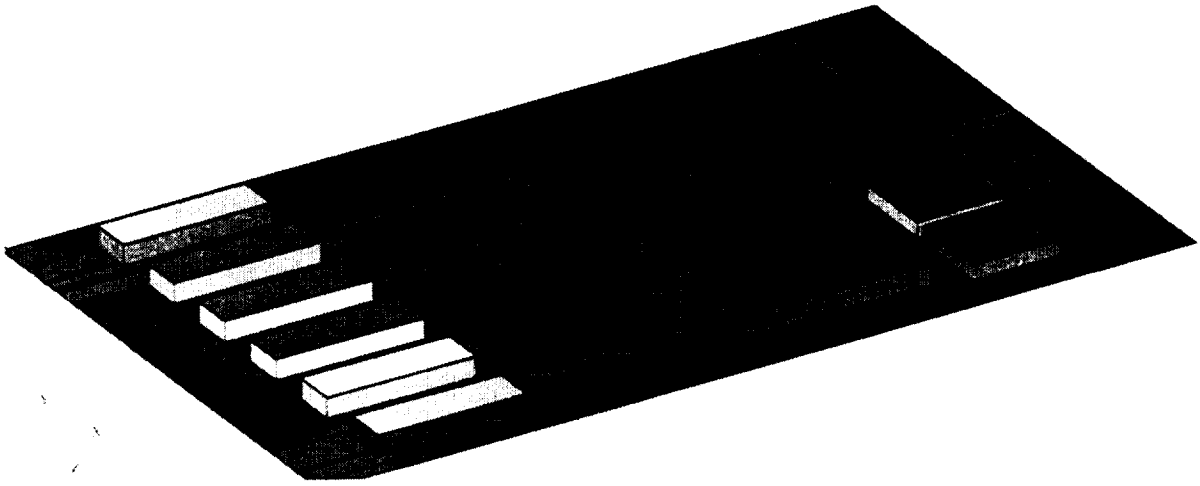

7 FLIGHT SYSTEM PRODUCTION

7.1 Flight Thruster Production

HED produced two flight-design thrusters for the NSTAR program.

7.1.1 Pathfinder

The Pathfinder Thruster (PFT) was built first ,using flight quality parts, to prove out the piece part designs and to develop and refine the thruster subassembly and assembly manufacturing processes. This included the development and qualification of brazing schedules, grit blasting for surface conditioning, schedules for spot welding, TIG welding and EB welding and the riveting processes for the grids and the discharge chamber assemblies. Detailed processing and assembly instructions called Operation Sheets (OS) were generated for each thruster assembly step. Piece part design drawings and assembly drawings were redlined when changes were made during the PFT fabrication. HED produced all the parts and assemblies for the PFT thruster except the swaged heater assemblies, which were fabricated by NASA GRC. HED performed the heater acceptance testing. HED also purchased swaged heaters from Semco for the purpose of qualifying them for the NSTAR program. Due to funding limitations, however, the Semco heaters were not qualification tested. Following the completion of final assembly, the PFT was delivered to NASA, GRC for performance testing. Following a series of rework operations, the thruster worked exactly as expected and met all the NSTAR performance requirements. The Pathfinder Thruster fabrication and test milestones are listed in Table 8. It was then installed into the DS1 spacecraft, where it successfully passed system level vibration, shock and solar thermal vacuum testing.

7.1.2 Flight Thruster 1

The first Flight Thruster (FT1) was built immediately following the PFT. Due to the tight schedule required for the DS1 spacecraft integration, NASA approved the use of redlined drawings and assembly instructions (OS) for the fabrication of the thruster. The FT1 was delivered to NASA where it was integrated with the PPU and DCIU. The Flight Thruster (FT1) fabrication milestones and rework operations are listed in Table 9. It successfully completed all flight acceptance testing and was installed in the DS1 spacecraft.

7.1.3 Pathfinder Refurbishment to Flight Thruster 2

Following spacecraft testing, the Pathfinder thruster was returned to HED and upgraded to the identical configuration of the first Flight Thruster (FT1) to become the second Flight Thruster (FT2). The upgrade of the PFT involved the addition of a discharge cathode magnetic pole piece, a new discharge cathode/keeper assembly, a new neutralizer cathode/keeper assembly, a new ion optics assembly, and a modified

power cable assembly. The resulting FT2 thruster was delivered to NASA for integration with the PPU and DCIU , followed by flight acceptance performance and environmental testing. The FT2 successfully met all NSTAR thruster requirements. The FT2 is currently being used in the 12,000 hour NSTAR Mission Profile Wear Test at JPL.

TABLE 8. PATHFINDER/FT2 THRUSTER MILESTONES

DATE	MILESTONE
02.25.97	Grid forming at GRC
03.13.97	GRC supplied cathode heaters
09.08.97	PFT assembled at HED
09.11.97	PFT delivered to GRC Machine screw-heads for clearance, replace ion optics insulators Grit-blast screws, replace cathode terminal screws
09.29.97	Start first functional test at GRC (SKITPACK)
10.13.97	PFT delivered to JPL Vibration Test on DS1
11.20.97	PFT delivered to HED HV isolator replacement Cathode braze repaired, Wiring replaced Install EMT4 ion optics
12.24.97	Start functional test #2 at JPL (JPL lab power supplies)
01.05.98	Delivered PFT to DS1 for STV (PPU 31, DCIU #1)
03.21.98	PFT delivered to GRC
03.24.98	Remove TCs and inspect PFT
04.09.98	Start rework; install ring pole-piece at cathode Replace cathode/keepers Replace ion optics with new set Replace helicoil on gimbal bracket Remove Kynar from cable Now PFT becomes FT2
05.06.98	Start FT2 functional and integration tests (PPU #1, DCIU #1)
05.27.98	Random vibration tests at JPL
06.01.98	Install reworked cable on FT2; install TCs near cable/thruster interface
06.02.99	Start functional and thermal vacuum tests (FT2, PPU #1, DCIU #1)
06.12.98	Post thermal-vacuum functional (SKITPACK)
08.12.98	Install 5 TCs and bring out SG lead in prep for MPT In addition to the NSTAR neutralizer, ship a low flow neutralizer (characterized on EMT40 to JPL for installation on FT2 prior to the ELT.

TABLE 9. FLIGHT THRUSTER (FT1) MILESTONES

DATE	MILESTONE
02.25.97	Grid forming at GRC
03.13.97	GRC supplied cathode heaters
07.28.97	Discharge chamber assembled, grit-blasted wire mesh assembled at GRC
10.30.97	Delivered to GRC; install Ta gasket around neutralizer box
11.03.97	Start first functional test at GRC (SKITPACK)
11.13.97	Replace wiring and some fasteners
12.05.97	Install the original PFT ion optics on FT1 Install gimbal bracket cover
12.08.97	Start second functional test (SKITPACK)
12.16.97	Rework including heater potting, fasteners, and HV isolator thermocouples
01.22.98	Start third functional test (SKITPACK)
01.30.98	Integrate PPU #2/DCIU #2/FT1b; functional test
.01.30.98	Start Thermal Vacuum Tests (PPU #2 and DCIU #2)
02.04.98	Hot PPU/cold FT1b; hot restart with RTD at 155°C
02.05.98	Cold PPU/cold FT1b; hot restart with RTD at 155°C
02.10.98	Rework: remove TCs, install one helicoil insert, install new shorter thruster cable.
02.25.98	Rework: remove Kynar shrink tube from cable, install Kapton wrap on thruster end of cable at JPL.
02.27.98	Vibration test at JPL
03.13.98	Functional test after vibration test (JPL power supplies)

7.2 Flight PPU Production

7.2.1 PPU1 and PPU2

Two Power Processor Units were designed and built by HED. The basic configuration has been discussed elsewhere in this report. The complexity of this device is immense. It contains over 2500 electronic components and is roughly 5 times more complex than a typical EPC (Electronic Power Conditioner – a high voltage power supply designed to run a travelling wave tube) built at HED. Each PPU contains approximately 750 separate wires (1500 solder connectors) running between densely packed modules.

7.2.2 Rework of PPU1 and PPU2

GRC and JPL thermal vacuum test data indicated large temperature gradients between the Screen Supply transformer cores and their heat sink brackets. The units were reworked to provide a mechanically tighter fit between the cores and their brackets. Furthermore on PPU2, the beam supply output inductor was removed and replaced with a new part using a new bond adhesive rated for higher temperature. During integration testing at JPL, spurious recycles were experienced with PPU2. This spontaneous events were traced to a spurious setting of the PPU fault flag on the slice board. This was apparently caused by switching noise present on the input to the digital latch. The DCIU interpreted the noise as a PPU fault, incremented the recycle counter and reset the PPU. DCIU software was modified to force the DCIU to poll the output of the Beam Supply when the fault flag was set, which must be zero in the case of a true PPU fault. Both conditions must now be met before the DCIU counts a recycle and performs a reset. This modification successfully eliminated this recycle problem.

The improvements incorporated into PPU2 as a result of experience with PPU1 assembly and test were then retrofitted into PPU1. This upgrade effort included added heatsinking of the beam power supply diodes, adding parallel diodes to the beam supply rectifier circuits, adding bypass wiring to the output relays, replacement of the beam supply output inductor, replacement of the RS-422 receiver chip on the slice board, addition of a chassis ground to the J6 connector, addition of heat-shrink tubing to selected wires, beam supply hexFETs were replaced as a precaution, and the select-in-test resistor controlling the Undervoltage Trip function was reduced to allow operation at a lower spacecraft bus line voltage. After rework, both units were again Qualification/Acceptance tested at NASA GRC. PPU1 became the flight unit on DS1 and PPU2 is scheduled to be part of the Extended Life Test at JPL.

7.3 Flight DCIU Production

7.3.1 DCIU1 and DCIU2

Both DCIUs were manufactured at Spectrum Astro, Inc for HED.
The original flight design incorporated three distinct printed wiring board modules in a card cage style aluminum box. Due to a desire for future mission flexibility, the box was expanded to include a spare board slot. This slot can be used for various functions such as increased DCIU memory, computing capability, or more valve drivers to handle more complex XFS systems.

In addition to the DCIU hardware, Spectrum Astro wrote the software code to operate the XFS and the PPU. Each DCIU is capable of operating 4 PPUs (8 Thrusters).

7.3.2 Rework of DCIU1 and DCIU2

The following DCIU rework was necessary:

1. The RS-422 chips were inadvertently damaged in test and replaced.
2. The 14 valve driver board opto-isolators were found to be from a suspect vendor lot and were replaced on each DCIU. Each DCIU went through penalty testing under NASA GRC direction.
3. The DCIU software was revised several times throughout the NSTAR test program - both during acceptance/qualification testing and during spacecraft integration.

7.4. Selected Subassembly Mass Breakdowns

Refer to Table 10.

Table 10 Selected Mass Breakdown Data

PPU1 MASS BREAKDOWN

SCREEN SUPPLY	2.800 kg
DISCHARGE SUPPLY	2.000
NEUTRALIZER/HEATERS SUPPLIES	2.150
SLICE and WALL	0.425
OUTPUT SECTION	0.850
INPUT FILTER	1.250
WIRING	1.100
BASEPLATE	0.890
BACK WALL	0.100
MOUNTING COLUMNS (4)	0.350
TOP COVER (MICROMETEOROID SHIELD)	2.055
SIDE WALLS (3)	0.590
MISCELLANEOUS HARDWARE	0.150
TOTAL	**14.51**

FLIGHT THRUSTER MASS BREAKDOWN

DISCHARGE CHAMBER and MOUNTING BRACKET ASSEMBLY	4.30 kg
OPTICS ASSEMBLY & MOUNTING INSULATORS	2.00
PLASMA SHIELD	0.44
FRONT MASK ASSEMBLY & SUPPORTS	0.30
DISCHARGE CATHODE/KEEPER ASSEMBLY	0.25
NEUTRALIZER CATHODE./KEEPER ASSEMBLY	0.41
INTERNAL WIRING	0.50
TOTAL	**8.20**

FLIGHT THRUSTER/PPU CABLE MASS BREAKDOWN

	Length (in)	Mass (kg)
CABLE FROM PPU TO FIELD JOINT:	120	0.95
CABLE FROM THRUSTER TO FIELD JOINT:	74	0.77
TOTAL	**194**	**1.72**

8 FLIGHT SYSTEM QUALIFICATION/ACCEPTANCE TESTING

8.1 Test flow chart

Refer to the following flow chart (Figure 37) and Table 11 for a summary of the testing plan for the NSTAR hardware/software. There were some modifications to this plan in the actual test implementation. Note that FT1, PPU1 and DCIU2 comprise the flight set flown on DS1. FT2, PPU2 and DCIU1 served initially as a flight set spare and were subsequently dedicated to the NSTAR Extended Life Test.

Figure 37. NSTAR Subsystem Test Flow

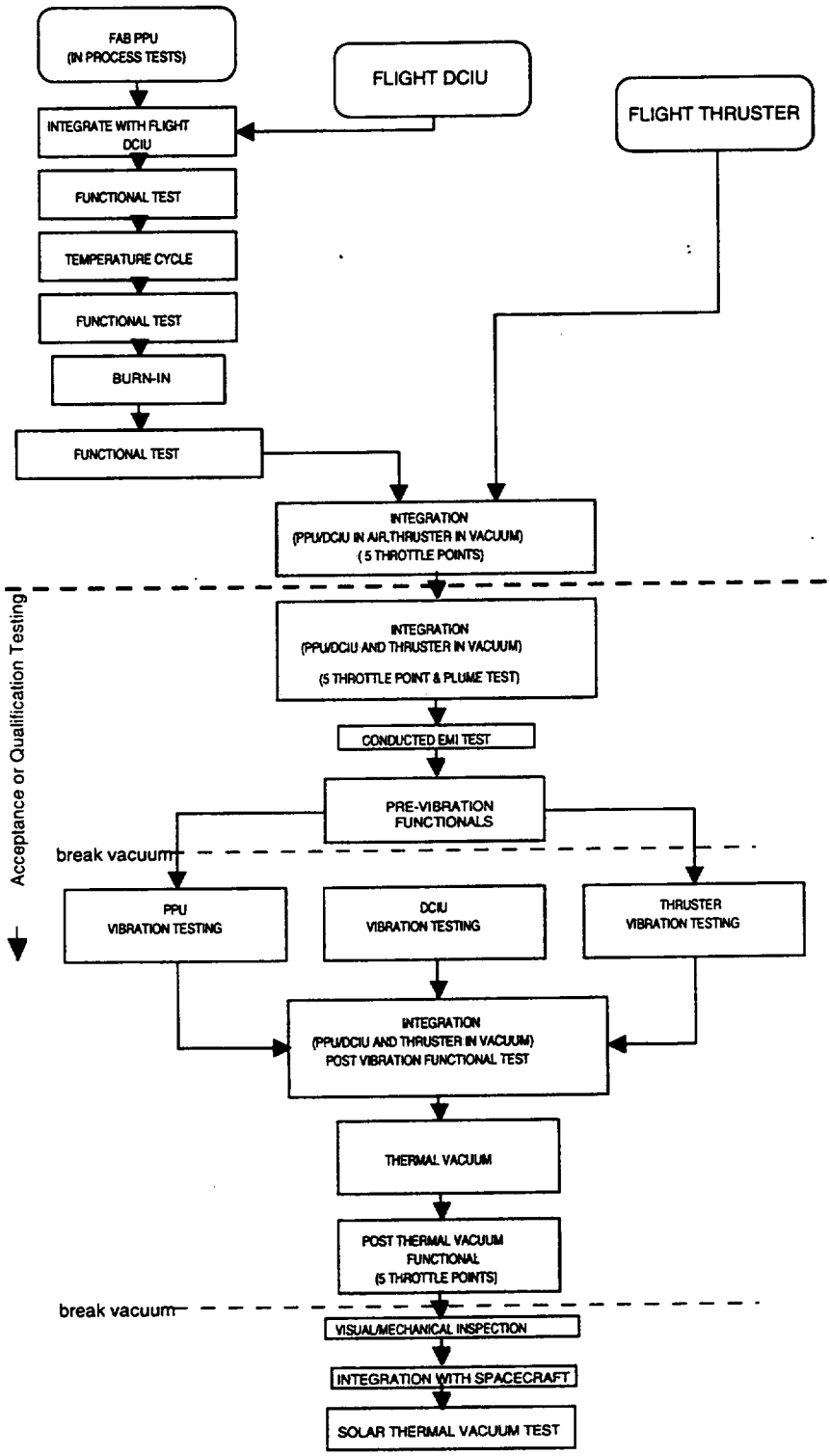

Table 11: Description of Tests

TEST BLOCK TITLE	TEST DESCRIPTION	INPUTS	LOAD
INTEGRATE WITH DCIU	Connect flight PPU and DCIU together. Test all DCIU command and telemetry modes	Power Supplies Computer interface to DCIU	Resistive Load Bank
FUNCTIONAL TEST	Test of all PPU operating modes, telemetry as well as fault protection/recovery @ 500W and 2500 W output levels	Power Supplies and Computer interface to DCIU	Resistive Load Bank
TEMPERATURE CYCLE	10 non-operating cycles between -20 and +70°C	Power Supplies Computer interface to DCIU	Resistive Load Bank
BURN-IN	100 hours operation in air at +50°C operating at the 2.5 kW level	Power Supplies and Computer interface to DCIU	Resistive Load Bank
INTEGRATION WITH THRUSTER (in air)	Setup: Thruster in vacuum. PPU and DCIU in air. Test: Basic functions of PPU at five output levels	Power Supplies and Computer interface to DCIU	Flight Thruster
INTEGRATION WITH THRUSTER (in vacuum)	Setup: Thruster, PPU and DCIU in vacuum. Test: Basic functions of PPU at five output levels	Power Supplies and Computer interface to DCIU	Flight Thruster
THERMAL VACUUM	Test: 8 thermal cycles in vacuum between -20 and +50°C	Power Supplies and Computer interface to DCIU	Flight Thruster
INTEGRATION WITH SPACECRAFT	Mount on DS1 Spacecraft. Test: Full functional testing on spacecraft.	Spacecraft power using a solar array simulator. Control via spacecraft computer.	Resistive Load Bank
SOLAR THERMAL VACUUM TEST	Mount on DS1 Spacecraft. Test: Full functional testing on spacecraft UNDER VACUUM. Thruster was fired for approx. 15 minutes.	Spacecraft power using a solar array simulator. Control via spacecraft computer.	Resistive Load Bank/THRUSTER

Flight-Set Tests and Delivery of Flight Hardware

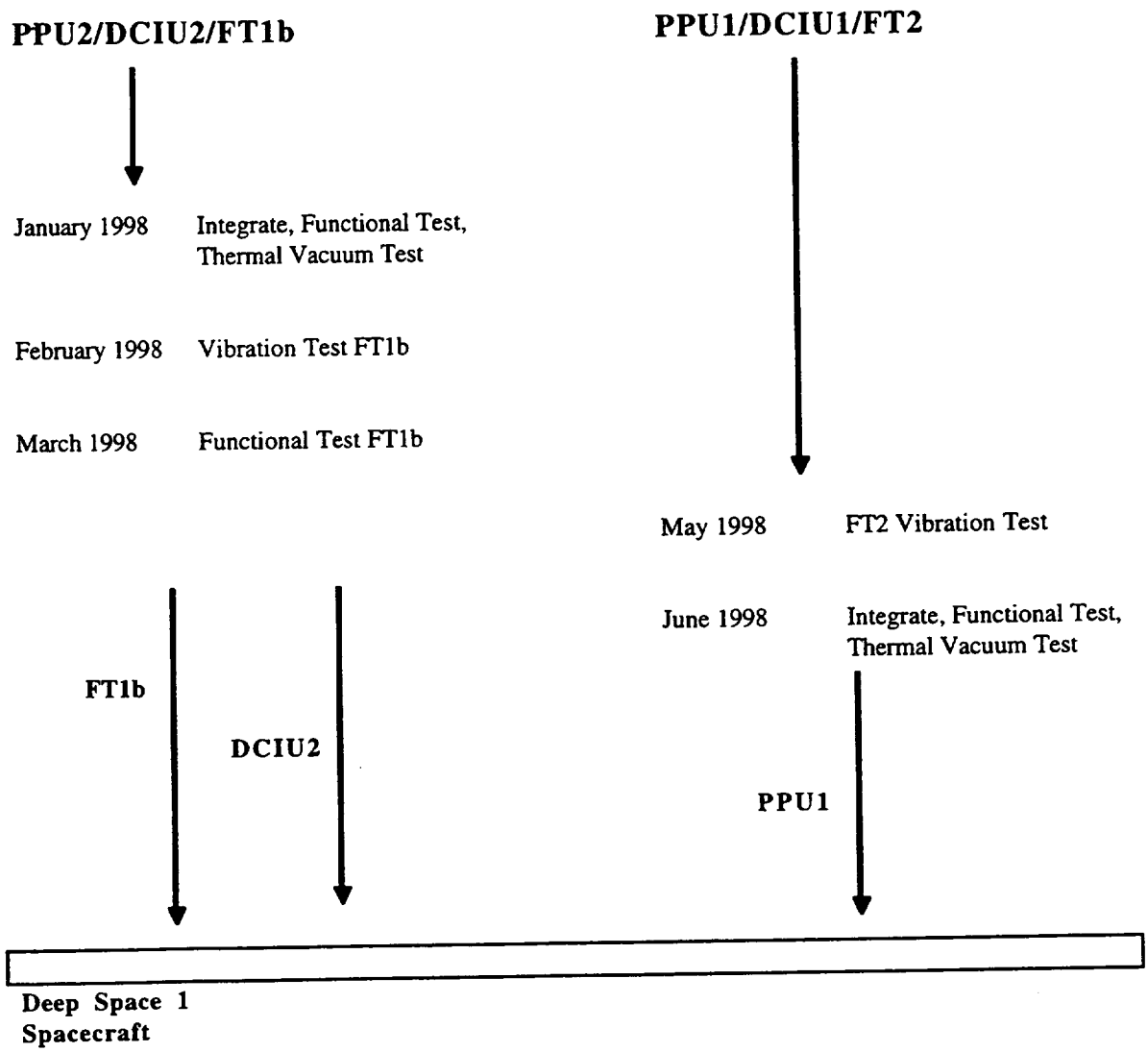

8.2. Flight Thruster Qualification/Acceptance Tests at NASA

8.2.1 Acceptance Test Plan

The Flight Thrusters performance and acceptance tests were performed at NASA GRC and JPL. The Pathfinder underwent thruster performance and thermal tests at GRC and then spacecraft level integration and thermal tests at JPL. After performance and environmental testing of FT1 was completed, it was installed onto the DS1 spacecraft. After Pathfinder was rebuilt to become FT2, performance and environmental testing was completed at GRC. After launch of FT1, FT2 was used in the ongoing 120 kg xenon throughput (equivalent to 12,000 hours operation at full power) mission profile test at JPL.

In this section, V. Rawlin of NASA GRC describes the results of the short term, in vacuum performance and thermal tests on the Pathfinder, FT1, and FT2 thrusters. These tests are described in greater detail in the published paper AIAA-98-3936.

Procedure

Planned thruster testing consisted of an initial Standard Functional Test which evaluated thruster performance over the power throttle range using the laboratory power system. This test characterized the neutralizer behavior as a function of xenon flow, first without beam extraction and later at full thruster power. Thruster performance was obtained at five or more of the NSTAR throttle points shown in Table 12 for comparison with earlier EMT performance or that of the other First Thruster.

Prior to the first ignition after exposure to air, the cathodes were prepared for operation with a 5 hour conditioning procedure. For normal thruster starts, the neutralizer was ignited first, followed immediately by ignition of the main discharge. Then, after 20 seconds, the beam extraction voltages were applied at the TH0 conditions of Table 12. The flows, beam voltage, and accelerator voltage were adjusted to TH15 values and then the discharge current was slowly increased until the beam current reached 1.76 A. After two hours (the thruster thermal time constant), a data set was obtained and thruster testing was usually terminated for the day. On the following day, the thruster was restarted at TH0, TH4, TH8, TH10, and TH15. However, some data were acquired at other power levels as the anticipated maximum thruster power level for DS1 varied over time.

In addition to electrical and propellant utilization efficiencies, each Standard Functional Test measured: the neutralizer characteristics, the optics perveance margin (difference between the Table 12 operating point and the minimum total accelerating voltage at the Table 12 beam current), the minimum accelerator grid voltage required to prevent electron backstreaming from the neutralized ion beam into the discharge chamber, and the ratio of doubly-to-single-charged ion currents emanating from a thin area across the thruster diameter. Standard Functional Tests were conducted after each thruster milestone; fabrication, Vibration Test, and Thermal Vacuum Test.

In addition to standard Functional Tests, each Flight Thruster was integrated with a Flight PPU/DCIU while following an abbreviated functional test plan (no neutralizer characterization, perveance margin, or electron backstreaming data were taken). Later, during the thruster Thermal Vacuum Test, the cold-soaked thruster was twice started and operated with the PPU/DCIU, once when the PPU/DCIU was hot and also when it was cold. Again, an abbreviated functional test was conducted.

Test Chronology

Table 13 lists, in chronological order, the tests conducted with each thruster. The order of testing varied due to the availability of facilities and/or a PPU/DCIU. A general description of each test and the major results are given here while detailed thruster performance is reported in the next section.

Pathfinder Thruster (PFT)

The first Standard Functional Test of the PFT started on October 1, 1997 with a pre-ignition cathode conditioning procedure and neutralizer characterization without beam extraction. Then, over the next few days the thruster was throttled to full power with dwell times at power levels TH0, TH11, and TH15 to obtain steady-state thruster temperatures. Next, the PFT was cold soaked to –92°C at the RTD. Discharge ignitions were successful. However, rapid throttle to full power was prohibited by insufficient electron backstreaming voltage margin, believed to be caused by a too-close initial grid-to-grid spacing when the high voltage was applied. To avoid this condition, the start-up accelerator grid power supply voltage was increased to 250 volts for 2 hours (the ion optics thermal time constant) and then reset to the appropriate lower run value.

After tests at GRC, the PFT was returned to HED to prepare it for DS1 spacecraft level vibration and thermal tests at JPL. After the vibration tests, the PFT's ion optics were removed to be used on FT1 and optics from EMT4 were used on the PFT for spacecraft thermal tests at JPL.

First Flight Thruster (FT1)

The first Standard Functional Test of FT1 was conducted in November 1997. Because the original kFT1 grid set had inadequate electron backstreaming margin, the ion optics assembly from the PFT was used on FT1.

Next, FT1 was successfully integrated with the second flight PPU/DCIU set yielding thruster performance identical to that with the laboratory power supplies. Both the thruster and power processor were started at room temperature conditions. The PPU2/DCIU2 set baseplates were maintained at 25°C, but, FT1 was allowed to rise to its normal operating temperatures. This combination was then used for Qualification level Thermal Vacuum Tests. PPU2/DCIU2 was subjected to several 12-hour thermal cycles, alternating between –30°C and +50°C, while operating into resistive load. During these cycles, the non-operating thruster was cooled to –97°C and then started using a hot (+50°C) PPU2/DCIU2 set (HPCT). Neutralizer ignition was delayed, as expected, due to the longer time required to reach approximately 1100°C with a fixed heater current. All thruster performance was nominal. The thruster was then turned off and cooled again to
–97°C. The next thermal cycle was started with a cold (–30°C) PPU2/DCIU2 set (CPCT). Again, neutralizer discharge ignition was delayed, as expected, and thruster performance was normal.

FT1 was then sent to JPL for Qualification level Vibration Tests, a final fourth Standard Functional Test with laboratory power supplies was performed, and installation onto the DS1 spacecraft was completed. FT1. PPU1 and DCIU2 were successfully flown on DS1 even though this combination of components was never integrated and tested on the ground. This demonstrates the interchangeability of the components.

Flight Thruster (FT2)

In February 1998, the PFT (with EMT4's ion optics) successfully completed an Ion Thruster Compatibility Test and Solar Thermal Vacuum Tests on the DS1 spacecraft. The entire NSTAR ion propulsion system, including the xenon feed system, the PFT, and PPU1/DCIU1 set, was

operated under spacecraft control in a large (7.6 m diameter) vacuum chamber with solar simulation. After the integration tests were completed, the PFT, PPU1, and DCIU1 were removed from the spacecraft to be reworked into flight-worthy hardware. The PFT received new propellant isolators, ion optics, a new discharge cathode assembly, and a new neutralizer assembly and was redesignated FT2.

On May 11, 1998, the first Standard Functional Test of FT2 was started and all operations were nominal. Shortly thereafter, FT2 was integrated with an upgraded PPU1/DCIU1 combination and, again, thruster performance was normal. FT2 was then sent to JPL for Vibration Tests and returned to GRC for a post-Vibration Test Standard Functional Test and Thermal Vacuum Testing. Meanwhile, PPU1/DCIU1 underwent Acceptance level Thermal Vacuum Testing with a resistive load. The second Standard Functional Test of FT2 was nominal as were its two abbreviated functional tests during the thruster Thermal Vacuum Test (hot, 55°C PPU1/DCIU1 set, the cold, –20°C PPU1/DCIU1 set). A third Standard Functional Test of FT2 (post-Thermal Vacuum Test) was conducted and also gave nominal performance. NSTAR testing GRC was complete and FT2 was removed from the vacuum chamber and stored as a Flight Spare. PPU1 was selected to become the Flight power processor and was installed onto the DS1 spacecraft.

Thruster Performance

This section discusses, in detail, the performance of each thruster for the tests shown in Table 13. First, PFT temperatures are compared with those of EMT4 in Table 14. Then, component performance for the neutralizer, discharge chamber, ion optics, and beam properties are compared. Finally, thruster efficiency and dispersion are discussed. An enormous quantity of performance data was accumulated and it cannot all be displayed here. The steady-state data for the first Standard Functional Test for each thruster are presented in Tables 15, 16, and 17, respectively. The format for each Table follows that used at GRC and JPL for short-term and endurance tests. Each Table gives the electrical parameters (power supply outputs), xenon flows, calculated performance, measured performance (when a thrust stand was used), optics performance, beam measurements, and facility measurements for each thruster operating point. Data for FT1's last Standard Functional Test at JPL is shown in Table 18. Table 19 shows all of the full-power data obtained with FT1 throughout its performance Acceptance and Qualification Testing.

PFT Temperature

The most temperature sensitive components of the thruster are the cathode inserts and the rare-earth permanent magnets. Insert temperatures are controlled by cathode design for the known emission current, but, magnet temperatures are a result of their environment. As the flight thruster design evolved due to mechanical and lifetime considerations, materials and surface treatments were altered to maintain maximum magnet temperatures below 310°C and provide margin from their stabilization temperature of 350°C, beyond which irreversible losses will occur. To verify temperature compliance, component temperatures of the PFT were measured and are compared to those of EMT4 in Table 14.

Steady-state temperatures of the PFT were obtained as TH0, TH11, and TH15 while those of EMT4 were taken at only TH11 and TH15. The aft and middle magnet rings were about 20°C lower for the PFT while the forward (optics end) magnets were similar or slightly warmer than EMT4. The ion optics mounting ring base temperature did not change, but, the accelerator grid stiffening ring was 18°C hotter than EMT4. The plasma screen mask temperatures were comparable for both thrusters, but, the titanium gimbal pads of the PFT were about 50°C hotter

than the stainless steel gimbal pads of EMT4. The adiabatic can covering the upstream portion of the thrusters was about 20°C hotter for the PFT.

It is believed that a more complete surface emissivity enhancement (grit-blasting) and the use of titanium magnet retainers (rather than aluminum as on EMT4) led to higher sheet metal temperatures between the magnet rings resulting in more heat radiation from those surfaces in the PFT and less heat conduction to the magnets. Additionally for the flight design, the insulators which were used to electrically isolate the grounded gimbal pads from the high-voltage discharge chamber were constructed from alumina which is thermally more conductive than the insulators used in the EMTs. Thus, the PFT titanium gimbal pads, which had a greater thermal input and were attached to the spacecraft simulator with thin, low thermal conductivity titanium straps, ran hotter than the stainless steel gimbal pads and thick aluminum mounting structure used for EMT4.

Neutralizer

In all room temperature thruster starts, the neutralizer keeper discharge lit within 15 seconds of the application of keeper voltage (32 volts DC and 5-700 volt ignition pulses), often without the igniter pulses.

After neutralizer ignition, the next part of the Standard Functional Test was to characterize the operation of the neutralizer assembly without the main discharge or ion beam. The neutralizer flow was increased from 3.6 sccm to 5 sccm and then slowly decreased as the DC and AC components of the keeper voltage and current were recorded. When the AC component of the voltage reached 5 volts peak-to-peak, an indication of "plume" mode operation, the parameters were noted and the flow returned to 3.6 sccm, the starting value. Operation was limited to 5 volts peak-to-peak to avoid excessive orifice plate erosion.

Figure 39 shows the keeper DC voltage characteristic for the first Functional Test of each of the three neutralizers. At 5 sccm, the DC voltage was approximately 16 volts and rose, as expected, with decreasing flow to about 26 volts at 2 sccm. Over this flow range the peak-to-peak AC voltage component increased from less than a volt to 5 volts.

Figure 40 shows the neutralizer characteristic for four Standard Functional Tests of FT1's neutralizer (the first test was repeated after a facility power interruption). Variations between thrusters and between tests with a given thruster were minor. The characteristics for FT2 (new neutralizer) were nearly identical to those for FT1.

With beam extraction and the thruster at full power, the neutralizer flow was reduced from the nominal flow of 3.6 sccm to the minimum possible value of 2 sccm while observing the DC and AC components of the keeper voltage and current and the thruster floating voltage. In all cases, there was little or no change (about 1 volt maximum) from the full power values shown in Tables 15-18 for a given thruster. This consistency also existed for the other thrusters.

Discharge Chamber

With the exception of initial neutralizer characterizations described above, the main discharge voltage was applied after the neutralizer ignited. In all cases, the main discharge ignited immediately upon application of 32 volts to the discharge keeper and anode. Then the thruster was power-throttled as mentioned earlier.

Figure 41 shows the optimum discharge losses, from the first Standard Functional Test of each thruster, as a function of thruster input power. The optimum discharge power (a trade between thruster efficiency and thruster lifetime) was found to occur at a discharge propellant efficiency of about 0.9, except at the lowest power-throttle levels where the fraction of neutrals lost of was

high. There, the discharge losses increased even at lower (about 0.83) propellant efficiencies. In general, the discharge losses, at near-constant propellant efficiency, decreased from about 230 W/A (also expressed as eV/ion) to about 190 W/A as the thruster power was increased from 0.5 kW to 2.3 kW. Table 19 shows that FT1 with FPT's optics had full-power discharge losses of 185+/–5 eV/ion for eight different functional tests at GRC covering a three-month period. Variations in discharge losses, for a given thruster or between thrusters, at any given power level were less than 12 percent. Figure 42 presents the required discharge current as a function of beam current for the first Standard Functional Test of each thruster. Relatively small variations resulted between thrusters at any value of beam current.

Perveance Margin

The perveance, or ion extraction capability, of NSTAR ion optics was determined by decreasing the beam power supply voltage at a constant beam current and observing the onset of ion beamlet defocusing. This is indicated by a rapid rise in the accelerator grid current due to direct ion impingement. The perveance was calculated as the beam current divided by the total ion accelerating voltage (beam power supply voltage plus the magnitude of the accelerator grid power supply voltage) raised to the three-half power. For NSTAR ion optics, the perveance increased from about 3×10^{-5} $A/V^{3/2}$ to 5.6×10^{-5} $A/V^{3/2}$ as the beam current was increased from 0.51 A to 1.76A. The increasing perveance was probably due to two factors: first, the hot grid spacing probably decreased with increasing beam current and discharge power and, secondly the ratio of discharge voltage to minimum total accelerating voltage decreased by nearly 50 percent. Variations in this ratio have been shown to impact perveance. The difference between the nominal-operating-point total voltage and that at the perveance limit was defined as perveance margin.

Figure 43 plots the perveance margin for the first Standard Functional Test of each thruster as a function of thruster input power. At THO, the nominal total voltage is only 800 volts, therefore, the margin was only about 125 volts even though the beam current was 0.51 A. The thruster deep throttle point (0.5 kW) at reduced beam voltage and specific impulse was selected to maximize the thrust-to-power ratio. Whenever spacecraft power allows operation at higher power levels, the beam voltage will be ramped up (to a maximum of 1100 volts), and then the flows and beam current will be raised. As the beam current was increased, the perveance margin dropped from about 600 volts at low power (TH4) to about 250 volts at 2.3 kW. Experience from extended tests of NSTAR thrusters indicates an increase in perveance with time can be expected as the accelerator grid hole diameters increase from wear.

Electron Backstreaming

The voltage value selected for the accelerator grid power supply is a trade between that required to prevent electrons from backstreaming into the discharge chamber from the neutralized ion beam and excessive erosion, primarily from charge-exchange ions. As given in Table 12, the accelerator grid voltage, with respect to neutralizer common, is –150 volts for all beam currents of 1.0 A and below and –180 volts for beam currents above 1.0 A. Figure 44 shows the magnitude of the accelerator grid backstreaming limit voltage as a function of beam current for the first Standard Functional Test of each thruster. At a constant beam voltage of 1100 V, the backstreaming limit voltage increases linearly with beam current. These values are expected to increase with time as the accelerator hole diameter increases from wear. Also shown are the nominal accelerator power supply values. The backstreaming limit voltage values for the PFT were as expected based on earlier EMT testing.

As mentioned earlier, an accelerator grid voltage of –250 volts is applied for the first two hours of operation to avoid the possibility of electron backstreaming conditions when a cold thruster is started. The center of the low mass screen grid rapidly moves downstream about a millimeter when the discharge power is applied. As the accelerator grid heats, it too moves downstream, the grid spacing opens, and the voltage required to prevent backstreaming decreases in magnitude. After two hours, approximately the time to reach thruster thermal equilibrium, the accelerator grid voltage is increased to its nominal value shown in Table 12.

Ion Beam Plume Measurements Near-Field Faraday Probe - The ion beam flatness parameter (ratio of average current density to the peak value) was measured during the post-Vibration Test Standard Functional Test at JPL and, as shown in Table 18, found to vary monotonically from 0.33 at THO to 0.43 at TH15. This range of values agrees favorably with that of EMT2, the thruster tested for 8000 hours in this LTD facility.

Momentum Analyzer - Identical momentum analyzer probes, with crossed electric and magnetic fields, were used at GRC and JPL to determine the ratio doubly-to-singly-charged ion currents in the ion beam emanating from a thin strip across a thruster diameter. In general, the ratio increased with thruster power going from about 2 percent at TH0 to about 15 percent at TH15 as seen in Tables 15-19. There appeared to be more scatter in the GRC data, possibly due to both the way the thruster was mounted to simulate the DS1 spacecraft and the greater distance (6.5 m) between the probe and the thruster, making the relative alignment more sensitive to thermal distortion. Integrated over the full thruster area, the total doubly-charged ion current fraction is expected to be less than 5 percent and thrust losses, due to multiply-charged ions less than 2 percent.

Thrust Vector - A probe consisting of an array of graphite rods, mounted at the end of the JPL chamber, was used primarily to locate and monitor the behavior of the thrust vector during the final Standard Functional Test of FT1. As seen in Table 18, the average steady-state vertical and horizontal thrust vector deviations from the ideal thrust axis were –0.98 degrees and 0.18 degrees, respectively. Over the power throttle range, the vertical angle went from a minimum value of –0.81 degrees at TH0 to a maximum value of –1.08 degrees at TH4 while the horizontal angle varied somewhat randomly from a minimum of 0.02 degrees at TH4 to a maximum of 0.39 degrees at TH15. By comparison, the thrust vector angles of EMT2, tested for 8000 hours at full-power in the LTD, increased from about –0.3 to –0.2 degrees in the vertical direction and decreased from about 1.2 to 0.4 degrees in the horizontal direction.

Measured Thrust

The thrust produced by FT1 was measured at JPL and is compared to the calculated thrust in Figure 45. Also shown in Figure 45 is a line of equal measured and calculated thrusts. The greatest deviation (about 10 percent) from the ideal is at the lowest value of thrust where uncertainties in corrections for cold flow and thrust due to discharge ions are relatively large. The desire to limit the beam-on time and number of discharge on/off cycles tempered the usual rigor of thrust stand data acquisition. Zero data (complete thruster and flow shutdown) were taken at the beginning and end of the test, but, during the throttle test only beam extraction was interrupted. Agreement between measured and calculated thrusts was excellent, except for the TH0 point.

Thruster Efficiency

Figure 46 shows the calculated thruster efficiency values for the first Standard Functional Test of each thruster as a function of thruster power. Not that the dispersion is quite small. At about 0.5

kW input power, thruster efficiency is about 0.41 and rises to a maximum of 0.63 at 1.8 kW and then drops to about 0.62 at 2.3 kW.

Figure 47 shows the same data plotted as a function of specific impulse. The points near 3000 seconds all have a beam voltage of 1100 volts and decrease in efficiency and specific impulse as the total propellant efficiency decreases . The points at 2000 seconds are low because the beam voltage is only 650 volts and the discharge losses and neutralizer power are a greater fraction of the total power.

Performance Dispersion

The data present have shown that for three different thrusters, with one tested in two different facilities, the performance of the neutralizer, discharge chamber, ion optics, and overall thruster efficiency are remarkably similar.

Table 12. Nominal NSTAR Operating Points

NSTAR power level	Thruster power, kW	main flow, sccm	discharge cathode flow, sccm	neutralizer cathode flow, sccm	Total flow, mg/s	Beam power supply voltage, V	Beam power supply current, A	Accel power supply voltage, V	Neutralizer keeper power supply current, A
TH 0	0.48	5.98	2.47	2.40	1.07	650	0.51	-150	2.0
TH 1	0.60	5.82	2.47	2.40	1.06	850	0.53	-150	2.0
TH 2	0.74	5.77	2.47	2.40	1.05	1100	0.52	-150	2.0
TH 3	0.85	6.85	2.47	2.40	1.16	1100	0.61	-150	2.0
TH 4	0.97	8.30	2.47	2.40	1.29	1100	0.71	-150	2.0
TH 5	1.09	9.82	2.47	2.40	1.45	1100	0.81	-150	2.0
TH 6	1.21	11.33	2.47	2.40	1.60	1100	0.91	-150	2.0
TH 7	1.33	12.90	2.47	2.40	1.75	1100	1.00	-150	2.0
TH 8	1.44	14.41	2.47	2.40	1.90	1100	1.10	-180	1.5
TH 9	1.57	15.98	2.47	2.40	2.06	1100	1.20	-180	1.5
TH10	1.70	17.22	2.56	2.49	2.19	1100	1.30	-180	1.5
TH11	1.82	18.51	2.72	2.65	2.35	1100	1.40	-180	1.5
TH12	1.94	19.86	2.89	2.81	2.51	1100	1.49	-180	1.5
TH13	2.06	20.95	3.06	2.98	2.65	1100	1.58	-180	1.5
TH14	2.17	22.19	3.35	3.26	2.83	1100	1.67	-180	1.5
TH15	2.29	23.43	3.70	3.60	3.03	1100	1.76	-180	1.5

Table 13. Test Chronology

DATE	THRUSTER	TEST/EVENT	RESULTS
10/1/97	PFT	First Functional Test started	Normal neutralizer characterization
10/2-6/97	PFT	First Functional Test completed	Steady-state temperatures at TH0, TH11, TH15
10/7-9/97	PFT	Cold-soak, start, go to full power rapidly	Successful ignitions, low initial electron backstreaming voltage margin at full power, (-250V V_A initiated)
Oct-97	PFT	Inspect, replace optics, install PFT onto DS1 spacecraft	
11/10/97	FT1	First Functional Test	
Nov-97	FT1	Use PFT optics on FT1	FT1 becomes FT1b
Dec-97	PFT	EMT4 ion optics installed on PFT	
12/12/97	FT1b	Second Functional Test	Nominal Operation
1/23-24/98	FT1b	Third Functional Test	Nominal Operation
1/30/98	FT1b	Integration with PPU2 and DCIU2	Successful integration, nominal thruster operation
2/4/98	FT1b	Thruster Thermal Vacuum Test, first cycle, hot PPU2/DCIU2-cold thruster(HPCT)	Successful ignitions and beam extraction
2/5/98	FT1b	Thruster Thermal Vacuum Test, second cycle, cold PPU2/DCIU2-cold thruster (CPCT)	Successful ignitions and beam extraction
2/10/98	FT1b	Integration with room temperature PPU2 and DCIU2	Successful operation, thruster to Vibration Tests, PPU/DCIU to Thermal Vacuum Tests
3/13-14/98	FT1b	Fourth Functional Test (post-vibration) at JPL	Successful operation, sent FT1b to DS1 spacecraft
Apr-98	PFT	Installed new discharge cathode, neutralizer assembly, propellant isolators,and ion optics	PFT becomes FT2
5/11-12/98	FT2	First Functional Test	Nominal Operation
5/13/98	FT2	Integration with PPU1 and DCIU1	Nominal Operation, thruster to VibrationTests, PPU1 and DCIU1 into thermal vacuum tests
6/4-5/98	FT2	Second Functional Test, (post vibration)	Nominal Operation
6/14/98	FT2	Thruster Thermal Vacuum Test, first cycle, hot PPU2/DCIU2-cold thruster(HPCT)	Successful ignitions and beam extraction
6/16/98	FT2	Thruster Thermal Vacuum Test, second cycle, cold PPU2/DCIU2-cold thruster (CPCT)	Successful ignitions and beam extraction
6/17/98	FT2	Third Functional Test	Nominal Operation, hold FT2 as flight spare

Table 14. Pathfinder and EMT4 Temperatures

	PFT	EMT4	PFT	EMT4	PFT
Thermocouple location	0.5 kW TH0	1.8 kW TH11	1.8 kW TH11	2.3kW TH15	2.3 kW TH15
aft magnet, cathode	172	261	238	288	262
middle ring magnet	144	219	206	249	230
middle ring magnet	142	222	209	252	233
forward magnet, optics	180	256	261	289	289
forward magnet, optics	181	252	268	285	297
optics support	135	188	192	213	214
accelerator ring	118	154	171	177	195
plasma screen mask, near neutralizer	76	113	109	128	127
plasma screen mask, near neutralizer (RTD)	73	na	108	na	126
plasma screenmask, opposite neutralizer	64	106	98	121	115
gimbal pads	108	108	155	124	174
titanium gimbal bracket, inner	89	na	128	na	144
titanium gimbal bracket, outer	53	na	74	na	85
adiabatic can	87	107	128	123	145

Table 15. . Pathfinder Thruster, First Functional Data

Operating Point	TH15	TH0	TH4	TH8	TH11	TH15
Facility/PPU	LeRC/console	LeRC/console	LeRC/console	LeRC/console	LeRC/console	LeRC/console
Test/date	10/3/97	10/3/97	10/3/97	10/5/97	10/5/97	10/5/97
Electrical Parameters						
Beam voltage, V	1100	650	1100	1100	1100	1100
Beam current, A	1.76	0.51	0.71	1.1	1.4	1.76
Accel voltage, V	180	150	150	180	180	180
Accel current, mA	6.5	1.3	1.8	3.3	4.8	6.9
Discharge voltage, V	23.47	25.01	24.92	24.16	24.48	23.35
Discharge current, A	13.85	4.79	6.41	9	10.62	13.93
C. Keeper Voltage, V	4.14	4.28	3.13	3.53	4.3	4.13
N. keeper voltage, V	14.03	15.24	15	14.78	14.44	14
N. keeper current, A	1.5	2	2	1.5	1.5	1.5
Floating voltage, V	13.47	12.38	12.53	13.5	13.39	13.32
Thruster Power, kW	2.291	0.484	0.973	1.454	1.828	2.291
Flow Rates						
Main flow+ingest, sccm	23.51	6.06	8.33	14.41	18.61	23.5
Cathode flow, sccm	3.7	2.5	2.5	2.5	2.72	3.7
Neutralizer flow, sccm	3.6	2.4	2.4	2.4	2.65	3.6
Total flow, mg/s	3.02	1.07	1.3	1.89	2.35	3.02
Calculated Performance						
Thrust, mN	92	21	37	58	73	92
Specific impulse, s	3114	1964	2931	3108	3179	3114
Ion Cost, eV/ion	185	235	226	198	186	186
Disch. propellant eff.	0.898	0.833	0.914	0.905	0.912	0.898
Total propellant eff.	0.793	0.65	0.747	0.792	0.811	0.793
Total Efficiency	0.616	0.412	0.55	0.605	0.626	0.615
Optics Performance						
Perveance Margin, V	240	150	510	430	350	250
e-backstreaming limit, V	151	66	118	130	139	150
Beam Measurements						
Double ion current fraction	0.106	0.032	0.046	0.068	0.1	0.103
Facility Measurements						
Tank pressure, µtorr	1.45	0.82	0.82	0.99	1.17	1.41

Table 16. Flight Thruster 1, First Functional Data

Operating Point	TH15	TH0	TH4	TH8	TH10	TH15
Facility/PPU	LeRC/console	LeRC/console	LeRC/console	LeRC/console	LeRC/console	LeRC/console
Test/date	12/13/97	12/13/97	12/13/97	12/13/97	12/13/97	12/13/97
Electrical Parameters						
Beam voltage, V	1100	650	1100	1100	1100	1100
Beam current, A	1.76	0.51	0.71	1.1	1.3	1.76
Accel voltage, V	180	150	150	180	180	180
Accel current, A	5.6	1.1	1.4	2.7	3.6	5.9
Discharge voltage, V	25.4	26	26.37	25.63	25.98	25.26
Discharge current, A	13	4.44	6.2	8.6	9.56	13.14
C. Keeper Voltage, V	4.7	3.9	2.8	3.4	4.1	4.7
N. keeper voltage, V	13.8	17.4	16.26	15.23	14.69	13.68
N. keeper current, A	1.5	2	2	1.5	1.5	1.5
Floating voltage, V	12.98	11.62	11.82	13.15	13.07	12.87
Thruster Power, kW	2.294	0.483	0.979	1.457	1.705	2.296
Flow Rates						
Main flow+ingest, sccm	23.5	5.99	8.3	14.44	17.25	23.5
Cathode flow, sccm	3.7	2.47	2.47	2.47	2.56	3.7
Neutralizer flow, sccm	3.6	2.4	2.4	2.4	2.49	3.6
Total flow, mg/s	3.02	1.07	1.29	1.9	2.19	3.02
Calculated Performance						
Thrust, mN	92.4	20.7	37.3	57.7	68.2	92.4
Specific impulse, s	3117	1974	2939	3108	3176	3117
Ion Cost, eV/ion	188	227	231	201	192	189
Dish. propellant eff.	0.899	0.838	0.917	0.904	0.912	0.899
Total propellant eff.	0.777	0.644	0.731	0.774	0.791	0.777
Total Efficiency	0.616	0.414	0.549	0.604	0.623	0.615
Optics Performance						
Perveance Margin, V	243	140	510	420	360	230
e-backstreaming limit, V	155	66	121	134	140	154
Beam Measurements						
Double ion current fraction	0.118	0.041	0.096	0.082	0.089	0.124
Facility Measurements						
Tank pressure, μtorr	1.19	0.56	0.59	0.77	0.84	1.19

Table 17.. Flight Thruster 2, First Functional Data

Operating Point	TH15	TH0	TH4	TH8	TH10	TH15
Facility/PPU	LeRC/console	LeRC/console	LeRC/console	LeRC/console	LeRC/console	LeRC/console
Test/date	5/11/98	5/12/98	5/12/98	5/12/98	5/12/98	5/12/98
Electrical Parameters						
Beam voltage, V	1100	650	1100	1100	1100	1100
Beam current, A	1.76	0.51	0.71	1.1	1.3	1.76
Accel voltage, V	180	150	150	180	180	180
Accel current, mA	6.6	1.1	1.5	2.9	3.8	6.3
Discharge voltage, V	25.23	25.5	25.71	25.41	25.83	25.16
Discharge current, A	13.12	4.74	6.46	8.67	9.77	13.36
C. Keeper Voltage, V	4.8	4.03	2.66	3.67	4.14	4.65
N. keeper voltage, V	14.5	17.56	16.57	15.2	15.24	14.37
N. keeper current, A	1.46	1.96	1.96	1.49	1.48	1.48
Floating voltage, V	13.34	11.85	12.09	13.7	13.32	13.19
Thruster Power, kW	2.297	0.488	0.981	1.457	1.71	2.302
Flow Rates						
Main flow+ingest, sccm	23.51	5.99	8.3	14.44	17.25	23.5
Cathode flow, sccm	3.7	2.47	2.47	2.47	2.56	3.7
Neutralizer flow, sccm	3.6	2.4	2.4	2.4	2.49	3.6
Total flow, mg/s	3.02	1.07	1.29	1.9	2.19	3.02
Calculated Performance						
Thrust, mN	92	21	37	58	68	92
Specific impulse, s	3115	1973	2938	3107	3175	3116
Ion Cost, eV/ion	189	238	234	201	195	192
Disch. propellant eff.	0.898	0.838	0.916	0.904	0.912	0.899
Total propellant eff.	0.793	0.653	0.749	0.792	0.81	0.794
Total Efficiency	0.614	0.409	0.547	0.603	0.621	0.613
Optics Performance						
Perveance Margin, V	285	115	530	450	380	260
e-backstreaming limit, V	160	68	127	139	146	161
Beam Measurements						
Double ion current fraction	0.094	0.017	0.052	0.073	0.113	0.107
Facility Measurements						
Tank pressure, µtorr	1.25	0.55	0.622	0.797	0.831	1.21

Table 18. Flight Thruster 1, Third Functional Data

Operating Point	TH0	TH4	TH8	TH10	TH15
Facility/PPU	JPL/lab supplies	JPL/lab supplies	JPL/lab supplies	JPL/lab supplies	JPL/lab supplies
Test/date	3/14/98	3/14/98	3/14/98	3/14/98	3/14/98
Electrical Parameters					
Beam voltage, V	651	1101	1101	1101	1102
Beam current, A	0.51	0.71	1.1	1.31	1.77
Accel voltage, V	151	151	181	180	181
Accel current, A	1.35	1.93	3.71	4.81	7.83
Discharge voltage, V	25.53	26.09	25	25.5	24.78
Discharge current, A	4.39	5.95	8.29	9.46	12.76
C. Keeper Voltage, V	3.94	2.73	3.39	3.73	4.03
N. keeper voltage, V	16.34	15.8	14.82	14.16	13.21
N. keeper current, A	2.01	2.01	1.5	1.49	1.5
Floating voltage, V	11.6	11.8	13.26	13.25	13.04
Thruster Power, kW	0.476	0.967	1.446	1.7	2.281
Flow Rates					
Main flow+ingest, sccm	5.98	8.29	14.39	17.26	23.43
Cathode flow, sccm	2.47	2.47	2.48	2.55	3.69
Neutralizer flow, sccm	2.4	2.39	2.4	2.48	3.59
Total flow, mg/s	1.06	1.29	1.9	2.19	3.02
Calculated Performance					
Thrust, mN	20.7	37.3	57.9	68.5	92.7
Specific impulse, s	1979	2940	3114	3189	3126
Ion Cost, eV/ion	217	218	189	186	180
Disch. propellant eff.	0.824	0.901	0.896	0.903	0.889
Total propellant eff.	0.65	0.746	0.791	0.809	0.792
Total Efficiency	0.422	0.555	0.614	0.63	0.624
Measured Performance					
Thrust, mN	22.8	36.7	57.8	68.5	92.5
Specific impulse, s	2195	2903	3104	3192	3125
Total Efficiency	0.515	0.54	0.608	0.63	0.621
Optics Performance					
Perveance Margin, V	150	515	424	362	259
e-backstreaming limit, V	64	117	130	134	149
Beam Measurements					
Double ion current fraction	0.025	0.095	0.081	0.159	0.146
Flatness parameter	0.33	0.34	0.38	0.4	0.43
Peak beam potential, V					
Thrust vector vertical, deg	0.11	0.02	0.16	0.21	0.39
Thrust vector horizontal, deg	-0.81	-1.08	-0.96	-1.04	-1.02
Facility Measurements					
Tank pressure, µtorr	1.62	1.88	2.66	3.03	4.08

Table 19. All Flight Thruster 1 Full Power (TH15) Data

Operating Point	TH15	TH15	TH15	TH15	TH15	TH15	TH15	TH15	TH15
Facility/PPU	LeRC/ console	LeRC/ console	LeRC/ console	LeRC/ console	LeRC/ PPU#2	LeRC/ PPU#2	LeRC/ PPU#2	LeRC/ PPU#2	JPL/lab supplies
Test/date	1st Fnctl 12/13/97	1st Fnctl 12/13/97	2nd Fnctl 1/23/98	2nd Fnctl 1/24/98	PPU integration 1/30/98	Qual TV. HPCT 2/4/98	Qual TV. CPCT 2/5/98	post-TV Fnctl 2/10/98	postVibe 3rd Fnctl 3/14/98
Electrical Parameters									
Beam voltage, V	1100	1100	1100	1100	1100	1100	1100	1100	1102
Beam current, A	1.76	1.76	1.76	1.76	1.76	1.76	1.77	1.76	1.77
Accel voltage, V	180	180	180	180	196	196	272	272	181
Accel current, A	5.6	5.9	6	6	6.3	6.2	6.2	6.1	7.83
Discharge voltage, V	25.4	25.26	25.27	25.14	25.08	25	24.95	25.07	24.78
Discharge current, A	13	13.14	13.1	13.08	13.04	12.72	12.16	12.92	12.76
C. Keeper Voltage, V	4.7	4.7	4.9	4.7	4.7	4.7	4.6	4.7	4.03
N. keeper voltage, V	13.8	13.68	13.93	14.03	14.01	14.33	14.13	14.1	13.21
N. keeper current, A	1.5	1.5	1.5	1.5	1.36	1.35	1.36	1.36	1.5
Floating voltage, V	12.98	12.87	12.88	12.89	13.22	13.5	13.43	13.25	13.04
Thruster Power, kW	2.294	2.296	2.292	2.294	2.296	2.287	2.274	2.286	2.281
Flow Rates									
Main flow+ingest, sccm	23.5	23.5	23.5	23.5	23.5	23.5	23.5	23.5	23.43
Cathode flow, sccm	3.7	3.7	3.7	3.7	3.7	3.7	3.7	3.7	3.69
Neutralizer flow, sccm	3.6	3.6	3.6	3.6	3.6	3.6	3.6	3.6	3.59
Total flow, mg/s	3.02	3.02	3.02	3.02	3.02	3.02	3.02	3.02	3.02
Calculated Performance									
Thrust, mN	92.4	92.4	92.2	92.4	92.6	92.5	92.5	92.3	92.7
Specific impulse, s	3117	3117	3112	3117	3124	3124	3126	3115	3126
Ion Cost, eV/ion	188	189	189	187	186	181	172	185	180
Disch. propellant eff.	0.899	0.899	0.897	0.899	0.901	0.901	0.902	0.898	0.889
Total propellant eff.	0.777	0.777	0.776	0.777	0.779	0.779	0.779	0.777	0.792
Total Efficiency	0.616	0.615	0.614	0.616	0.618	0.62	0.624	0.617	0.624
Measured Performance									
Thrust, mN									92.5
Specific impulse, s									3125
Total Efficiency									0.621
Optics Performance									
Perveance Margin, V	243	230	240	240	na	na	na	na	259
e-backstreaming limit, V	155	154	152	153	na	na	na	na	149
Beam Measurements									
Double ion current fraction	0.118	0.124	0.121	0.109	0.103	0.086	0.079	0.076	0.146
Flatness parameter									0.43
Thrust vector vertical, deg									0.39
Thrust vector horizontal, deg									-1.02
Facility Measurements									
Tank pressure, µtorr	1.19	1.19	1.19	1.22	1.08	1.08	1.08	1.08	4.08

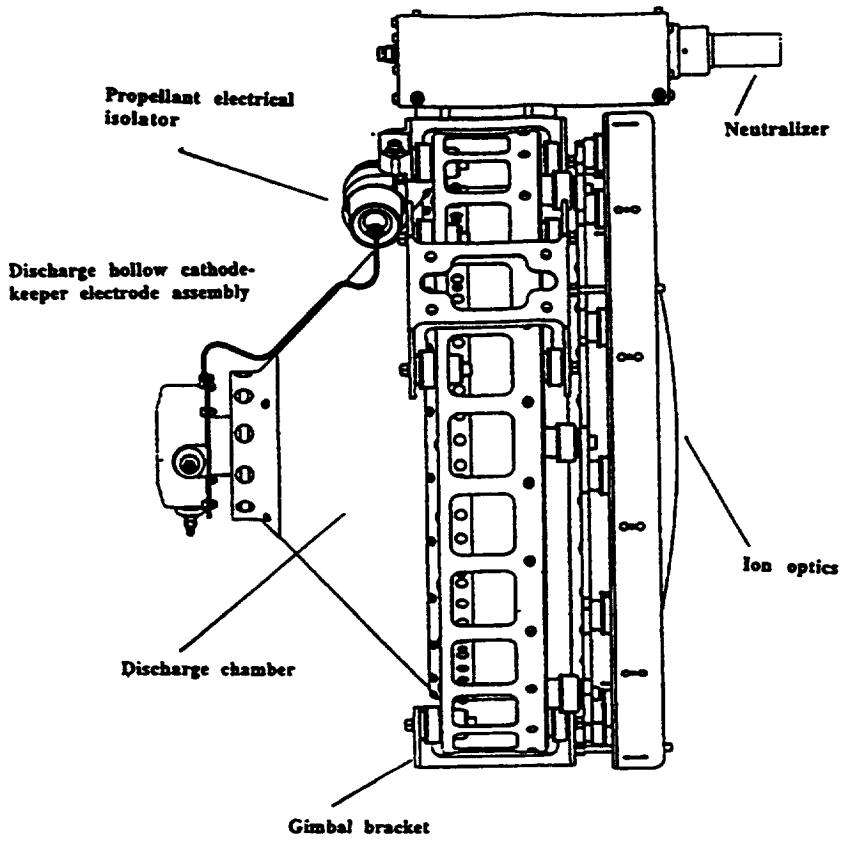

Figure 38. Graphic of the NSTAR ion thruster without the plasma screen.

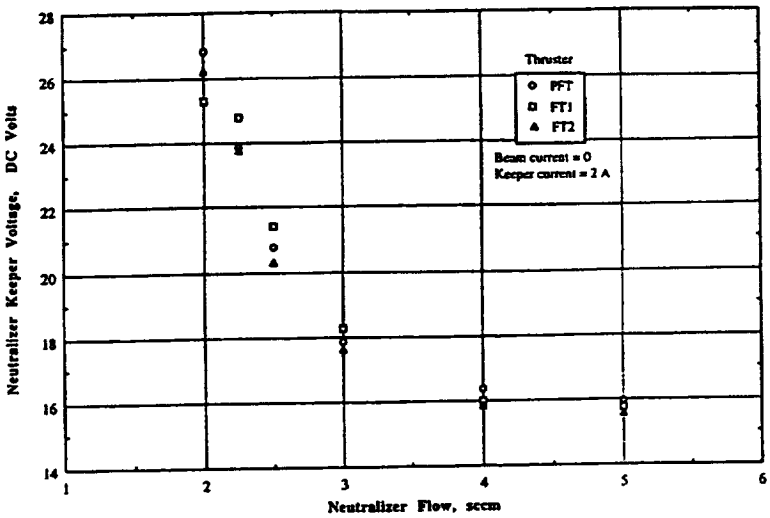

Figure 39. Neutralizer voltage as a function of neutralizer flow

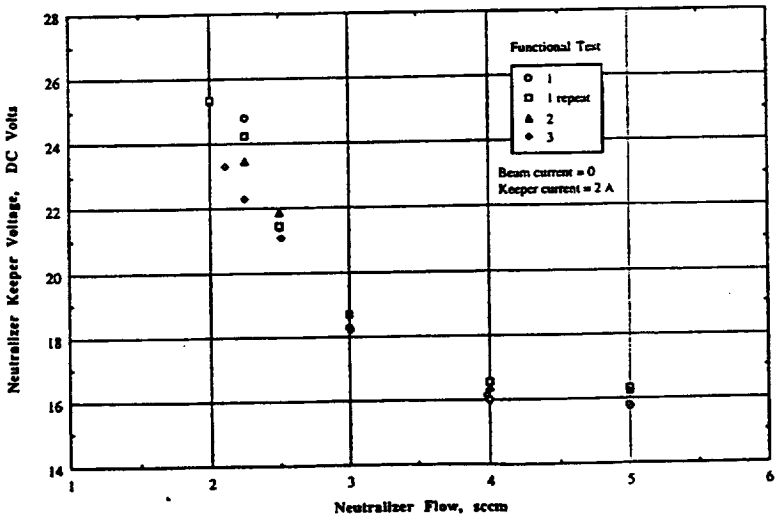

Figure 40. FT1 neutralizer voltage as a function of neutralizer flow

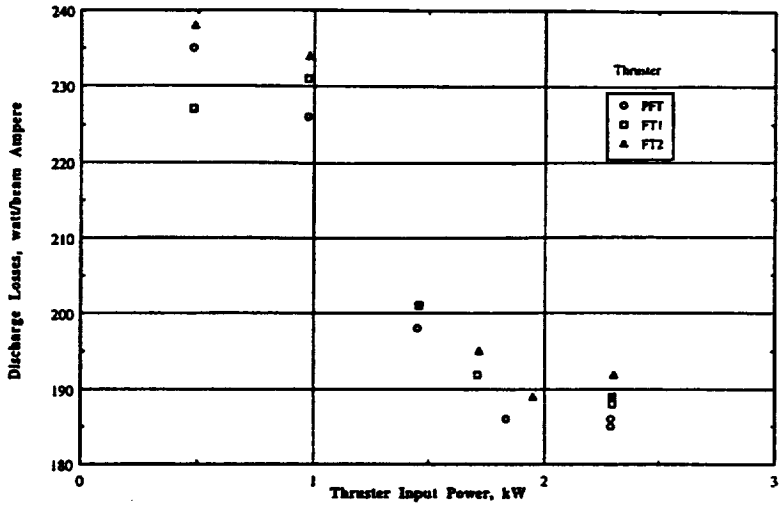

Figure 41. Optimum discharge losses as a function of input power, 1st Functional Test

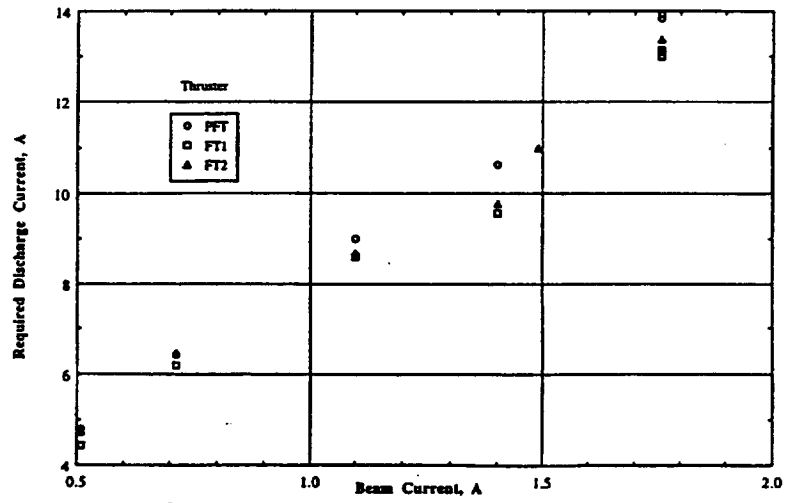

Figure 42. Required discharge current as a function of beam current, 1st Functional Test

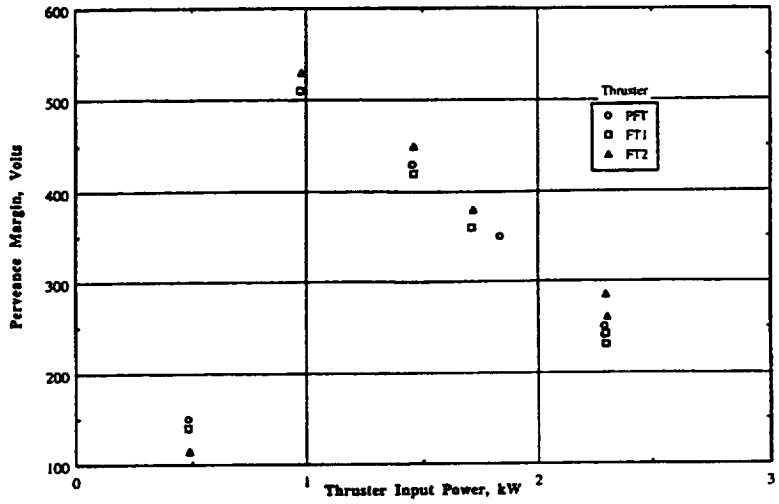

Figure 43. Perveance margin as a function of thruster input power, 1st Functional Test

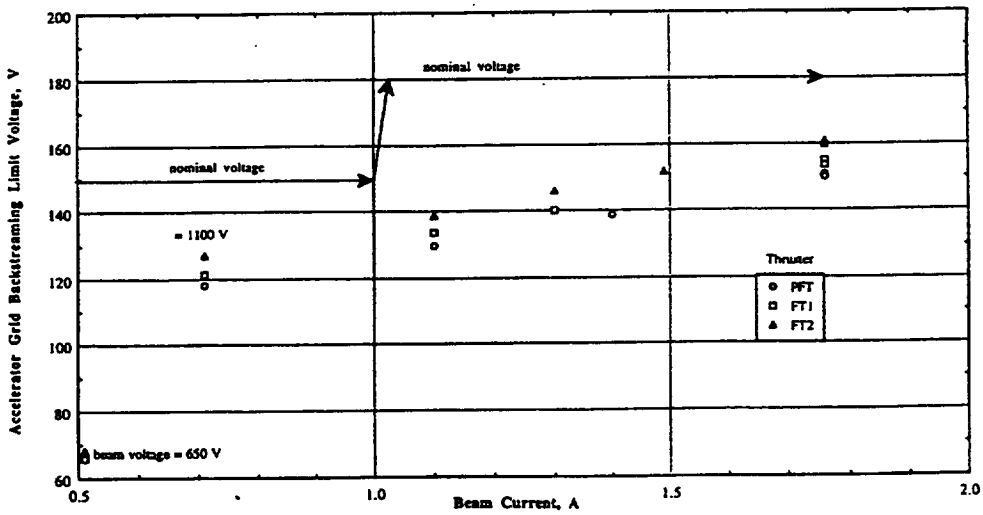

Figure 44. Accelerator grid backstreaming limit voltage as a function of beam current, 1st Functional Test

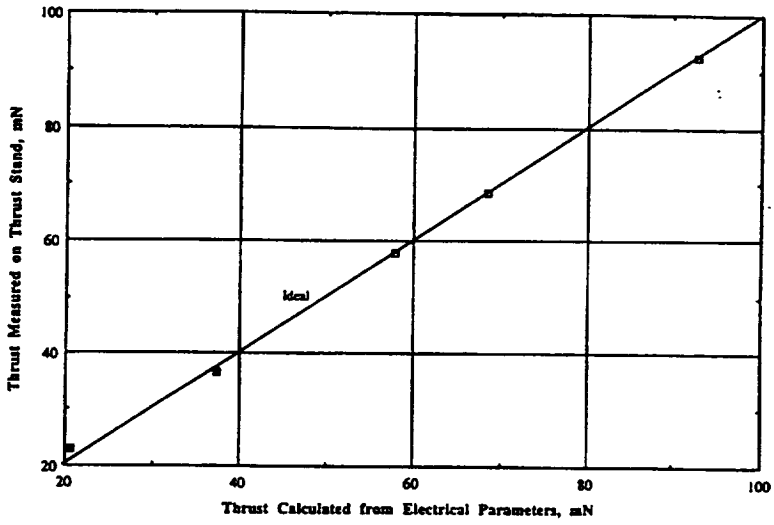

Figure 45. Comparison of calculated and measured thrust for FT1 final Functional Test

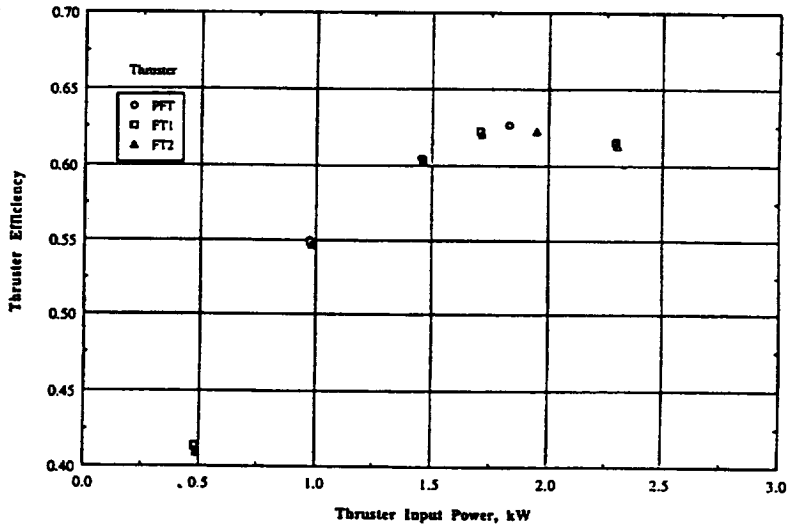

Figure 46. Thruster efficiency as a function of thruster input power, 1st Functional Test

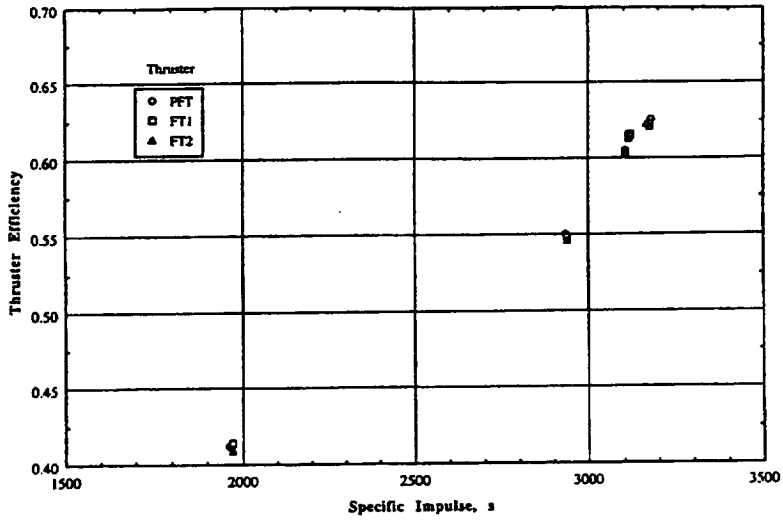

Figure 47. Thruster efficiency as a function of specific impulse, 1st Functional Test

8.3 Flight PPU Testing at Hughes

The Deep Space 1 flight hardware is identified as FT1, PPU1 and DCIU2.

8.3.1 Tests with Test Console

8.3.1.1 Functional Testing

PPU1 and PPU2 were functionally tested with the SPOTH test console. The data was reported to NASA GRC.

8.3.1.2 Combined Survival, Burn-in and Thermal Cycle performance Testing

PPU1 was subjected to the following sequence of tests in October 1997:

One Survival Temperature Cycle (-40°C to +70°C)

One Operational Temperature Cycle (-20°C to +50°)

High Temperature (+50°) Operating Burn-in (Level 15) (70hrs)

During this testing, a total of 43 random recycle events were recorded. This problem was later attributed to the Test Console.

PPU2 (the flight spare) was also subjected to these tests in November 1997.

8.3.2 Tests Integrated with Flight DCIU

Functional Testing was performed on PPU2 and DCIU2 S/N 00473 as an integrated pair. The testing was similar to that of the PPU with the test console only, but also included tests of the DCIU software. The flight PPU1 and DCIU1 were also subjected to integration testing. Figure 48 compares flight efficiency to that obtained during ground testing. The agreement is very good.

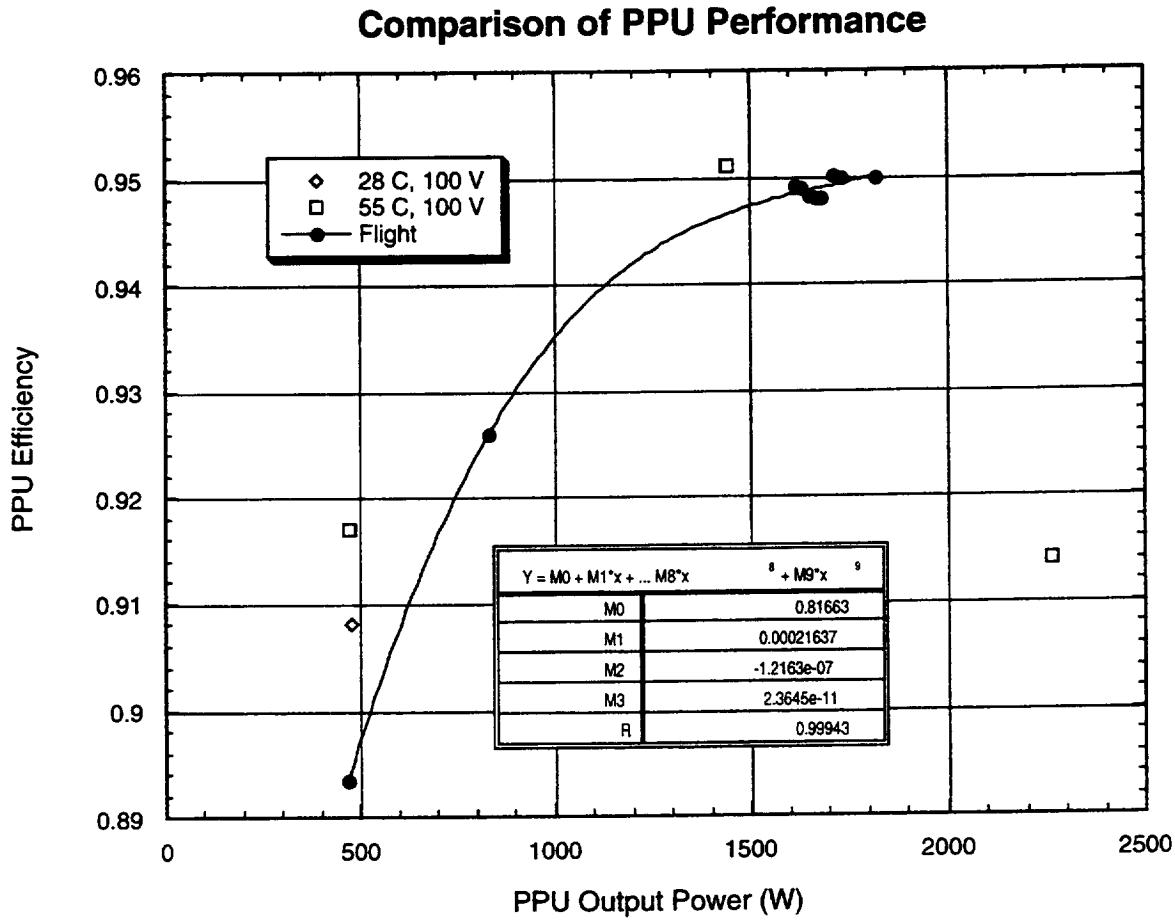

Figure 48. PPU Flight Efficiency Compared to Ground Test Data

8.4 Flight PPU Testing at NASA

8.4.1 Qualification Test Plan (Integration with Flight Thruster and DCIU)

The PPUs and DCIUs were integrated in vacuum port S77 of tank #5 at GRC with the thruster installed in the main portion of tank #5. FT1, PPU2 and DCIU2 were Thermal Vacuum tested in January 1998. FT2, PPU1 and DCIU1 were Thermal Vacuum tested in June 1998. The test flow was as follows:

Cathode Conditioning
Thruster start at Power Level 0
Throttle up to Power Level 4
Throttle up to Power Level 10
Throttle up to Power Level 15
Throttle down to Power Level 8
Throttle up to Power Level 15
Multiple Recycle Test
Continuous Recycle Test
Thruster Shutdown
Thermal Vacuum Test*
- PPU/DCIU Survival Cycle (+70°C to -40°C)
- PPU/DCIU Cold Operation (-30°C into Resistive Load)
- PPU/DCIU Hot Operation (+50°C into Resistive Load)
- Hot PPU/DCIU; Cold Thruster (-97°C) Start – Level 0
- Throttle up to Level 8
- Throttle up to Level 15
- Recycle Test
- Throttle down to Level 8
- Throttle up to Level 15
- Multiple Recycle Test
- Heat Thruster to Hot Survival (+153°C)
- Hot PPU/DCIU/Thruster Turn On Level 15
- Thruster Shutdown and Cool to -97°C
- Cold PPU/DCIU/Thruster Start Level 0
- Throttle up to Level 8
- Throttle up to Level 15
- Recycle Test
- Throttle down to Level 8
- Throttle up to Level 15
- Multiple Recycle Test
- Heat Thruster to +153°C

Cold PPU/DCIU; Hot Thruster Start Level 15
Shutdown Thruster
Break Vacuum for Component Vibration Testing
Post Vibration Test (Limited Functional)

*FT1, PPU #2, and DCIU #2 tested January 1998
FT2, PPU #1, and DCIU #1 tested June 1998

8.4.2 PPU Qualification Vibration Test

A vibration test on PPU S/N 002 and DCIU #2 (S/N 00473) was conducted at NASA GRC in December 1997. Both units were subjected on all three coordinate axes to the specified random vibration spectrum (in accordance with JPL document D-13638) having a total acceleration level of 12.98 g's-rms for a duration of 60 seconds. Resonate frequencies were determined using a 0.5g sweep in each axis. Both units successfully passed the test as documented in NASA GRC report no. SDL-TR 97-49. This test was repeated after the PPU was upgraded thermally (see NASA GRC Test Report No. SDL-TR 97-49 dated January 1998).

The second set of flight units (PPU S/N 001 and DCIU1 S/N 00472) were also subjected to vibration testing at GRC – again with success.(See NASA GRC Test Report No. SDL-TR 98-06 dated April 1, 1998.

8.4.3 EMI Testing

Conducted emissions testing of the NSTAR PPU S/N 002 and DCIU S/N 00473 was conducted at vacuum tank #5 of the Electrical Propulsion Laboratory (NASA GRC) in January 1998. Testing was done to MIL-461-C test limits in accordance with MIL-462 test procedures. Test data was generated with the NSTAR subsystem driving a resistive load and driving the flight thruster. Both the DCIU and the PPU failed to pass the MIL-462-C CE03 requirements. Due to the nature of these units, this was the expected result. The EMI noise was considered to be acceptable by the DS1 Program. Refer to NASA Test Report No. EMI RPT 127 for detail.

8.5 Flight DCIU Testing at Spectrum Astro

Acceptance Testing of both flight DCIUs was performed at Spectrum Astro, Inc. with HED participation. The test flow was as follows:

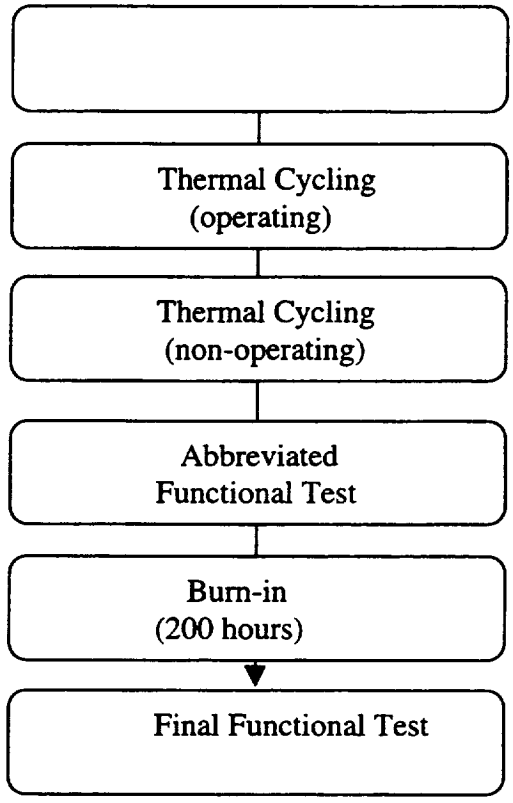

The Functional Testing consisted of an automated test sequence designed to exercise all modes of both hardware and software.
The Operating Thermal Cycling Test consisted of 5 cycles between -24°C and +61°C.
The Non-operating (survival) Thermal Cycle Test consisted of 1 cycle between the extremes of -35°C and +70°C.

Some rework of the DCIU required replacement of opto-isolators and the addition of a DCIU to Slice reset circuitry. Final tests of DCIU #2 were completed in March 1998, and the final confidence tests of DCIU #1 were completed in May 1998.

8.6 Flight DCIU Testing at Hughes

8.6.1 Tests Integrated with Flight PPU

Both PPUs were integrated pairwise with each of the two DCIUs for a functional test. All major DCIU software algorithms were verified. The setup for this test is shown below.

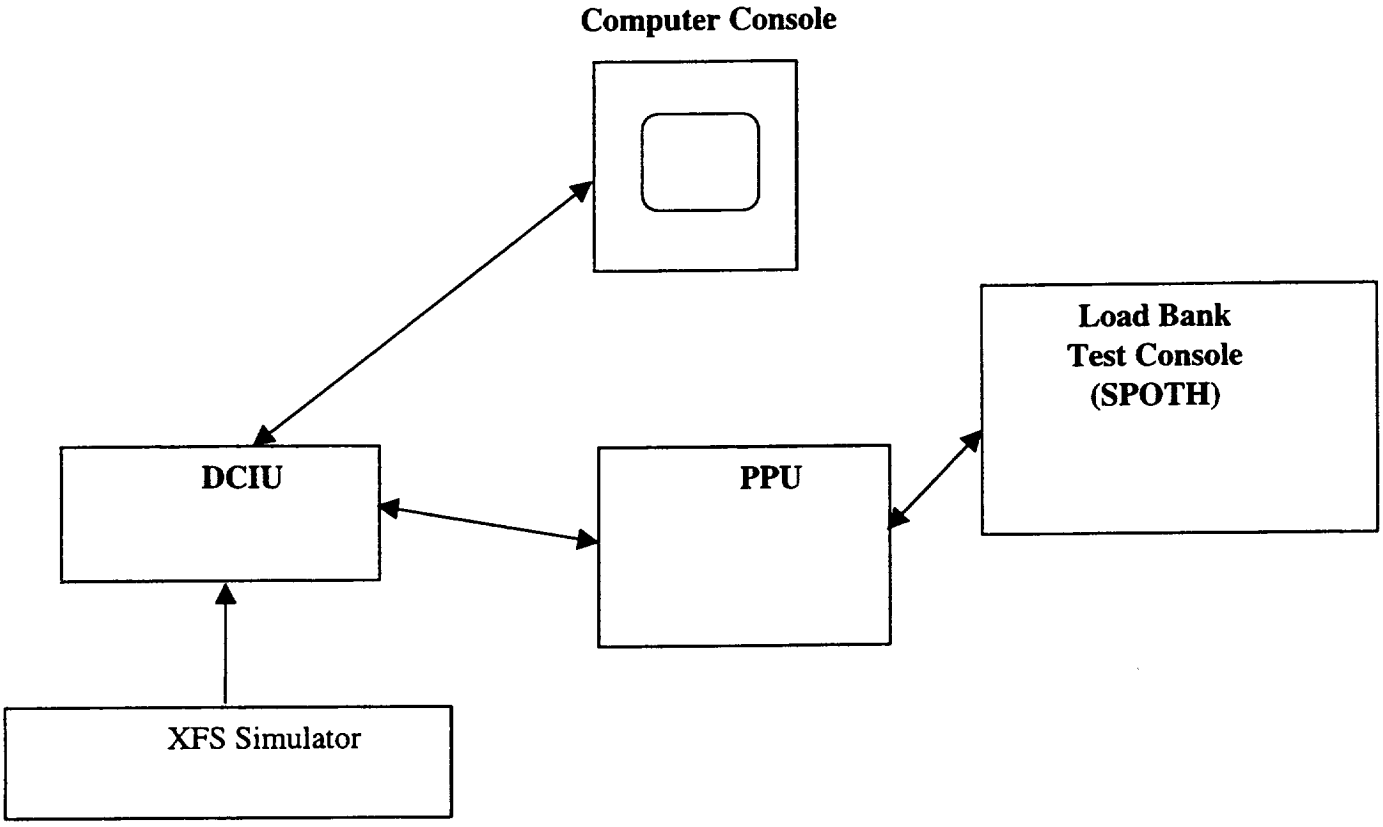

8.7 Flight DCIU Testing at NASA

8.7.1 DCIU Qualification Vibration Test

A vibration test on PPU S/N 002 and DCIU S/N 00473 was conducted at NASA GRC in December 1997. Both units were subjected on all three coordinate axes to the specified random vibration spectrum (in accordance with JPL document D-13638) having a total acceleration level of 12.98 g's-rms for a duration of 60 seconds. Resonate frequencies were determined using a 0.5g sweep in each axis. Both units successfully passed the test as documented in NASA GRC report no. SDL-TR 97-49. This test was repeated after the PPU was upgraded thermally (see NASA GRC Test Report No. SDL-TR 98-06 dated March 1998).

The second set of flight units (PPU S/N 001 and DCIU S/N 00472) were also subjected to vibration testing at GRC – again with success.

8.7.2 EMI Testing

Conducted emissions testing of the NSTAR PPU S/N 002 and DCIU S/N 00473 was conducted at vacuum tank #5 of the Electrical Propulsion Laboratory (NASA GRC) in January 1998. Testing was done to MIL-461-C test limits in accordance with MIL-462 test procedures. Test data was generated with the NSTAR subsystem driving a resistive load and driving the flight thruster. Both the DCIU and the PPU failed to pass the MIL-462-C CE03 requirements. Due to the nature of these units, this was the expected result. The EMI noise was considered to be acceptable by the DS1 Program. Refer to NASA Test Report No. EMI RPT 127 for detail.

8.7.3 Functional Full Integration Test

PPU S/N 002 and DCIU #2 (S/N 00473) were integrated in vacuum port S77 of tank #5 at GRC with the flight thruster in the main portion of tank #5. This test was conducted in January 1998.The test flow was as follows:

Cathode Conditioning
Thruster start at Power Level 0
Throttle up to Power Level 4
Throttle up to Power Level 10
Throttle up to Power Level 15
Throttle down to Power Level 8
Throttle up to Power Level 15
Multiple Recycle Test
Continuous Recycle Test
Thruster Shutdown
Thermal Vacuum Test

PPU/DCIU Survival Cycle (+70°C to -40°C)
PPU/DCIU Cold Operation (-30°C into Resistive Load)
PPU/DCIU Hot Operation (+50°C into Resistive Load)
Hot PPU/DCIU; Cold Thruster (-97°C) Start – Level 0
Throttle up to Level 8
Throttle up to Level 15
Recycle Test
Throttle down to Level 8
Throttle up to Level 15
Multiple Recycle Test
Heat Thruster to Hot Survival (+153°C)
Hot PPU/DCIU/Thruster Turn On Level 15
Thruster Shutdown and Cool to -97°C
Cold PPU/DCIU/Thruster Start Level 0
Throttle up to Level 8
Throttle up to Level 15
Recycle Test
Throttle down to Level 8
Throttle up to Level 15
Multiple Recycle Test
Heat Thruster to +153°C
Cold PPU/DCIU; Hot Thruster Start Level 15
Shutdown Thruster
Break Vacuum for Component Vibration Testing
Post Vibration Test (Limited Functional)

No DCIU hardware problems were found. Minor software problems were corrected by Spectrum Astro during the course of the integration testing. during the thermal vacuum testing of FT2, the PPU/DCIU failed to respond properly to a simulated thruster fault. The PPU beam and accelerator power supplies powered off normally and the discharge current was cut back. The DCIU failed to detect the recycle and the system remained in this state. As part of the CCB-directed trouble shooting, the PPU was placed on a resistive load, and recycles were nominal. This test verified the operation of the PPU/slice hardware and focused attention on the version 1.08 software loaded in the DCIU since previous thruster tests with PPU1 and DCIU1 were conducted with v1.07 software. V1.08 contained improved recycle detection logic, per ECR N036 which was designed to ignore the spurious setting of the PPU fault flag due to electronic noise on the digital input channels of the slice board. The ECR logic assessed the state of the PPU, via telemetry data, to ensure that the beam and accelerator supplies were in fact off when the PPU fault flag was set. The v1.08 code was reviewed and it was found that erroneous variable names caused the DCIU to look at discharge voltage and discharge cathode heater voltage rather than beam and accelerator voltages when the PPU fault flag was set. Coincidentally, these parameters were within limits when a recycle was attempted with the resistive load and not with the thruster. The coding error was corrected and new software v1.09 was uploaded. The acceptance test cycles verified the fix. This coding error also

explains the unexpected recycles still obtained with the v1.08 code during earlier PPU/DCIU thermal vacuum tests in May. Note: An outline of all software modifications to the DCIU software is contained in JPL interoffice memo No. IOM-8310-99-02 dated January 25, 1999.

Note: PPU S/N 001 and DCIU #1 (S/N 0047) were also subjected to this integration test in May 1998.

9 LESSONS LEARNED

9.1 The Thruster

Overall, the fabrication and assembly of the NSTAR Flight Thruster is straightforward and repeatable. The processes are capable of achieving flight quality with high manufacturing yields. However, there are some parts design and fabrication issues that should be addressed on the next NSTAR flight thruster program that will improve the quality of the thrusters and reduce the assembly labor. These are listed below:

1. The electron beam weld of the discharge cathode orifice OD to the cathode support tube was a low yield process that caused stress cracks in the orifice plate on several of the assemblies. This should be changed to a face weld, similar to the neutralizer cathode orifice to cathode support tube design. The face weld was performed with a high yield and no stress cracks.

2. The electrical connection to the swaged coaxial heater used on both the discharge and neutralizer cathode assemblies should be redesigned to eliminate the sauerisen cement and reduce the stress on the heater center conductor during assembly.

3. Semco produced swaged heaters of the NSTAR design for the purpose of supplier qualification. NASA produced the heaters that were used on the NSTAR program. Qualification testing of these heaters should be performed.

4. The spin forming of the titanium discharge chamber and front mask parts was very difficult for the HED supplier. This resulted in schedule delays and excessive machining required to achieve the required dimensions and flatness. Alternate spin forming suppliers with better process control or alternate forming methods need to be explored.

5. The flatness of the spun-formed front mask is difficult to control. It is attached to the thruster by means of four posts that are 90 degrees apart. The use of additional posts (6 or 8) would help to pull the front mask into the desired flatness and achieve a more

consistent gap from the front mask to the optics assembly. The threads on the posts should be 6-32 rather than 4-40.

6. The internal wiring was replaced by NASA during the flight thruster acceptance testing to incorporate insulated shielding and reduce the bend radii near the box beam. These improvements should be incorporated in the thruster design drawings and assembly processes.

7. The gimbal brackets should be redesigned to eliminate the helicoil inserts and the large hole in the center of each of the brackets. The brackets are made from titanium and do not require helicoil inserts. On the NSTAR thrusters, metal sheet stock was used to cover the large holes in the brackets to prevent possible electron backstreaming

8. The power cable termination at the thruster should have the Kynar wrap replaced with a Kapton wrap and metal tie-wraps.

9. The fit of the neutralizer cover should be improved to reduce the interface gaps to less than .020 inches.

10. The terminal assemblies (insulators and shields) used in the neutralizer and discharge cathode housings were difficult to align during the internal wiring of the thruster. The design of these assemblies should be changed to make them self-aligning or prealigned.

11. Some contamination of the neutralizer keeper insulator was seen on the NSTAR thruster which may have occurred during one of the assembly operations. Methods should be developed to keep this insulator clean and shielded from possible contamination from sputtered material.

12. It is recommended that the unique grid riveting process be documented.

13. Consideration should be given to eliminating the lightening holes in the magnet retainers. The rare earth magnet material is extremely brittle and chipping does occur during discharge chamber assembly. While it is assumed that the magnetic field holds the chips in place, they are small enough to come through the retainer holes during thruster handling or launch. This risk would be eliminated with only a small weigh penalty if the holes are removed.

14. A review should be conducted of the as-built data that should be recorded during thruster assembly. In Process Records (IPRs) should be created to capture this data in the equipment logs. All Operation Sheets should be updated prior to the next thruster production.

15. An HED thruster Acceptance Test Procedure needs to be written to document the tests that NASA performed on the NSTAR program.

9.2 The PPU

9.2.1 Engineering Model

Due to time and budget constraints, no Engineering Model PPU was built.
Transition from the breadboard PPU to the Flight model was difficult.
The fabrication experience of an EM PPU would have led to a better PPU mechanical design:

Increased built-in test capability
Easier assembly and test (less point-to-point solder connections)
Improved heat sinking

9.2.2 Fault Diagnostics

By design, the PPU/DCIU combine 5 different fault conditions – any of which set the recycle flag. This makes it very awkward if not impossible to determine if an in-flight "recycle" is actually due to a thruster arc or short. Again, hindsight suggests that the various significant fault conditions have their own telemetry flags.

9.2.3 Baseplate Temperature Range

Due to the risk of overheating the beam power supply transformers, the PPU baseplate temperature was limited to +55 C maximum. At the +55 C baseplate, the acceptance tests were conducted over a bus voltage range of 120 V to 80 V at the full thruster power of 2.3 kW. The estimated safe operating envelope of the PPU output power at a +55 C baseplate temperature is 2.3 kW from a bus voltage of 80 to 120 V, decreasing linearly to 1.8 kW output power at a bus voltage of 160 V.

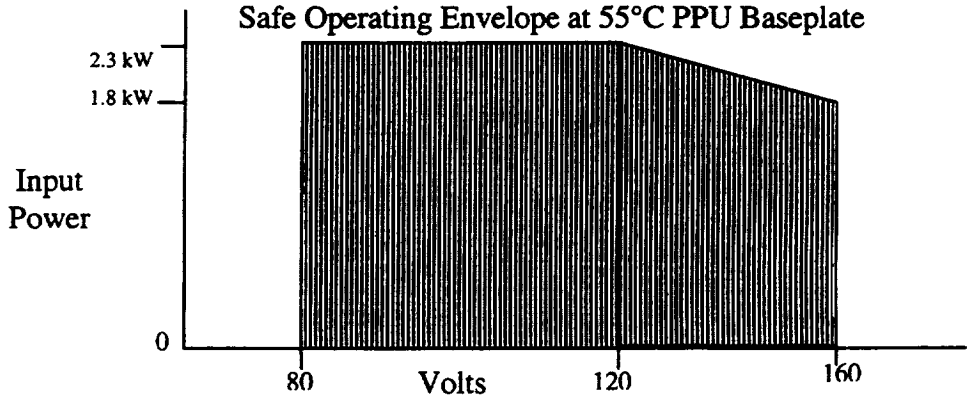

9.3. The DCIU

9.3.1 Software

The DCIU software is very complex and difficult to test. This is further complicated by the fact that the DCIU interfaces with so much other hardware (e.g. - Spacecraft computer, XFS valves, XFS temperature sensors, XFS pressure sensors, and the PPU). The next program should budget more time for software integration/validation.

10. CONCLUSIONS AND RECOMMENDATIONS

The Flight Model Thruster, the Power Processor Unit, and the Digital Control and Interface Unit have successfully completed acceptance and qualification tests and to date have successfully operated aboard the DS1 spacecraft for 1798 hours. The performance of the first flight design thruster PFT was completely consistent with the NASA EM thrusters. The completion of the 12,000 hour Extended Life Test will demonstrate the life of the thruster, the power processor unit, and the digital control interface unit.

Most of the assembly processes used in the production of the NSTAR thrusters have proven to be robust and repeatable, based on the experience with the first three thrusters. The PPU and DCIU have also passed their baptism by fire and are ready for future production with relatively minor changes. The incorporation of the improvements listed in Section 9 Lessons Learned should increase the quality of the parts and assemblies and reduce the assembly labor and cost. It should be noted that in the case of the NSTAR thruster, many of the assemblies and manufacturing processes are similar to the HED 25 cm thruster being produced for the Hughes 702 Communications Satellites. The experience being gained on the production of the Hughes thrusters will directly benefit the future NSTAR thruster programs.

ABBREVIATIONS AND ACRONYMS

The following list defines the abbreviations and acronyms that are used within this test specification:

AG	Accel Grid
ATP	Acceptance Test Plan
BOL	Beginning of Life
CDS	Command Data Subsystem
CVS	Component Verification Specification
DCIU	Digital Control and Interface Unit
DS1	Deep Space One
ELT	Extended Life Test
EMC	Electromagnetic Compatibility
EMI	Electromagnetic Interference
EM	Engineering Model
EMT	Engineering Model Thruster
EPC	Electronic Power Conditioner
EOL	End of Life
ESD	Electrostatic Discharge
FEM	Finite Element Model
FET	Field Effect Transistor
FM	Flight Model
FMT	Flight Model Thruster
FPGA	Flight Programmable Gate Array
FT	Flight Thruster
GRC	NASA Glenn Research Center

GSE	Ground Support Equipment
HED	Hughes Electron Dynamics
HV	High Voltage
IPS	Ion Propulsion System
JPL	Jet Propulsion Laboratory
LeRC	NASA Lewis Research Center (now GRC)
MPT	Mission Profile Test
NSTAR	NASA Solar-Electric-Power Technology Application Readiness
OS	Operations Sheet (HED Lot Traveler)
PDU	Power Distribution Unit
PFT	Pathfinder Thruster
PPS	Power/Pyrotechnic Subsystem
PPU	Power Processor Unit
PSD	Power Spectral Density
QTP	Qualification Test Plan
RDM	Radiation Design Margin
SAI	Spectrum Astro, Inc.
SEGR	Single-Event Gate Rupture
SEB	Single-Event Burnout
SEL	Single-Event Latchup
SEPS	Solar Electric Propulsion System
SEU	Single-Event Upset
SG	Screen Grid
SOW	Statement of Work
SPF	Single-Point Failure

STV	Solar Thermal Vacuum
TC	Thermocouple
TID	Total Ionizing Dose
TF	Transfer Function
XFS	Xenon Feed System
XIPS	Xenon Ion Propulsion Subsystem

LIST OF SELECTED REFERENCES

1. Bond, Thomas A. et al., "The NSTAR Ion Propulsion Subsystem for DS1," AIAA Paper 99-2972, June 1999.

2. Bond, Thomas A. et al., " NSTAR Ion Engine Power Processor Unit Performance: Ground Test and Flight Experience," SAE Paper 99APSC-47, April 1999.

3. Christensen, J., et al., "Design and Fabrication of a Flight Model 2.3 kW Ion Thruster for the Deep Space 1 Mission," AIAA Paper 98-3327, July 1998.

4. Hamley, J. A., et al., "The Design and Performance Characteristics of the NSTAR PPU and DCIU," AIAA Paper 98-3938, July 1998.

5. Rawlin, V. K., et al., "NSTAR Flight Thruster Qualification Testing," AIAA Paper 98-3936. July 1998.

6. Rawlin, V., Patterson, M., and Becker, R., "Thermal Environmental Testing of the NSTAR Engineering Model Ion Thruster," IEPC Paper 97-051, 1997.

7. Polk, J. E. et al., "The Effect of Engine Wear on Performance in the NSTAR 8000 Hour Ion Engine Endurance Test," AIAA Paper 97-3387, July 1997.

8. Sovey, J. S., et al., "Development of an Ion Thruster and Power Processor for New Millennium's Deep Space 1 Mission," AIAA Paper 97-2778, July 1997.

9. Bushway, E. D., et al., "NSTAR Ion Engine Xenon Feed System: Introduction to the System Design and Development," IEPC Paper 97-044, August 1997.

10. Patterson, M. J., et al., "NASA 30 cm Ion Thruster Development Status," AIAA Paper 94-2849, June 1994.

APPENDIX

1. PPU Grid Clear description (John Hamley)
2. PPU/Thruster Power Cable & Interface Drawings
3. The NSTAR Interface Control Drawings

PPU Grid Clear description (John Hamley)

GRID CLEARING

- Corrective action when conductive debris is lodged between the screen and accelerator grid.

- Electrical path exists between grids which precludes application of accelerating voltages.

- Results in high beam current
  - Direct short to Accel supply
  - Electron backstreaming

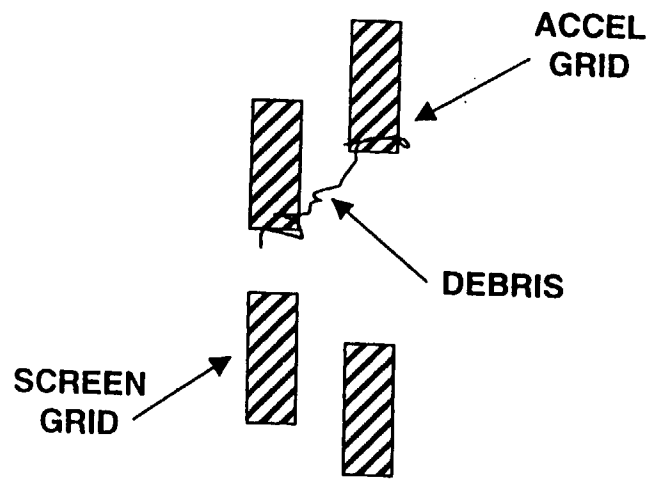

MANIFESTED BY HIGH OR CONTINUOUS RECYCLES

NSTAR ION OPTICS SCHEMATIC

- Screen Grid connected to discharge cathode
- Anode connected to Discharge & Beam +
- Beam & Accel referenced to Neut. Common

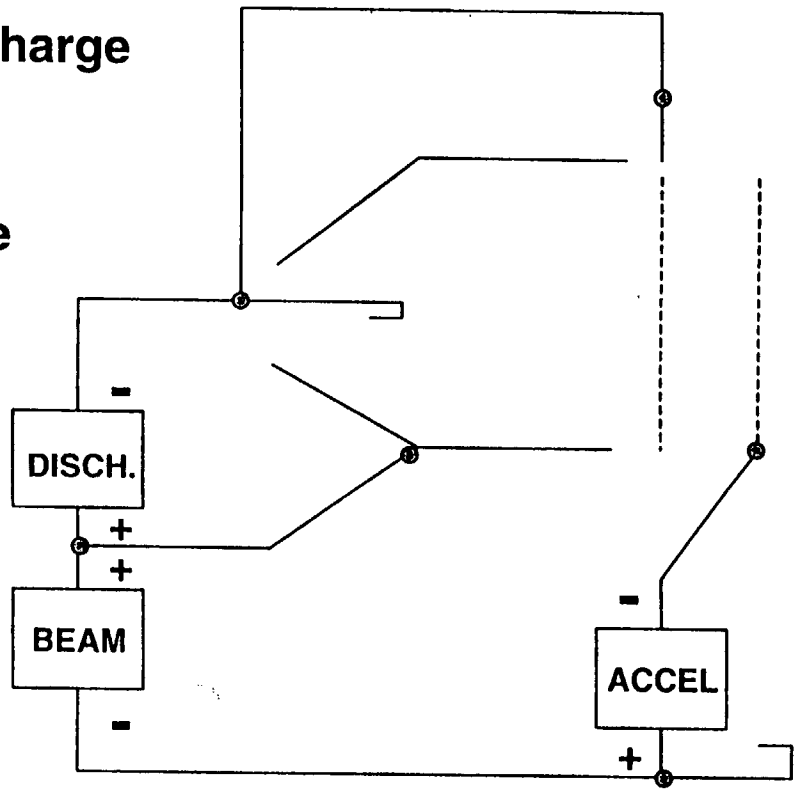

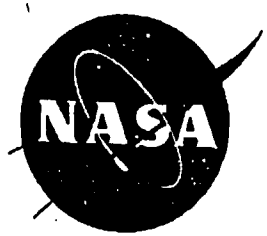

National Aeronautics and
Space Administration
Glenn Research Center

GRID CLEARING

- Grid-to-Grid shorts are reported in ground and flight data in most programs, NASA and commercial.
  - Back-sputtered facility material in Ground tests
  - Flight data from HSC and DS1 (Also SERT II)

- Grid clearing circuits included in HSC and DS1 PPU due to established need

LITTLE EMPIRICAL DATA ON GRID CLEARING IS IN THE LITERATURE

NSTAR GRID CLEARING

- Internal PPU relay (R1) is commanded closed
- Discharge supply is commanded ON
  - Hardware Interlocks limit current to 3.75-4.0 A
- DCIU monitors discharge current
  - Ends grid clearing if $J_D = 0$ or if 30 sec elapses with $J_D > 0$

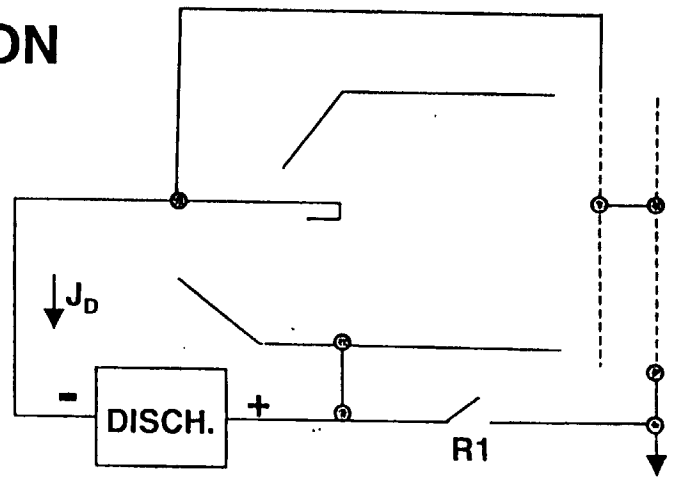

BENIGN PROCEDURE WITH NO HOT SWITCHING AND LIMITED ENERGY

PPU/Thruster Power Cable & Interface Drawings

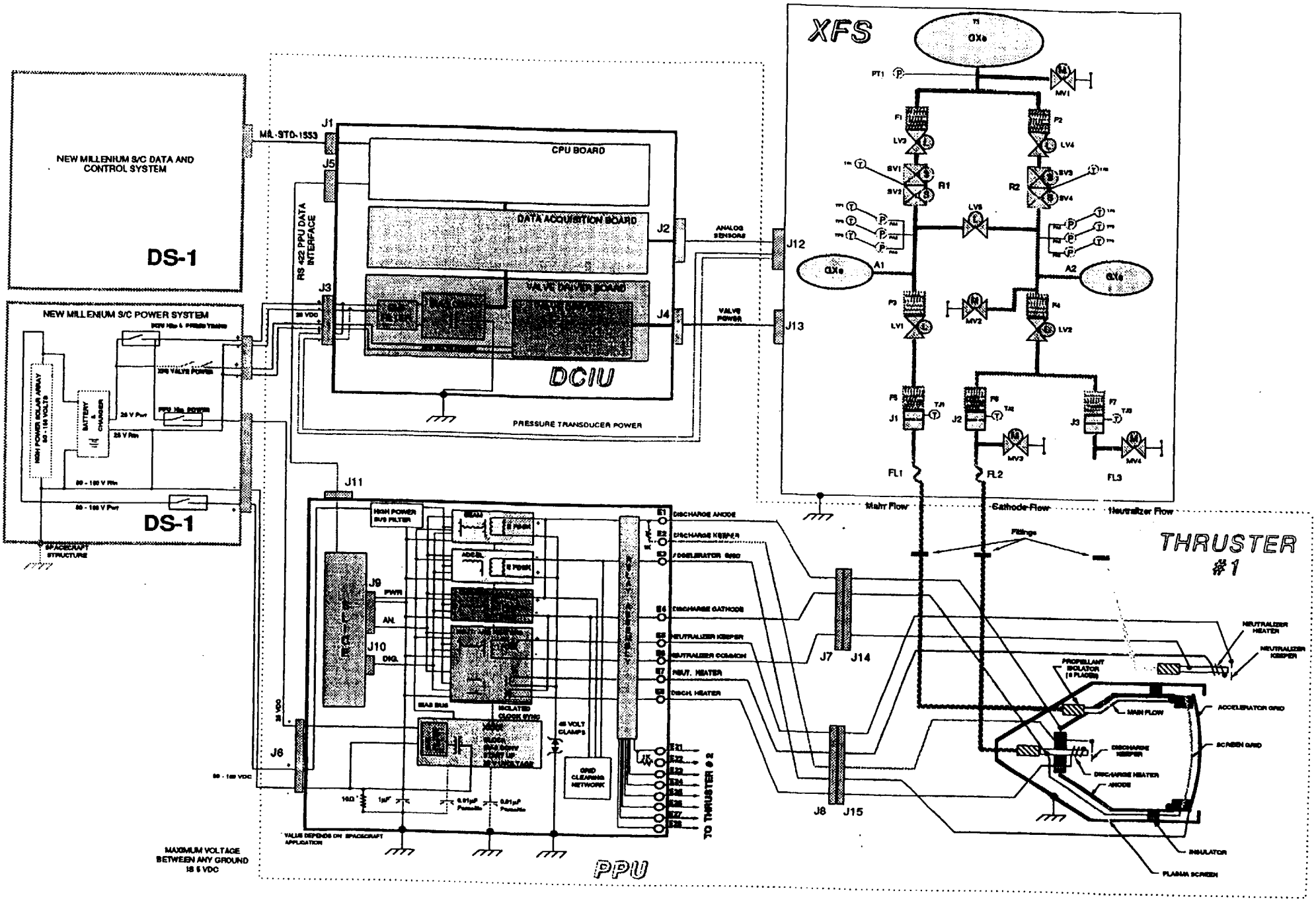

NSTAR Thruster Element Block Diagram

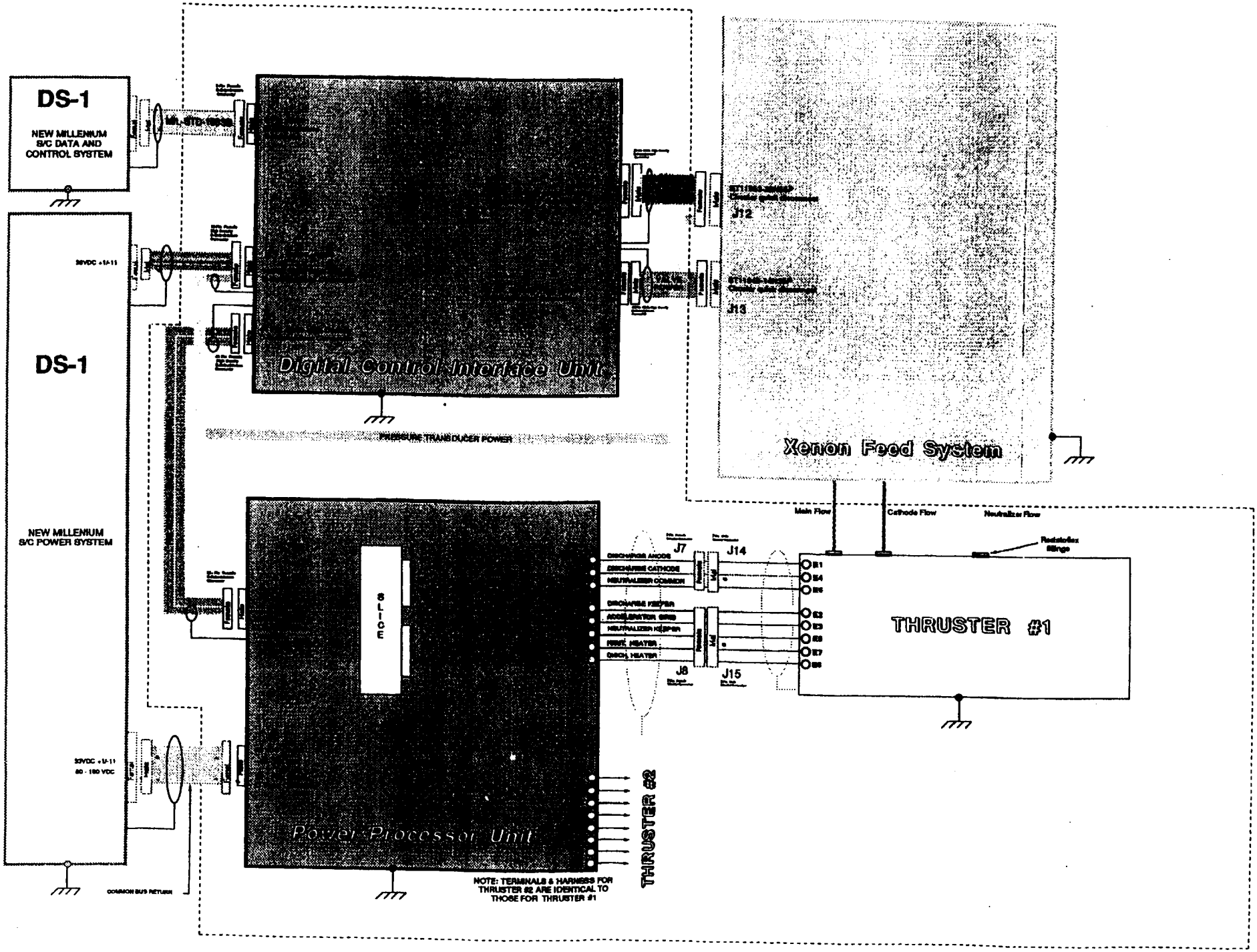
DS-1
NEW MILLENIUM S/C DATA AND CONTROL SYSTEM
DS-1
NEW MILLENIUM S/C POWER SYSTEM
Digital Control Interface Unit
Power Processor Unit
SLICE
PRESSURE TRANSDUCER POWER
Xenon Feed System
Main Flow
Cathode Flow
Neutralizer Flow
J12
J13
J7
J14
J8
J15
THRUSTER #1
THRUSTER #2
NOTE: TERMINALS & HARNESS FOR THRUSTER #2 ARE IDENTICAL TO THOSE FOR THRUSTER #1

PPU / Thruster CABLE Harness

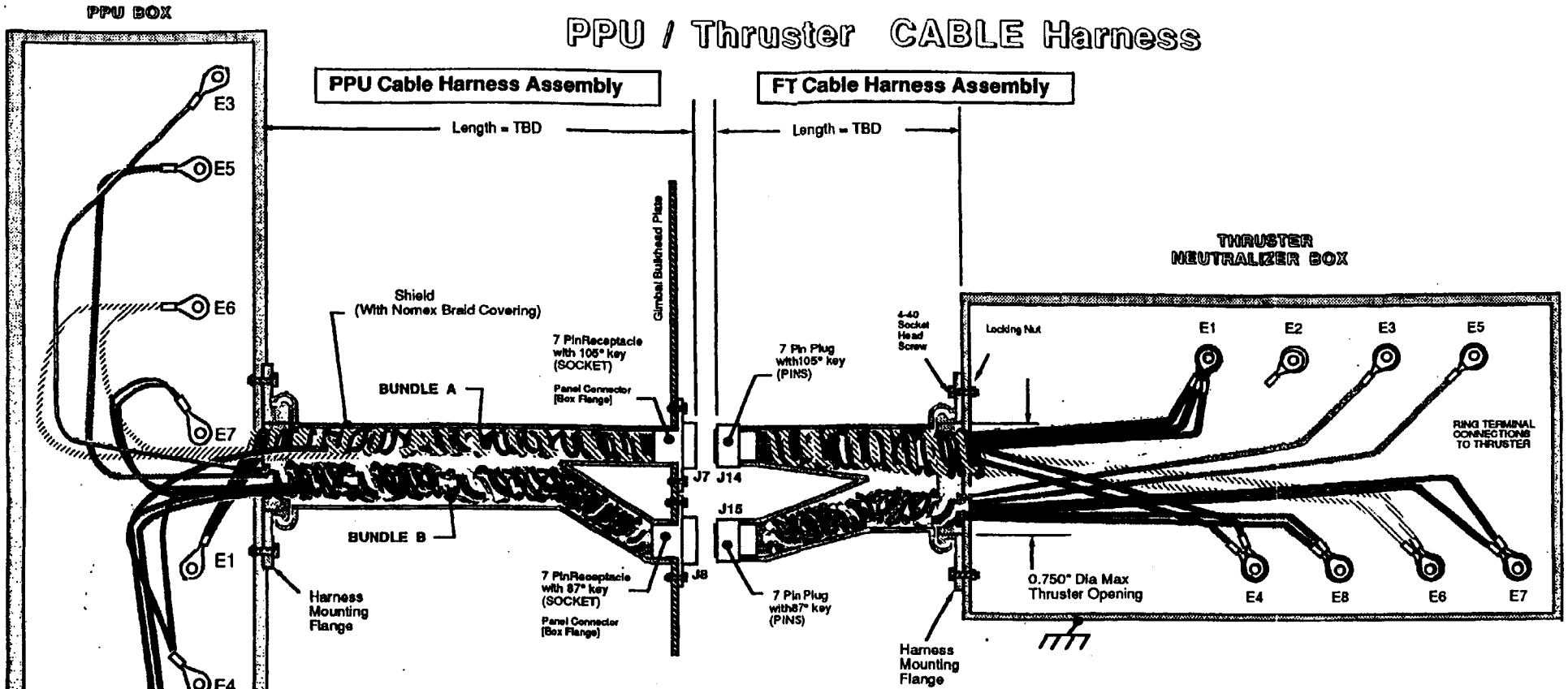

Ref. #	Description	# of wires	Wire gauge	Max I dc (A)
E1	Disch Anode	3	16	18
E2	Disch Keeper	1	20	1.2
E3	Accelerator	1	16	0.02*
E4	Disch Cath	2	16	16
E5	Neutr Keeper	1	20	2
E6	Neutr Common	2	18	9
E7	Neutr Htr	2	20	9
E8	Disch Htr	2	20	9

NOTE: 1. * E3 must carry 12 amperes (@35Vdc) for 30 seconds for Grid clearing between the Screen and Accel Grid.

2. Temperature rating: -55°C to + 125°C

BUNDLE A	BUNDLE B
WIRES	WIRES
E1-1	E2
E1-2	
E1-3	E3
E4-1	E5
E4-2	
	E7-1
E6-1	E7-2
E6-2	
	E8-1
	E8-2
7 Wires	7 Wires

MATERIAL	DESCRIPTION
(1). Ring Terminals	(1). Amp Inc. Part Number 321864, Uninsulated Ring Tongue Terminal, Crimp.
(2). Insulated Wire	(2). Teflon insulated silver plated high voltage stranded wire built to MIL-W-22759.
(3). Shield	(3). 32 gauge, 85% minimum coverage, silver plated.
(4). Sheath	(4). Nomex Braid
(5). Connector	(5). Reynolds Part Number TBD
(6). Harness Mounting Flange	(6). Nickel Plated Aluminum Alloy 6061
(7). Strap	(7). Reynolds Part Number TBD

PPU Thruster Harness Diagram

The NSTAR Interface Control Drawings

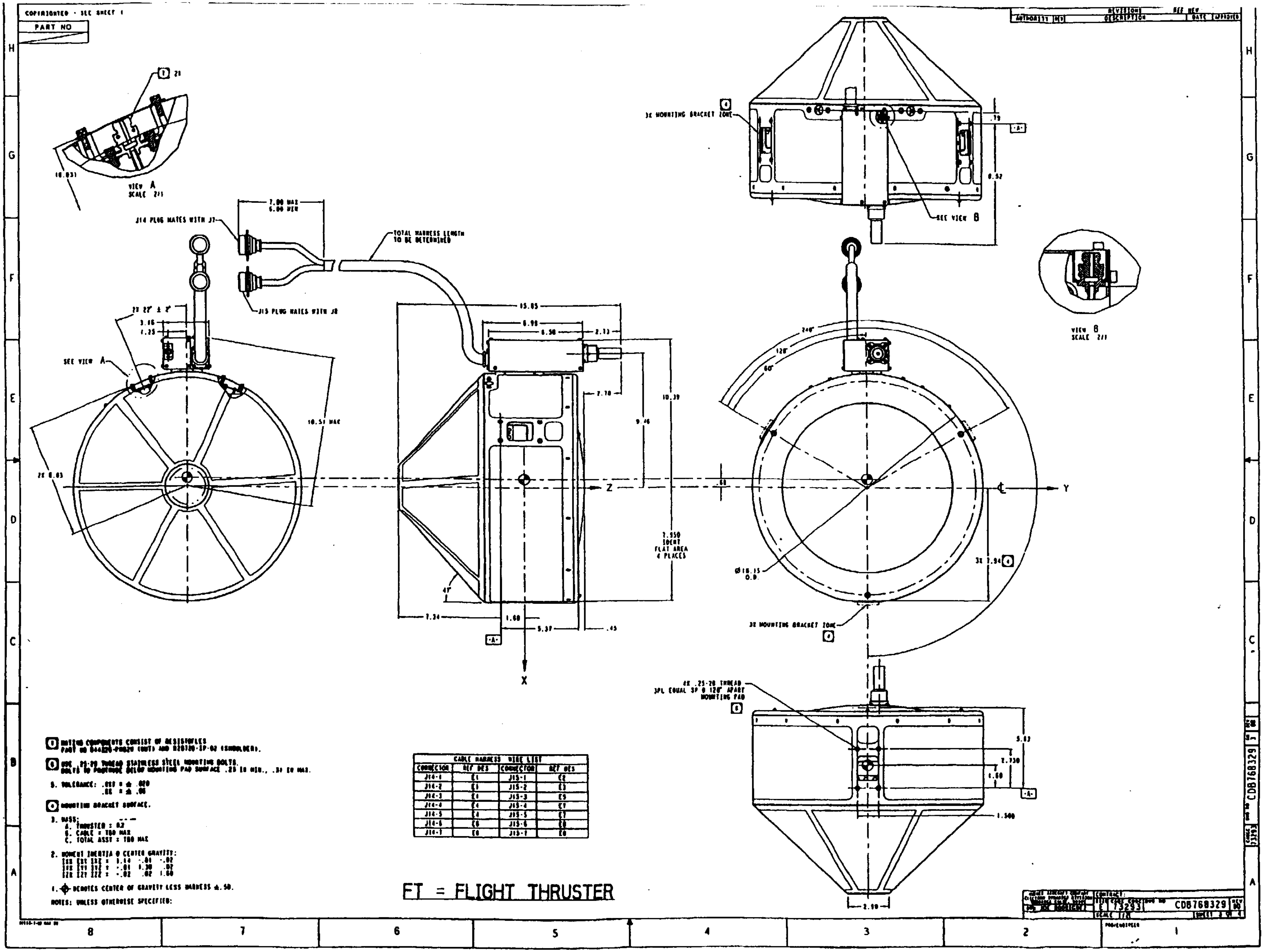
PART NO
VIEW A
SCALE 2/1
VIEW B
SCALE 2/1
TOTAL HARNESS LENGTH
TO BE DETERMINED
J14 PLUG MATES WITH J7
J15 PLUG MATES WITH J8
SEE VIEW A
SEE VIEW B
3X MOUNTING BRACKET ZONE
CABLE HARNESS WIRE LIST
NOTES: UNLESS OTHERWISE SPECIFIED:
CDB768329
FT = FLIGHT THRUSTER

PART NO: C0B768329-001

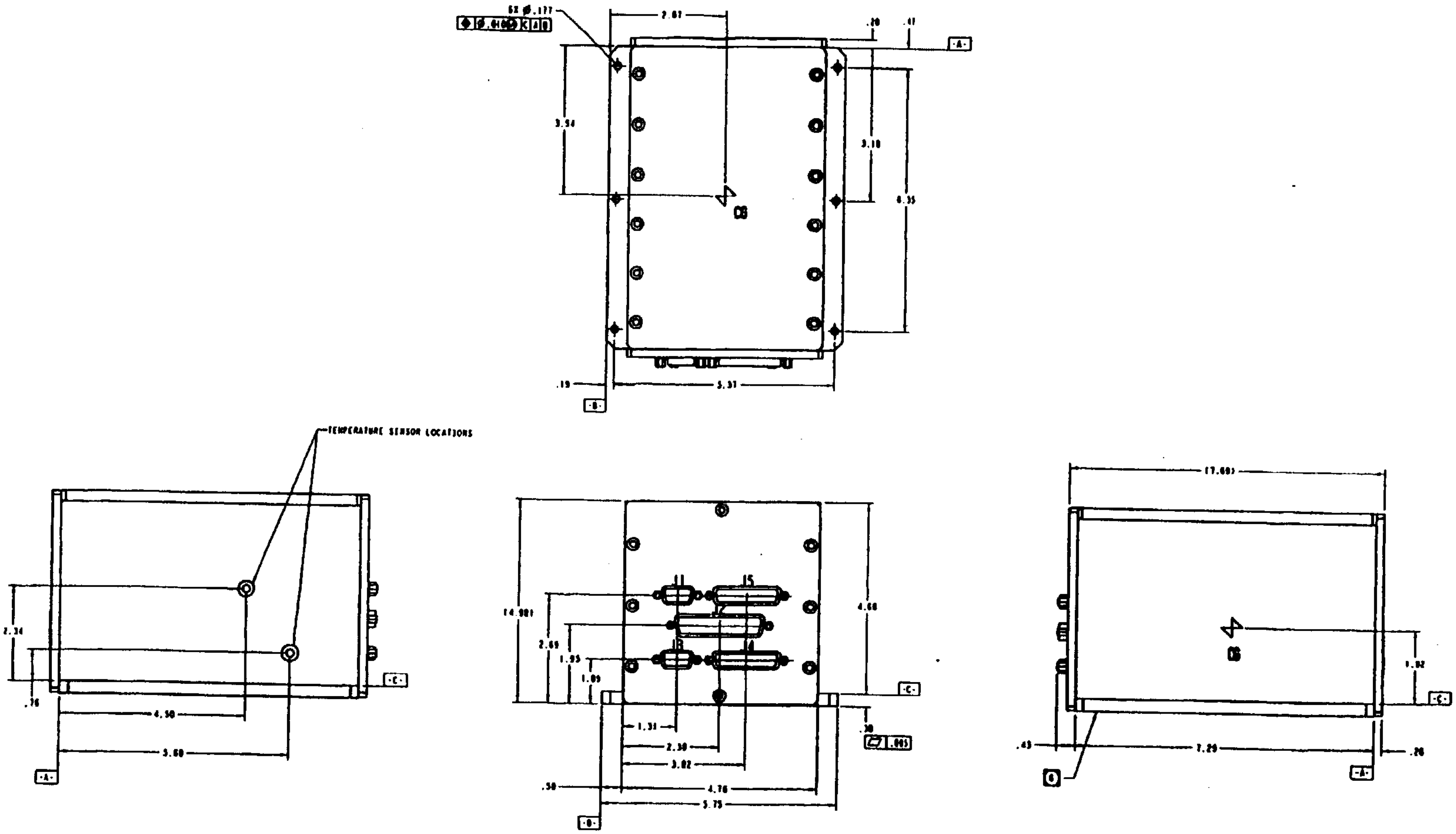

DCIU = DIGITAL CONTROL INTERFACE UNIT

NOTES: UNLESS OTHERWISE SPECIFIED

1. APPROXIMATE WEIGHT: 2.25KG
2. FINISH: CHEM FILM PER MIL-C-5541, CLASS 1A, YELLOW
3. SURFACE FINISH: 63 MICROINCHES RMS
4. MAXIMUM POWER DISSIPATION: 10 WATTS
5. MATERIAL: 6061-T651
6. SURFACE INDICATED SHALL NOT BE ANODIZED
7. REFER TO SH 4 FOR ELECTRICAL PIN OUTS.

REV STATUS OF SHEETS	LTR	00	00	00	00
	SH	1	2	3	4

HUGHES AIRCRAFT COMPANY
ELECTRON DYNAMICS DIVISION
TORRANCE, CALIF 90509

NSTAR THRUSTER ELEMENT SYSTEM

SIZE E | CAGE CODE 73293 | DWG NO C0B768329 | REV 00

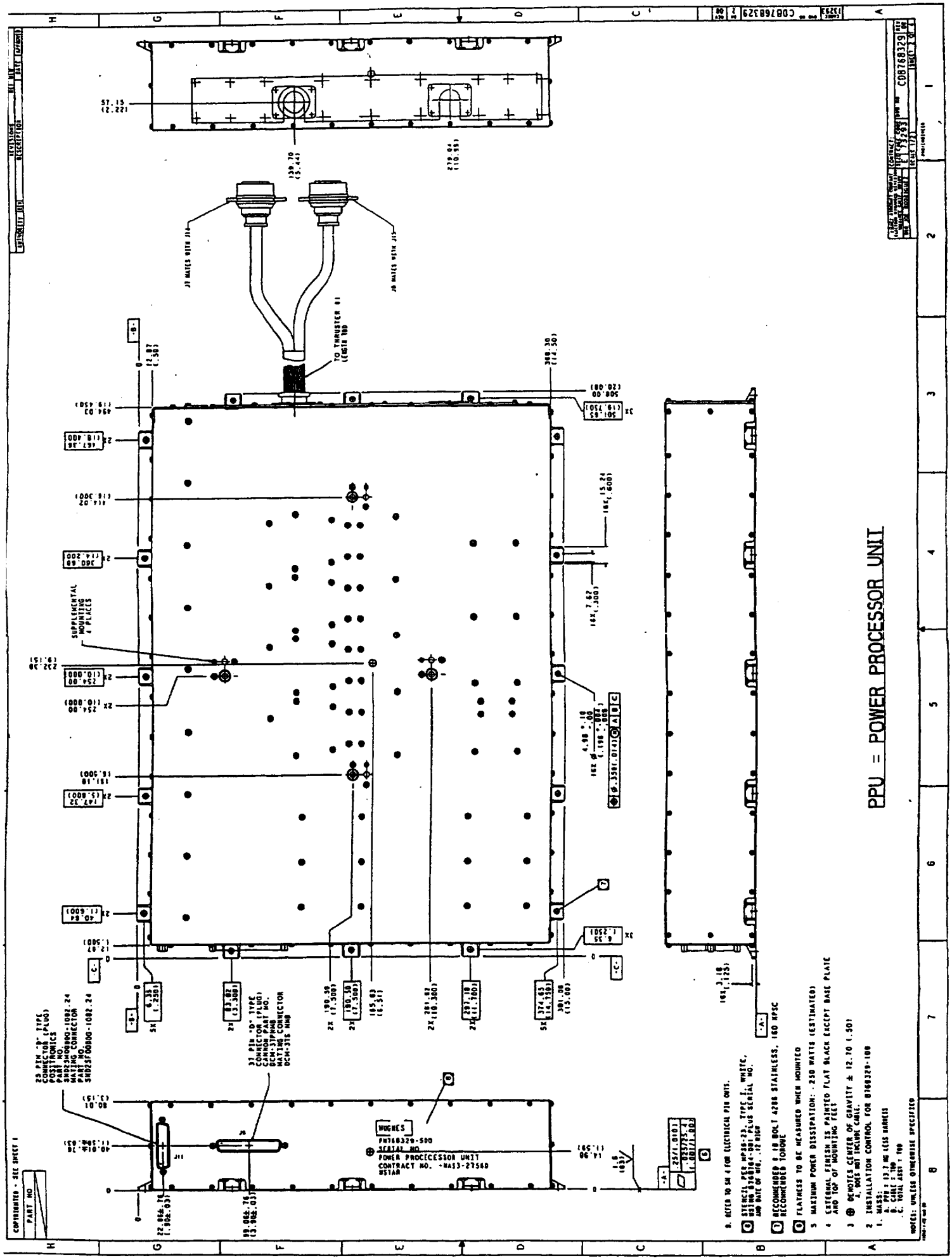
PPU = POWER PROCESSOR UNIT
HUGHES
PN7680329-500
SERIAL NO.
POWER PROCCESSOR UNIT
CONTRACT NO. -NAS3-27560
HSTAR
TO THRUSTER #1
(CCW VIEW)
J7 MATES WITH J15
J8 MATES WITH J16
SUPPLEMENTAL MOUNTING 4 PLACES
23 PIN "P" TYPE CONNECTOR (PLUG) CANNON ELECTRONICS PART NO. SRDE3M00B0-1082.24 MATING CONNECTOR PART NO. SRDE3F00B0G-1082.24
37 PIN "D" TYPE CONNECTOR (PLUG) CANNON ELECTRONICS PART NO. DCM-37PM48 MATING CONNECTOR DCM-37S M48
NOTES: UNLESS OTHERWISE SPECIFIED
1. MASS: A. CASE : 13.2 KG LESS HARNESS B. CARE : 700 C. TOTAL ASSY : 900
2. INSTALLATION CONTROL FOR 8168329-108
3. ⊕ DENOTES CENTER OF GRAVITY ± 12.70 (.50) A, DOES NOT INCLUDE CABLE.
4. EXTERNAL FINISH IS PAINTED FLAT BLACK EXCEPT BASE PLATE AND TOP OF MOUNTING FEET
5. MAXIMUM POWER DISSIPATION: - 250 WATTS (ESTIMATED)
6. FLATNESS TO BE MEASURED WHEN MOUNTED
7. RECOMMENDED 8-18 BOLT 4288 STAINLESS, 180 KPSC RECOMMENDED TORQUE
8. REFER TO SH 4 FOR ELECTRICAL PIN OUTS.
9. STENCIL PER MP88-23, TYPE I, WHITE, USING 8368164-001 PLUS SERIAL NO. AND DATE OF MFG. .12 HIGH

"Connector J1, GSFC311P409-1P-H-12"

Pin	Signal
1	Tx/Rx Channel A+
2	Tx/Rx Channel A-
3	N/C
4	Channel B Shield
5	N/C
6	Channel A Shield
7	N/C
8	Tx/Rx Channel B+
9	Tx/Rx Channel B+

"Connector J2, GSFC 311P407-5S-H-12"

Pin	Signal
1	N/C
2	XFS Low Pressure PA1+
3	XFS Low Pressure PA1-
4	XFS Low Pressure PA2 Shield
5	XFS Low Pressure PA3+
6	XFS Low Pressure PA3-
7	XFS Low Pressure PA4 Shield
8	N/C
9	XFS High Pressure PT1 Shield
10	XFSHigh Pressure Spare 1+
11	XFS High Pressure Spare 1-
12	XFS Temperature T9 Shield
13	XFS Temperature T10
14	XFS Temperature T10 Return
15	XFS Temperature T1 Shield
16	XFS Temperature T2
17	XFS Temperature T2 Return
18	XFS Temperature T3 Shield
19	XFS Temperature T4
20	XFS Temperature T4 Return
21	N/C
22	XFS Low Pressure PA1 Shield
23	XFS Low Pressure PA2+
24	XFS Low Pressure PA2-
25	XFS Low Pressure PA3 Shield
26	XFS Low Pressure PA4+
27	XFS Low Pressure PA4-
28	XFS Low Pressure PT1+
30	XFS High Pressure Spare 1 Shield
31	XFS Temperature T9
32	XFS Temperature T9 Return
33	XFS Temperature T10 Shield
34	XFS Temperature T1
35	XFS Temperature T1 Return
36	XFS Temperature T2 Shield
37	XFS Temperature T3
38	XFS Temperature T3 Return
39	XFS Temperature T4 Shield
40	N/C
41	XFS Low Pressure PA5+
42	XFS Low Pressure PA5-
43	XFS Low Pressure PA6 Shield
44	N/C
45	N/C
46	N/C
47	N/C
48	XFS High Pressure Spare 2 Shield
49	XFS High Pressure Spare 3+
50	XFS High Pressure Spare 3-
51	XFS Temperature TSpare Shield
52	XFS Temperature T11
53	XFS Temperature T11 Return
54	XFS Temperature T5 Shield
55	XFS Temperature T6
56	XFS Temperature T6 Return
57	XFS Temperature T7 Shield
58	XFS Temperature T8
59	XFS Temperature T8 Return
60	N/C
61	XFS Low Pressure PA5 Shield
62	XFS Low Pressure PA6+
63	XFS Low Pressure PA6-
64	N/C
65	N/C
66	N/C
67	XFS High Pressure Spare 2+
68	XFS High Pressure Spare 2-
69	XFS High Pressure Spare 3 Shield
70	XFS Temperature TSpare
71	XFS Temperature TSpare Return
72	XFS Temperature T11 Shield
73	XFS Temperature T5
74	XFS Temperature T5 Return
75	XFS Temperature T6 Shield
76	XFS Temperature T7
77	XFS Temperature T7 Return
78	XFS Temperature T8 Shield

"Connector J3, GSFC 311P407-3P-H-12"

Pin	Signal
1	+28V DCIU HouseLooping Power
2	N/C
3	+28V Valve Driver Power
4	N/C
5	+28V XFS Transducer Power
6	+28V DCIU Housekeeping Power
7	+28V Housekeeping Return
8	+ 28V Valve Driver Power
9	+28V Valve Driver Return
10	+28V XFS Transducer Power
11	+28V DCIU Housekeeping Return
12	N/C
13	+28V Valve Driver Return
14	+28V XFS Transducer Return
15	+28V XFS Transducer Return

"Connector J4, GSFC 311P407-3S-H-12"

Pin	Signal
1	Solenoid Valve SV1+
2	Solenoid Valve SV2+
3	Solenoid Valve SV3+
4	Solenoid Valve SV4+
5	Latch Valve LV10+
6	Latch Valve LV20+
7	Latch Valve LV30+
8	Latch Valve LV40+
9	Latch Valve LV50+
10	Latch Valve LV10+
11	Latch Valve LV20+
12	Latch Valve LV30+
13	Latch Valve LV40+
14	Latch Valve LV50+
15	N/C
16	Solenoid Valve SV1-
17	Solenoid Valve SV2-
18	Solenoid Valve SV3-
19	Solenoid Valve SV4-
20	Latch Valve LV10-
21	Latch Valve LV20-
22	Latch Valve LV30-
23	Latch Valve LV40-
24	Latch Valve LV50-
25	Latch Valve LV10-
26	Latch Valve LV20-
27	Latch Valve LV30-
28	Latch Valve LV40-
29	Latch Valve LV50-
30	N/C
31	Shield (Chassis Ground)
32	Shield (Chassis Ground)
33	Shield (Chassis Ground)
34	Shield (Chassis Ground)
35	Shield (Chassis Ground)
36	Shield (Chassis Ground)
37	Shield (Chassis Ground)
38	Shield (Chassis Ground)
39	Shield (Chassis Ground)
40	Shield (Chassis Ground)
41	Shield (Chassis Ground)
42	Shield (Chassis Ground)
43	Shield (Chassis Ground)
44	Shield (Chassis Ground)

"Connector J5, GSFC 311P407-3P-H-12"

Pin	Signal
1	Shift Clock 1+
2	Command Enable 1+
3	Command Data 1+
4	Telemetry Enable 1+
5	Telemetry Data 1+
6	N/C
7	Shift Clock 2+
8	Slice Reset Pulse +
9	Command Data 2+
10	Slice Signal Spare+
11	Telemetry Data 2+
12	N/C
13	UART TX+
14	UART RX+
15	N/C
16	Command Clock 1-
17	Command Enable 1-
18	Command Data 1-
19	Telemetry Enable 1-
20	Telemetry Data 1-
21	N/C
22	Shift Clock 2-
23	Slice Reset Pulse -
24	Command Data 2-
25	Slice Signal Spare-
26	Telemetry Data 2-
27	N/C
28	UART TX-
29	UART RX-
30	N/C
31	Shift Clock 1 Shield (Chassis Ground)
32	Command Enable 1 Shield (Chassis Ground)
33	Command Data 1 Shield (Chassis Ground)
34	Telemetry Enable 1 Shield (Chassis Ground)
35	Chassis Ground
36	N/C
37	Shift Clock 2 Shield (Chassis Ground)
38	Slice Reset Pulse Shield (Chassis Ground)
39	Command Data 2 Shield (Chassis Ground)
40	Slice Signal Spare Shield (Chassis Ground)
41	Telemetry Data 2 Shield (Chassis Ground)
42	N/C
43	Digital Ground (DGND)
44	Digital Ground (DGND)

DCIU ELECTRICAL PIN OUTS

Cable Harness Wire List

Connector	Ref Des	Connector	Ref Des
J7-1	E1	J8-1	E2
J7-2	E1	J8-2	E3
J7-3	E1	J8-3	E5
J7-4	E4	J8-4	E7
J7-5	E4	J8-5	E7
J7-6	E6	J8-6	E8
J7-7	E6	J8-7	E8

J6 Pin Assignment

Pin No.	Function	Pin No.	Function
1	+100V	20	+100V
2	+100V	21	+100V
3	+100V	22	+100V
4	+100V	23	+100V
5	+100V	24	+100V
6	+100V	25	+100V
7	+100V	26	Spare
8	Spare	27	Spare
9	Spare	28	+28V
10	+28V	29	Spare
11	Spare	30	Return
12	Return	31	Return
13	Return	32	Return
14	Return	33	Return
15	Return	34	Return
16	Return	35	Return
17	Return	36	Return
18	Return	37	Return
19	Chassis Ground		

J11 Pin Assignment

Pin No.	Function
1	Slice Reset Pulse+
2	Shift Clock+
3	Shift Clock-
4	Chassis Ground
5	Command Enable+
6	Command Enable-
7	Telemetry Data Shield (Chassis Ground)
8	Telemetry Enable+
9	Telemetry Enable-
10	Digital Ground
11	N/C
12	N/C Slice Signal Spare+
13	N/C
14	Slice Reset Pulse-
15	Chassis Ground
16	Command Data+
17	Command Data-
18	Chassis Ground
19	Telemetry Data+
20	Telemetry Data-
21	Chassis Ground
22	Digital Ground
23	N/C
24	N/C Slice Signal Spare
25	Chassis Ground

Thruster Outputs:	To Thruster - 1		To Thruster - 2
Pin No.	Assignment	Pin No.	Assignment
E1	Discharge Anode	E21	Discharge Anode
E2	Discharge Keeper	E22	Discharge Keeper
E3	Accelerator Grid	E23	Accelerator Grid
E4	Discharge Cathode	E24	Discharge Cathode
E5	Neutralizer Keeper	E25	Neutralizer Keeper
E6	Neutralizer Common	E26	Neutralizer Common
E7	Neutralizer Heater	E27	Neutralizer Heater
E8	Discharge Heater	E28	Discharge Heater

PPU ELECTRICAL PIN OUTS

NSTAR ELECTRICAL PIN OUTS

Drawing Number: CDB768329

Engineer: James Sovey **Date: 09.28.98**

Approved: **Date:**

Sheet 4 of 4 **Revision 2**

REPORT DOCUMENTATION PAGE

Form Approved
OMB No. 0704-0188

1. AGENCY USE ONLY (*Leave blank*)	2. REPORT DATE	3. REPORT TYPE AND DATES COVERED
	November 1999	Final Contractor Report

4. TITLE AND SUBTITLE

NSTAR Ion Thrusters and Power Processors

5. FUNDING NUMBERS

WU-242-70-01-00
NAS3-27560

6. AUTHOR(S)

T.A. Bond and J.A. Christensen

7. PERFORMING ORGANIZATION NAME(S) AND ADDRESS(ES)

Hughes Electron Dynamics
3100 West Lomita Blvd.
Torrance, California 90509-2999

8. PERFORMING ORGANIZATION REPORT NUMBER

E-11730

9. SPONSORING/MONITORING AGENCY NAME(S) AND ADDRESS(ES)

National Aeronautics and Space Administration
John H. Glenn Research Center at Lewis Field
Cleveland, Ohio 44135-3191

10. SPONSORING/MONITORING AGENCY REPORT NUMBER

NASA CR—1999-209162

11. SUPPLEMENTARY NOTES

Project Manager, James Sovey, Power and On-Board Propulsion Technology Division, NASA Glenn Research Center, organization code 5430, (216) 977-7454.

12a. DISTRIBUTION/AVAILABILITY STATEMENT

Unclassified - Unlimited
Subject Category: 20 Distribution: Nonstandard

This publication is available from the NASA Center for AeroSpace Information, (301) 621-0390.

12b. DISTRIBUTION CODE

13. ABSTRACT ***(Maximum 200 words)***

The purpose of the NASA Solar Electric Propulsion Technology Applications Readiness (NSTAR) project is to validate ion propulsion technology for use on future NASA deep space missions. This program, which was initiated in September 1995, focused on the development of two sets of flight quality ion thrusters, power processors, and controllers that provided the same performance as engineering model hardware and also met the dynamic and environmental requirements of the Deep Space 1 Project. One of the flight sets was used for primary propulsion for the Deep Space 1 spacecraft which was launched in October 1998.

14. SUBJECT TERMS

Propulsion; Electric propulsion; Spacecraft; Plasma applications; Ion propulsion

15. NUMBER OF PAGES

152

16. PRICE CODE

A08

17. SECURITY CLASSIFICATION OF REPORT	18. SECURITY CLASSIFICATION OF THIS PAGE	19. SECURITY CLASSIFICATION OF ABSTRACT	20. LIMITATION OF ABSTRACT
Unclassified	Unclassified	Unclassified	